

UNIVERSITÉ DU QUÉBEC À MONTRÉAL

ACCUMULATION DU CARBONE DANS LES TOURBIÈRES BORÉALES :
ANALYSE DE SENSIBILITÉ ET INTÉGRATION DE DONNÉES
PALÉOÉCOLOGIQUES

THÈSE
PRÉSENTÉE
COMME EXIGENCE PARTIELLE
DU DOCTORAT EN SCIENCES DE L'ENVIRONNEMENT

PAR
ANNE QUILLET

JANVIER 2013

UNIVERSITÉ DU QUÉBEC À MONTRÉAL
Service des bibliothèques

Avertissement

La diffusion de cette thèse se fait dans le respect des droits de son auteur, qui a signé le formulaire *Autorisation de reproduire et de diffuser un travail de recherche de cycles supérieurs* (SDU-522 – Rév.01-2006). Cette autorisation stipule que «conformément à l'article 11 du Règlement no 8 des études de cycles supérieurs, [l'auteur] concède à l'Université du Québec à Montréal une licence non exclusive d'utilisation et de publication de la totalité ou d'une partie importante de [son] travail de recherche pour des fins pédagogiques et non commerciales. Plus précisément, [l'auteur] autorise l'Université du Québec à Montréal à reproduire, diffuser, prêter, distribuer ou vendre des copies de [son] travail de recherche à des fins non commerciales sur quelque support que ce soit, y compris l'Internet. Cette licence et cette autorisation n'entraînent pas une renonciation de [la] part [de l'auteur] à [ses] droits moraux ni à [ses] droits de propriété intellectuelle. Sauf entente contraire, [l'auteur] conserve la liberté de diffuser et de commercialiser ou non ce travail dont [il] possède un exemplaire.»

REMERCIEMENTS

Je tiens tout particulièrement à remercier ma directrice de thèse Michelle Garneau pour l'opportunité qu'elle m'a offerte de contribuer à la recherche, pour sa confiance, sa patience et son soutien pluriel et inébranlable durant toutes ces longues années, et touchant à la fois les aspects scientifique, humain et matériel. Je remercie également Steve Frolking (University New Hampshire) pour son engagement bénévole dans ce projet, sa disponibilité et sa contribution scientifique sans laquelle cette thèse n'aurait pu être menée à bien.

Je suis reconnaissante à Nigel Roulet (McGill University) et à Changhui Peng pour m'avoir permis de participer à ce projet et pour leur soutien scientifique. Merci à Simon van Bellen (University of Aberdeen) de m'avoir soutenue au quotidien et d'avoir participé à de nombreuses envolées scientifiques. Je remercie aussi Julie Talbot (Université de Montréal) et Eeva-Stiina Tuittila (University of Eastern Finland) pour leur curiosité, leur motivation et les discussions enrichissantes.

Par ailleurs, la contribution technique et scientifique de Stefano Tarantola (Joint Research Center, Italy) a été essentielle à l'aboutissement des expériences scientifiques. Sa disponibilité et son indulgence ont été de plus très appréciées. Une importante contribution matérielle revient à Dina Oudjehani et à son équipe du Sitel (UQAM) qui ont permis la réalisation technique des expériences. Je suis également reconnaissante à Alain Tremblay (Environnement/Production, Hydro-Québec) d'avoir pu découvrir et prendre part au grand projet d'Eastmain 1. Le soutien moral ainsi que logistique de Nancy Lambert et Marty Lee ont grandement contribué à l'avancement du projet et ont été très appréciés.

Je remercie également mes acolytes tourbeux pour leur support, leurs encouragements et les riches discussions que nous avons eues. Je souhaite ajouter une mention spéciale pour mes amis, ma famille et plus particulièrement pour Marie-Christine Adam et Luc Pellecier qui m'ont aidée et soutenue, même au cœur de la tempête.

Je souhaiterais ajouter une mention spéciale pour mes amis, ma famille et plus particulièrement pour Marie-Christine Adam et Luc Pellecuer qui m'ont aidée et soutenue, même au cœur de la tempête.

AVANT-PROPOS

La présente thèse est constituée de trois articles, chacun présenté dans un chapitre et soumis à une revue à comité de lecture. Je suis la principale auteure de chacun de ces articles et j'ai effectué les tâches expérimentales, analytiques et interprétatives, ainsi que la préparation, la rédaction et le suivi de ces manuscrits. Les co-auteurs des différents articles m'ont assistée en me fournissant des outils ou des données, ou encore ont apporté leur contribution en discutant les manuscrits.

Le premier article est intitulé « *Assessing the role of parameter interactions in the sensitivity analysis of a model of peatland dynamics* » et a été publié en 2013 dans le journal *Ecological Modelling*. Les co-auteurs de cet article sont Steve Frolking (University New Hampshire), ma directrice de thèse Michelle Garneau, Julie Talbot (Université de Montréal) ainsi que mon co-directeur de thèse Changhui Peng. Steve Frolking a fourni le modèle (Holocene Peat Model) et a participé, en compagnie de Julie Talbot, à de nombreux échanges.

Le second article a pour titre: « *What drives carbon accumulation in peatlands? A global sensitivity analysis of the Holocene Peat Model* » et été accepté pour publication dans le *Journal of Geophysical Research: Biogeosciences*. Cet article a été rédigé en collaboration avec ma directrice de thèse Michelle Garneau et Steve Frolking.

Le troisième article: « *Integration of multi-proxy datasets in a peatland modelling exercise: new tools for palaeo-ecological studies* » a été soumis au *Journal of Ecology*. Les co-auteurs de cet article sont ma directrice de thèse Michelle Garneau, Simon van Bellen (Aberdeen University) et Steve Frolking et Eeva-Stiina Tuittila (University of Eastern Finland). Simon van Bellen a fourni les données de reconstruction de niveaux de nappe phréatique, les analyses de perte au feu et de macrorestes végétaux nécessaires à l'évaluation du modèle.

TABLE DES MATIÈRES

| | |
|--|------|
| REMERCIEMENTS..... | ii |
| AVANT-PROPOS..... | iii |
| TABLE DES MATIÈRES..... | iv |
| LISTE DES FIGURES..... | viii |
| LISTE DES TABLEAUX..... | xii |
| LISTE DES ABBRÉVIATIONS..... | xiii |
| RÉSUMÉ..... | xiv |
| INTRODUCTION..... | 1 |
| CHAPITRE I | |
| ASSESSING THE ROLE OF PARAMETER INTERACTIONS IN THE SENSITIVITY ANALYSIS OF A MODEL OF PEATLAND DYNAMICS..... | 8 |
| 1.1 Introduction..... | 11 |
| 1.2 Model description..... | 14 |
| 1.2.1 General scope..... | 14 |
| 1.2.2 Main mechanisms of peatland development..... | 15 |
| 1.2.3 Calibration and spin-up..... | 17 |
| 1.2.4 Evaluation..... | 18 |
| 1.3 Methods..... | 18 |
| 1.3.1 Output of interest..... | 19 |
| 1.3.2 Local sensitivity analysis..... | 19 |
| 1.3.3. Screening method..... | 20 |

| | | |
|-------------|---|----|
| 1.4 | Results | 23 |
| 1.4.1 | Local sensitivity analysis..... | 23 |
| 1.4.2 | Morris' screening method..... | 27 |
| 1.5 | Discussion..... | 31 |
| 1.6 | Conclusions | 35 |
| | Acknowledgments..... | 37 |
| | References | 37 |
| CHAPITRE II | | |
| | SOBOL' SENSITIVITY ANALYSIS OF THE HOLOCENE PEAT MODEL: WHAT DRIVES CARBON ACCUMULATION IN PEATLANDS?..... | 46 |
| 2.1 | Introduction..... | 49 |
| 2.2 | The Holocene Peat Model | 51 |
| 2.2.1 | Vegetation representation and productivity..... | 51 |
| 2.2.2 | Water balance and hydraulic properties | 52 |
| 2.2.3 | Peat decomposition..... | 52 |
| 2.2.4 | Peat accumulation..... | 53 |
| 2.2.5 | Model calibration and initiation | 53 |
| 2.3 | Global sensitivity analysis | 54 |
| 2.3.1 | Screening method | 55 |
| 2.3.2 | Sobol' indices | 55 |
| 2.3.3 | Experimental setting..... | 56 |
| 2.4 | Results | 57 |
| 2.4.1 | Main processes affecting carbon mass | 58 |

| | |
|--|-----|
| 2.4.2 Relationships between PFTs and accumulated carbon mass..... | 60 |
| 2.5 Discussion..... | 64 |
| 2.6 Conclusions | 68 |
| Acknowledgments..... | 68 |
| References | 69 |
| CHAPITRE III | |
| INTEGRATION OF MULTI-PROXY DATASETS IN A PEATLAND MODELLING EXERCISE: A NEW TOOL FOR PALAEO-ECOLOGICAL STUDIES..... | |
| 3.1 Introduction..... | 84 |
| 3.2 Palaeoecological analyses..... | 86 |
| 3.2.1 Sites | 86 |
| 3.2.2 Material collected and analyses..... | 87 |
| 3.2.3 Water table depth reconstruction..... | 87 |
| 3.3 The forcing exercise | 88 |
| 3.3.1 The Holocene Peat Model | 88 |
| 3.3.2 Methods | 88 |
| 3.4 Results | 92 |
| 3.4.1 Precipitation and water table depth | 92 |
| 3.4.2 Carbon accumulation..... | 93 |
| 3.4.3 Vegetation distribution | 96 |
| 3.5 Discussion..... | 99 |
| 3.5.1 Model limitations..... | 99 |
| 3.5.2 The role of water table depth forcing in the simulation results..... | 100 |

| | | |
|-------|---|-----|
| 3.5.3 | Long-term net carbon loss | 102 |
| 3.5.4 | Tracing vegetation history in relation to climate and other forcing . | 103 |
| 3.5.5 | Multiple proxies..... | 104 |
| 3.6 | Conclusion | 105 |
| | Acknowledgments..... | 106 |
| | References | 106 |
| | CONCLUSION..... | 121 |
| | REFERENCES..... | 128 |

LISTE DES FIGURES

| Figure | Page |
|---|------|
| 0.1 Schéma du Holocene Peat Model (HPM). z_{WT} et h_{PD} représentent respectivement le niveau de la nappe phréatique et la hauteur totale de tourbe. (Frolking et al., 2010)..... | 4 |
| 0.2 Schéma méthodologique de la thèse. Les hypothèses sont présentées dans des cadres blancs..... | 6 |
| 1.1 Total carbon mass after 5000 simulation years for different parameters values of a) maximum potential NPP (NPP_{pot}), b) minimum bulk density (ρ_{min}), c) anoxia scale length (c_2) and d) precipitation (P). In these one-at-a-time (OAT) sensitivity analyses one parameter changes at a time and all other parameters remain constant at nominal values. In (a)–(c), filled circles represent simulations with precipitation nominal value 0.9 m yr^{-1} , hollow squares and triangles represent simulations with precipitation scenarios of 0.7 m yr^{-1} and 1.1 m yr^{-1} respectively (all other parameters remain constant)..... | 43 |
| 1.2 Total carbon mass after 5000 simulation years for different combination of parameters according to the random sampling method applied for the elementary effects calculation. Here 1280 simulations are performed with parameters combinations based on all the model parameters (127); each parameter may take a different value within its range (Table 1.2). The central mark of the box is the median, the bottom and the top of the box represent the 25 th and 75 th percentiles, the whiskers extend to the most extreme data points not considered outliers, and outliers are plotted individually..... | 44 |

- 1.3 Mean (μ) and standard deviation (σ) of the distribution of elementary effects of each model parameter for total carbon mass after 5000 simulation years. Triangles, squares and hollow circles represent groups of parameters related to water outflows, bulk density and PFTs respectively. All other parameters are represented by filled circles. μ gives an insight of the overall influence of a parameter on the total carbon mass. σ is an indicator of non-linearity and interactions with other parameters..... 45
- 2.1 Sobol' indices (S_i) calculated for the total carbon mass after 5000 simulation years: a) first-order effect of each parameter, b) sum of the second-order effects for each parameter and c) total effect of each parameter. The magnitude of the first-order effect represents the direct influence of that parameter on the variance in model output assessed, i.e., total carbon mass; note that the first-order effect is very small for some parameters. The magnitude of the second-order effect represents the variance of the output related to a parameter's interactions with other parameters. The total effect includes first- and second-order effects as well as all the higher-order interactions (i.e. 3 or more parameters) and represents the variance in the output that would remain if only this parameter were to stay undetermined..... 76
- 2.2 Sobol' indices: second-order effects for each of the 26 parameters. Each parameter is designated by its abbreviation; details on each parameter are in Table 2.1. Only positive values are shown, zero or negative values are not significant, and those parameters are omitted.. 77
- 2.3 a) Average response of total carbon mass (kg) for different values of maximum potential NPP (NPP_{pot}) and minimum profile relative transmissivity (T_0), b) average response of water table depth (positive down) for different values of NPP_{pot} and T_0 , and c) number of simulation for each combination of parameter values. See note in Figure 2.3 caption..... 78

| | | |
|-----|--|-----|
| 2.4 | a) Average response of total carbon mass (kg) for different decomposition rates for hummock- <i>Sphagnum</i> (k_{0_8}) and different values of relative productivity of lawn- <i>Sphagnum</i> (NPP_{rel7}) and b) number of simulation for each combination of parameter values. See note in Figure 2.3 caption. | 79 |
| 2.5 | a) Average response of total carbon mass (kg) for different values of productivity optimum peat depth for lawn- <i>Sphagnum</i> (h_{PD7}^{opt}) and anoxia scale length (c_2), b) response amplitude of total carbon mass for different values of h_{PD7}^{opt} and c_2 and c) number of simulation for each combination of parameter values. See note in Figure 2.3 caption..... | 80 |
| 3.1 | Location of the two peatlands..... | 112 |
| 3.2 | Conceptual diagram of HPM. Dashed-lines represent feedbacks. | 113 |
| 3.3 | a) Precipitation in the Eastmain watershed reconstructed from pollen data (Viau and Gajewski, 2009). For b) LLC and c) MOS: water table reconstructions from testate amoebae (white solid line) with their standard errors (gray shade)(van Bellen, Garneau and Booth, 2011) and simulated water table depths from the simulation with reconstructed precipitation (black solid line). Water table depths are positive down..... | 114 |
| 3.4 | Accumulated carbon mass for a) LLC and b) MOS from loss on ignition results (black solid lines with 95% confidence interval in dashed lines), simulations with reconstructed precipitation (solid light gray) and with water table depth forcing (solid dark gray)..... | 115 |
| 3.5 | Carbon accumulation rates from loss on ignition analyses compared with simulated final core carbon content with reconstructed precipitation and with water table depth forcing for a) LLC and b) MOS and with simulated net annual carbon balance with reconstructed precipitation and with water table depth forcing for c) LLC and d) MOS..... | 116 |

- 3.6 a) Macrofossil profile summary, b) distribution of the mass fraction of the different PFTs for P_{LLC} and c) for W_{LLC} . For sake of comparison, HPM's 12 PFTs (see Appendix 3.1) are aggregated into 7 groups of species identifiable in a peat core..... 117
- 3.7 a) Macrofossil profile summary, b) distribution of the mass fraction of the different PFTs for P_{MOS} and c) for W_{MOS} . For sake of comparison, HPM's 12 PFTs (see Appendix 3.1) are aggregated into 7 groups of species identifiable in a peat core..... 118

LISTE DES TABLEAUX

| Tableau | Page |
|---|------|
| 1.1 Nominal values of plant functional types (PFTs), after Froking <i>et al.</i> (2010)..... | 41 |
| 1.2 Model parameters characteristics and associated range and distribution for the sensitivity analysis | 42 |
| 2.1 Characteristics of the 26 selected model parameters and their associated range and distribution for the sensitivity analysis, after Quillet <i>et al.</i> (2013) .. | 74 |
| 2.2 Nominal values of plant functional types (PFTs), after Froking <i>et al.</i> (2010)..... | 75 |
| 3.1 HPM parameters: description and values. Differences between sites are in bold type | 119 |

LISTE DES ABRÉVIATIONS, SIGLES ET ACRONYMES

| | |
|--------|---|
| cal BP | calibrated years before present |
| CAR | Carbon Accumulation Rate |
| FPAR | Fraction of Photosynthetically Active Radiation |
| GSA | Global Sensitivity Analysis |
| HPM | Holocene Peat Model |
| LLC | Tourbière du Lac Le Caron |
| MOS | Tourbière Mosaik |
| NPP | Net Primary Production |
| PAR | Photosynthetically Active Radiation |
| PFT | Plant Functional Type |
| PD | Peat Depth |
| PPN | Productivité Primaire Nette |
| SA | Sensitivity Analysis |
| SE | Standard Error |
| TFP | Type Fonctionnel de Plante |
| UOM | Unidentified Organic Matter |
| WTD | Water Table Depth |

RÉSUMÉ

Les tourbières nordiques, sont des écosystèmes humides ayant la particularité de produire plus de matière organique qu'elles n'en décomposent. Elles ont ainsi accumulé de formidables quantités de carbone depuis le début de la dernière déglaciation. C'est pour cette raison qu'elles représentent un intérêt particulier pour la modélisation du climat global. En effet, contenant environ un tiers du carbone des sols tout en ne couvrant qu'environ 3% de la surface terrestre, les tourbières émettent également de grandes quantités de méthane, qui a un pouvoir de réchauffement climatique 23 fois plus important que le dioxyde de carbone. Afin de pouvoir intégrer ces différents facteurs dans les modèles globaux du climat et d'estimer leur incidence sur le cycle global du carbone, il est nécessaire de mieux connaître la dynamique du carbone dans les tourbières elles-mêmes.

Les tourbières nordiques ont la capacité d'archiver des informations rapportant les différents changements qu'elles ont subis depuis leur développement. Ces changements incluent les changements climatiques régionaux, qui ont affecté leur végétation et la dynamique du carbone, mais aussi des changements autogènes, c'est-à-dire propres à leur dynamique interne. Il est donc nécessaire de prendre en compte ces différents facteurs en vue de reproduire leur dynamique.

Cette thèse a pour objectif d'évaluer la connaissance de la dynamique du carbone dans les tourbières par le biais de l'évaluation du Holocene Peat Model (Frolking et al. 2010). Ce modèle comprend une description des processus d'accumulation, de décomposition, du bilan hydrique et une représentation de la végétation par 12 groupes fonctionnels de plantes ainsi que les boucles de rétroaction entre ces différents processus. Son évaluation a été effectuée en deux étapes.

Dans un premier temps, une analyse de sensibilité a permis de déceler les paramètres du modèle ayant une influence sur la quantité totale de carbone dans les simulations, puis les interactions entre les paramètres ont également été analysées. Les résultats montrent que certains paramètres représentent des sources d'incertitude importantes et devraient être l'objet de plus amples recherches (tels que la conductivité hydraulique, le gradient d'anoxie, certains paramètres contrôlant le bilan hydrique et la densité sèche). De plus, parmi les milliers de simulations effectuées, on observe que plusieurs types de développements des tourbières sont possibles, bien que la méthodologie mette l'accent sur les processus autogènes et contraigne les processus allogènes à un régime de précipitation et une productivité primaire nette (PPN, servant d'indicateur climatique) constants. Par ailleurs, il apparaît que les sphaignes ont une influence sur le type de développement de la tourbière, ce qui affecte par conséquent l'accumulation du carbone.

Dans un second temps, le modèle est calibré pour deux sites de la région de la Baie James au Québec. Il s'agit de deux tourbières ombrotrophes ouvertes ayant des caractéristiques écohydrologiques et des taux d'accumulation de carbone différents. Pour chacun de ces sites, deux simulations sont réalisées : la première est basée sur une reconstruction des précipitations et la seconde sur une reconstruction des niveaux de nappe phréatique. Il est notable que les résultats des simulations révèlent des périodes durant lesquelles les tourbières présentent des pertes nettes de carbone. En comparant les résultats des simulations avec les taux d'accumulation de carbone et les résultats des analyses de macrorestes végétaux, on constate que le modèle reproduit, de façon générale, les variations observées dans ces séries de données. De plus, il est conclu que ce modèle peut être utilisé comme outil d'identification des causes de variations de l'assemblage végétal.

Bien que de certains processus doivent être étudiés plus avant afin de limiter les incertitudes du modèle, cette thèse a permis d'établir la validité des concepts de dynamique du carbone dans les tourbières en intégrant l'évaluation des dynamiques d'échelle globale et locale.

Mots-clés : Tourbière, modélisation, évaluation, analyse de sensibilité, forçage, fonction de transfert.

INTRODUCTION

Les tourbières boréales et subarctiques, bien que non répertoriées dans leur totalité, couvrent environ 3% de la surface terrestre (Charman, 2002). Elles sont particulièrement abondantes à des latitudes supérieures à 50° et sous des climats froids et humides (Yu, Beilman et Jones, 2009) et, malgré leur étendue, demeurent mal connues. Jusqu'à récemment, ces écosystèmes humides ont été peu étudiés à l'état naturel car ils ont été gravement affectés par leur exploitation comme source de combustible, notamment en Europe, mais aussi du fait de leur éloignement des centres urbains et des infrastructures routières. De plus, en vue de dresser un portrait global des tourbières, il est nécessaire de procéder à un grand nombre d'études locales en raison de la variabilité de la dynamique écosystémique entre les sites et les régions.

L'étude des tourbières suscite toutefois un intérêt grandissant dans le cadre de la compréhension du système climatique global. En effet, il apparaît essentiel de comprendre les interactions entre les écosystèmes terrestres et l'atmosphère et plus particulièrement en ce qui a trait au cycle global du carbone (Denman et al., 2007). Les tourbières jouent un rôle prépondérant dans ces recherches puisqu'elles renferment environ la moitié du carbone total contenu dans les sols, ce qui représente environ entre 473 et 621 PgC (Yu et al., 2010), et qu'elles exercent un forçage radiatif négatif sur le climat (Frolking et Roulet, 2007).

L'accumulation de carbone dans les tourbières est particulièrement liée à l'humidité du milieu. Les conditions anaérobies qui prévalent limitent la décomposition de la matière organique, et en conséquence une tourbière produit plus de biomasse organique qu'elle n'en décompose. Toutefois, les processus qui contrôlent les taux d'accumulation de tourbe et du carbone qui lui est associé demeurent peu compris. En effet, les tourbières nordiques stockent des quantités de carbone très différentes selon

leur mode de développement, les conditions hydrologiques, les conditions climatiques régionales ou encore leur stade de développement (ex: Turunen et al., 2002a ; Yu, Beilman et Jones, 2009). À ceci s'ajoute, au sein d'une même tourbière, une forte variabilité de la microtopographie de surface, des propriétés hydrauliques, du pH et des ressources en nutriments (ex: Waddington et al., 2010), ce qui limite l'extrapolation spatiale des résultats. Par conséquent, l'établissement des causes des variations de l'accumulation de carbone doit tenir compte de ces différents facteurs ainsi que des interactions possibles entre eux.

Afin de comprendre les processus d'accumulation de carbone dans les tourbières, leur contenu en matière organique et en carbone est analysé. Des études paléoécologiques sont effectuées en vue de corrélérer les changements d'accumulation avec différents événements enregistrés parmi les horizons tels que des changements dans la composition de la végétation ou la présence de niveaux de charbons. Ces études montrent que des facteurs autant autogènes qu'allogènes peuvent être à l'origine de modifications de l'accumulation du carbone d'une tourbière (ex: Anderson, Foster et Motzkin, 2003 ; Beaulieu-Audy et al., 2009 ; Lamentowicz, Obremska et Mitchell, 2008 ; Tuittila et al., 2007). L'identification de l'origine d'une variation d'accumulation de carbone demeure toutefois complexe du fait de la rétroaction de différents processus dans la dynamique interne de la tourbière mais aussi du fait des incertitudes liées à la limite d'interprétation des paléoindicateurs (proxies) et des chronologies qui leur sont associées (Blaauw, 2012).

Dans les années 1980, Clymo (1984b) propose un premier modèle d'accumulation de tourbe applicable aux tourbières ombrotrophes. Il s'agit d'une première tentative d'évaluation des connaissances; le but étant de retrouver dans une représentation mathématique les observations faites sur le terrain et en laboratoire. Par la suite, de nombreux auteurs proposent leur modèle des processus d'accumulation dans les tourbières (ex: Clymo, 1992 ; Frohling et al., 2001 ; Frohling et al., 2010 ;

Heinemeyer et al., 2010 ; Hilbert, Roulet et Moore, 2000 ; Ise et al., 2008 ; St-Hilaire et al., 2010). Ces travaux sont pour la plupart basés sur le modèle d'accumulation de Clymo (1984b). Ils intègrent différentes caractéristiques et rétroactions propres aux tourbières (ex : biogéochimie, hydrologie, végétation, etc.) et sont développés pour des échelles spatiales variées allant du local au global.

Bien que quelques études aient déjà pris en compte les tourbières dans des modèles climatiques ou systémiques globaux (ex: Kleinen, Brovkin et Getzieh, 2011 ; St-Hilaire et al., 2010 ; Wania, Ross et Prentice, 2009), leur représentation reste marginale et simplifiée. En vue d'intégrer la dynamique des tourbières nordiques dans les modèles globaux de simulation de végétation de surface et du cycle du carbone nécessaires aux modèles climatiques et considérant la complexité des interactions entre les tourbières et le climat, il est essentiel de s'assurer de la représentativité des modèles de dynamique des tourbières existants.

Certains modèles ont déjà été partiellement évalués soit en comparant les simulations avec des données de terrain (ex: Heijmans et al., 2008 ; Heinemeyer et al., 2010 ; Lai, 2009 ; Tuittila et al., 2013), soit en procédant à des analyses de sensibilité partielle (ex: Hilbert, Roulet et Moore, 2000 ; Li et al., 2010 ; St-Hilaire et al., 2010 ; Tang et al., 2010 ; Wania, Ross et Prentice, 2009 ; Yu et al., 2001a). Il est important de procéder à une évaluation rigoureuse des fondements des modèles, de façon à évaluer les connaissances dans le domaine mais également afin de s'assurer que le rôle des tourbières dans les bilans globaux du carbone soit adéquatement représenté.

Pour ce faire, il est important de comprendre quels sont les différents facteurs qui contrôlent la dynamique du carbone dans les tourbières et de quelle façon ils l'influencent. A partir d'un modèle dynamique de ces écosystèmes, il est possible d'évaluer les représentations mathématiques et d'estimer le rôle des interactions entre les différents processus représentés.

Le « Holocene Peat Model » (HPM, Figure 1) développé par Frohling et al. (2010) est un modèle simulant le développement d'une tourbière ombrotrophe. Il inclut les processus d'accumulation et de décomposition calculés annuellement en intégrant 12 types fonctionnels de plante (TFP), chacun d'entre eux étant caractérisé par une productivité et une décomposition spécifiques, et également par un biotope (gradient d'humidité) et des conditions d'accès aux nutriments particuliers (par le biais d'un gradient de profondeur de tourbe). HPM comprend également différentes boucles de rétroaction intégrant la productivité, la décomposition, les propriétés hydrauliques de la tourbe, le bilan hydrique et les différents TFP.

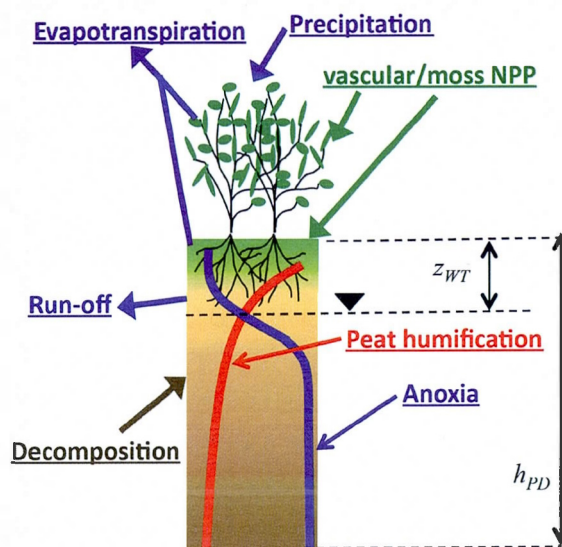


Figure 1 : Schéma du « Holocene Peat Model » (HPM). z_{WT} et h_{PD} représentent respectivement le niveau de la nappe phréatique et la hauteur totale de tourbe. (Frohling *et al.*, 2010)

Bien que ce modèle ne comporte qu'une dimension, et ne représente par conséquent ni la microtopographie, ni l'expansion latérale des tourbières au cours de leur développement, il est, au vu des connaissances actuelles, très complet en ce qui a trait à la dynamique du carbone dans les tourbières à l'échelle millénaire.

À l'aide de la représentation des connaissances actuelles de la dynamique des tourbières fournie par le HPM, la thèse présentée ici a pour objectif principal d'évaluer les processus d'accumulation de carbone dans les tourbières tout au long de leur développement et d'apprécier les connaissances et les lacunes dans ce domaine sur le plan systémique. Au-delà de l'évaluation intrinsèque du HPM, cette thèse vise à améliorer la compréhension des processus contrôlant l'accumulation de carbone dans les tourbières par l'analyse de l'influence des boucles de rétroaction sur l'équilibre des systèmes tourbeux.

Les sous-objectifs de cette thèse sont les suivants :

- Développer une méthodologie d'évaluation de la représentativité de la dynamique du carbone du HPM;
- Évaluer la capacité du HPM à reproduire les processus de développement d'une tourbière de façon réaliste;
- Évaluer la sensibilité de l'accumulation du carbone aux paramètres utilisés pour contrôler les différents modules de HPM;
- Évaluer le rôle des interactions entre les paramètres sur l'accumulation simulée de carbone;
- Identifier les processus causant des incertitudes dans les simulations en vue d'améliorer le modèle.

Le schéma conceptuel présenté à la Figure 2 associe la démarche méthodologique et les hypothèses de travail. Deux approches différentes ont été utilisées pour réaliser cette étude. L'analyse de sensibilité du HPM, elle-même effectuée en deux temps, établit tout d'abord l'importance du choix dans la méthode d'évaluation et souligne la

portée des interactions entre les paramètres dans l'évaluation des résultats d'un modèle. Cette première analyse est présentée au chapitre 2 et constitue le sujet de l'article intitulé « *Assessing the role of parameter interactions in the sensitivity analysis of a model of peatland dynamics* » publié en 2013 dans le journal *Ecological Modelling*.

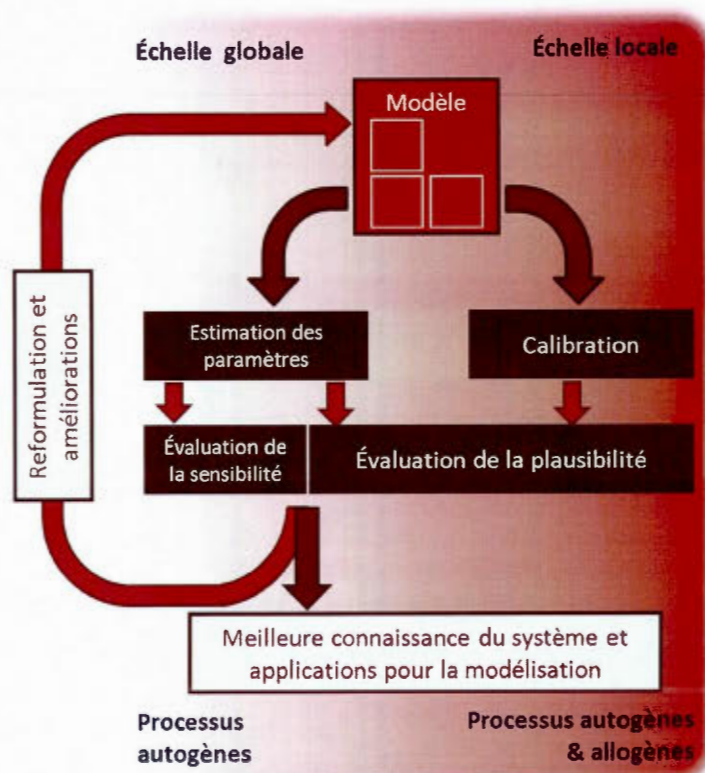


Figure 2 : Schéma méthodologique de la thèse. Les hypothèses sont présentées dans des cadres blancs.

L'analyse de sensibilité du HPM est enrichie d'une analyse de sensibilité globale permettant de quantifier l'influence des interactions entre les paramètres sur l'accumulation totale de carbone. De plus, cette étude permet l'analyse de l'influence des processus autogènes sur la dynamique du système. Le chapitre 3 présente cette

analyse dans un article intitulé « *What drives carbon accumulation in peatlands? A global sensitivity analysis of the Holocene Peat Model* » sous presse dans le *Journal of Geophysical Research: Biogeosciences*.

Ces deux études mènent également à l'identification des sources d'incertitude dans le modèle et permettent d'avancer des pistes d'amélioration. Toutefois, c'est en comparant les résultats des simulations avec des résultats d'analyses paléoécologiques provenant de tourbières ombrotrophes de la région boréale de la Baie James au Québec qu'il est possible d'évaluer la capacité du HPM à reproduire le développement d'un système naturel. Cette analyse fait l'objet d'un troisième article qui met également l'accent sur le développement d'une nouvelle méthode alliant la modélisation aux données paléoécologiques et pouvant s'avérer utile pour identifier les causes de variation d'accumulation du carbone dans un système. Le chapitre 4 présente cet article intitulé « *Integration of multi-proxy datasets in a peatland modelling exercise: new tools for palaeo-ecological studies* » et soumis au *Journal of Ecology*.

Finalement, le chapitre 5 présente les conclusions de la thèse en incluant ses limites, sa portée ainsi que plusieurs pistes de recherche pour des études ultérieures.

CHAPITRE I

ASSESSING THE ROLE OF PARAMETER INTERACTIONS IN THE SENSITIVITY ANALYSIS OF A MODEL OF PEATLAND DYNAMICS

Anne Quillet¹, Steve Frohking², Michelle Garneau³, Julie Talbot⁴ and Changhui Peng⁵

¹ GÉOTOP et Chaire DÉCLIQUE-Hydro-Québec, Université du Québec à Montréal, succ. centre-ville, CP 8888, Montréal QC. H3C 3P8, Canada.

² Institute for the Study of Earth, Oceans, and Space, University of New Hampshire, 8 College Road, Durham, NH 03824-3525, USA.

³ GÉOTOP, Chaire DÉCLIQUE-Hydro-Québec & Département de Géographie, Université du Québec à Montréal, succ. centre-ville, CP 8888, Montréal QC. H3C 3P8, Canada.

⁴ Département de Géographie, Université de Montréal, 520, chemin de la Côte-Ste-Catherine, Montréal QC. H2V 2B8, Canada.

⁵ Institut des Sciences de l'Environnement, Université du Québec à Montréal, succ. centre-ville, CP 8888, Montréal QC. H3C 3P8, Canada.

Article publié en 2013 dans le journal *Ecological Modelling*, vol. 248, p. 30-40,
doi: 10.1016/j.ecolmodel.2012.08.023.

Résumé

L'identification des processus contrôlant le budget du carbone dans les tourbières nordiques est cruciale pour leur intégration dans les modèles globaux du climat. Dans un premier temps, les modèles actuels de dynamique des tourbières doivent être adéquatement évalués afin de s'assurer de la solidité des processus représentés et que ces modèles répondent à leurs objectifs.

Nous comparons ici la sensibilité de la quantité totale de carbone d'une tourbière simulée par le Holocene Peat Model (HPM) en utilisant différentes analyses de sensibilité : une analyse de sensibilité locale classique et une approche globale par le biais d'une méthode de criblage.

Les conclusions tirées des différentes méthodes sont très différentes les unes des autres et il est déconseillé de tirer quelque conclusion générale que ce soit d'une analyse locale de type one-at-a-time (OAT, c'est-à-dire « un à la fois ») étant donné que l'espace du modèle qui y est représenté est très limité. Les résultats également que la représentation dans le modèle de certains processus, tels que le ruissellement ou la décomposition de la tourbe sous différents degrés de saturation, est limitée par le manque de données empiriques et de connaissances. Au-delà de l'évaluation du modèle en tant que telle, l'exploration de ses comportements permet l'observation dans les simulations de deux modes de transition fen-bog.

Cette étude montre que les interactions entre les paramètres devraient être prises en compte lors de l'évaluation d'un modèle de dynamique des tourbières. Les résultats de la méthode de criblage permettent de plus la simplification et l'amélioration du modèle. En outre, cette méthode permet une exploration détaillée des processus modélisés et apporte une ouverture sur la dynamique des systèmes tourbeux.

Abstract

Identifying the processes controlling the carbon balance in northern peatlands is crucial for their integration in global climate models. As a first step, current models of peatlands dynamics need to be adequately evaluated to verify the consistency of processes before their integration in global models.

We compared here the sensitivity of the total carbon mass of a peatland simulated by the Holocene Peat Model (HPM) derived from different sensitivity methods: a 'classic' local sensitivity analysis method and a global approach with the screening method.

We observed that the conclusions drawn by the different methods are very different and, moreover, that it is not advisable to draw any general conclusion from a local one-at-a-time (OAT) experiment because the model space represented is very limited. The results also stressed that the representation of several processes, such as runoff or peat decomposition under different saturation conditions, lack sufficient empirical data and knowledge to be adequately represented in the model. In addition to the evaluation of the model per se, the exploration of its behaviour allowed us to observe simulations of two fen-bog transition patterns.

This study showed that interactions between parameters should be taken into account when evaluating peatland dynamics models. The results of the screening method are useful for model improvement and simplification. Moreover, this method enables the exploration of model processes in detail, thus providing insight into peatland system dynamics.

1.1 Introduction

Northern peatlands accumulate large quantities of organic matter because their net production exceeds their total decomposition. Northern peatlands sequester between 270 and 550 PgC (Gorham, 1991 ; Turunen *et al.*, 2002 ; Yu *et al.*, 2010), and they are thus identified as a major long-term sink of terrestrial carbon at the global scale.

Processes underlying this sequestration ability are manifold and interact with each other. Species growing in northern peatlands are relatively decay resistant and their productivity is naturally limited by cold temperatures, low photosynthetically active radiation and low nutrient availability. Additionally, acidity and permanent saturation of the deeper peat layers account for a slow decomposition rate of the plant-derived organic matter. Recently produced peat layers are in an oxic zone above the water table and decompose more rapidly. Thus water level and peat hydraulic properties are of great importance and influence the overall carbon balance of the peatland. Peat water content and peat saturation also affect the amount of methane released by the peatland. Peat accumulation and decomposition patterns vary depending on different criteria, such as climate conditions, water level, nutrient availability, or vegetation composition.

In global scale models, processes of peatland dynamics and their interactions are often ignored for the sake of simplification, so that northern peatlands are commonly replaced by boreal forest vegetation or tundra (Frolking, Roulet and Lawrence, 2009). Only few modelling studies aim to integrate peatlands and wetlands in global vegetation or carbon models (Kleinen, Brovkin and Schuldt, 2012 ; St-Hilaire *et al.*, 2010 ; Wania, Ross and Prentice, 2009). The challenge resides in the quantification of the carbon balance. Indeed, peatlands sequester carbon through photosynthesis but these wet ecosystems also release large amount of carbon in form of methane. Moreover, the balance between both processes might lead to opposite feedbacks on

climate (Frolking and Roulet, 2007). Identifying the processes of peatland dynamics controlling the balance between sink and source is thus an essential question.

Modelling peat accumulation and peatland development and dynamics was initiated with the model of peat bog growth (Clymo, 1984, 1992). Several models followed Clymo's concepts of accumulation and decomposition (Frolking *et al.*, 2001 ; Heinemeyer *et al.*, 2010 ; Hilbert, Roulet and Moore, 2000 ; Yu *et al.*, 2001a). The Holocene Peat Model (Frolking *et al.*, 2010), which also relies on those accumulation and decomposition concepts, aims at integrating dynamical feedbacks between environmental, hydrological and ecological processes. Several attempts have also been made to represent peatlands dynamics in a 3D model (Borren and Bleuten, 2006 ; Korhola *et al.*, 1996 ; Morris, Baird and Belyea, 2012). In Baird, Morris and Belyea (2012), the new DigiBog model includes a more complex representation of hydrological processes. However, this model needs to be further improved and tested for its reliability in its 3D version (Morris, Baird and Belyea, 2012).

At this time, model evaluation appears to be essential to verify the consistency of processes and to ensure that peatland models adequately represent peatland dynamics. Commonly, evaluation is made by comparing simulation results with field data and is often limited to a small number of sites so that it is difficult to infer their bioclimatological and biogeochemical representativeness. Additionally, observing reasonable results at the end of a simulation does not insure that the processes of peatland dynamics are properly reproduced. Thus, in order to evaluate the functioning of a model, it is important to focus on understanding mechanisms influencing the model results rather than only comparing model results with field data.

Sensitivity analysis aims at identifying the factors or parameters of a model that are responsible for variation in the output. The model is tested with different parameter values, and changes in behaviour associated with parameter changes are observed. Testing all possible conditions and parameter configurations requires a large number

of model runs so that it is rarely feasible for complex models having a large number of parameters. The numerous runs needed take substantial computer time. A variety of sensitivity methods are available (Saltelli *et al.*, 2008). Sampling-based methods rely on the assumption that the uncertainty of an output depends on the uncertainty of the parameters. Each parameter takes a number of different values, and the influence of each parameter on the variance of the output is quantified. The different parameter values taken by the parameters are commonly chosen at random (Monte-Carlo methods) or follow a pseudo-random sampling method (Helton *et al.*, 2006 ; Saltelli *et al.*, 2008).

When the value of only one parameter changes between consecutive simulations, the method is called a 'one-at a time' (OAT) method. This 'local' method determines the influence of the variation of one parameter on the output, while all other parameters remain constant. This allows a quantification of the partial derivative of the output. On the other hand, 'global' sensitivity analyses aim at quantifying the influence of several parameters simultaneously, thereby identifying which combinations of parameters influence the output. In order to limit the number of runs of a sensitivity analysis, it is possible to carry out a screening method, which identifies the most influential parameters with limited computing cost (Morris, 1991 ; Saltelli *et al.*, 2004).

The objective of this study was to evaluate the Holocene Peat Model (Frolking *et al.*, 2010). This model includes several sub-models and interactions between the sub-models, so that the number of parameters is high. An earlier sensitivity experiment with HPM was presented in Frolking *et al.* (2010). In their study, as in other peatland/wetland modelling studies (e.g. Hilbert, Roulet and Moore, 2000 ; Li *et al.*, 2010 ; St-Hilaire *et al.*, 2010 ; Tang *et al.*, 2010 ; Wania, Ross and Prentice, 2009 ; Yu *et al.*, 2001a), only a very limited number of parameters were taken into account in a local sensitivity analysis. We argue that an intuition-driven choice of parameters

carried out by the modeller or the ecologist is not necessarily representative of the model behaviour and might lead to incorrect interpretation of the results. We hypothesize that a low-cost sensitivity method taking into account all the parameters of the model will reveal additional and different results from those obtained after an “intuitive” sensitivity analysis.

In this paper, we propose to compare the sensitivity of the total carbon mass of a peatland simulated by the HPM model derived from two different methods: a ‘classic’ local sensitivity analysis, changing one parameter value at a time and, subsequently, a global sensitivity analysis with the use of the parameter screening approach.

1.2 Model description

1.2.1 General scope

HPM aims to reproduce the temporal development of a peatland in one dimension (vertical) over centuries to millennia, using an annual time step. The model thus simulates the development of a peatland at its centre and delivers a year by year reconstruction of accumulation, decomposition, hydraulic properties and vegetation assemblages. Outputs are peat depth, peat composition, carbon accumulation and water table depth; HPM keeps track of each annual peat cohort. The main mechanisms of HPM are described in the following section; a more detailed description can be found in Frohking *et al.* (2010). HPM, in its original version, is parameterized to represent peatlands located in northern latitudes, registering a fen-bog transition, with negligible tree cover and soil mineral effects. HPM is a semi-empirical model based on laboratory and field data (e.g. decomposition rate of plant litter of different species) as well as on numerical representations (e.g. hydraulic properties derived from known functions, see Frohking *et al.* (2010) for details).

In HPM, besides the site-specific input parameters (e.g., annual potential evapotranspiration), several categories of parameters are used: initialization parameters, curve fitting parameters and descriptive parameters for a total of 127 parameters (Table 1.2). These parameters concern the core equations of the model (e.g. bulk density calculation, peat porosity) but also more ecological descriptions of peat and vegetation (e.g. decay rates, water table depth ranges for productivity).

1.2.2 Main mechanisms of peatland development

1.2.2.1 Vegetation representation

The model is based on the assumption that water table depth influences vegetation composition. This premise takes into account litter properties of each plant functional type and their respective decomposability. HPM includes 12 plant functional types (PFTs) differentiated through their ability to grow in different water table depths and under different conditions of nutrient availability, with the use of peat depth as a proxy for nutrient status (based on Tuittila *et al.* (2007) and Välranta *et al.* (2007)). For example, very wet, minerotrophic species (such as herbaceous species or brown mosses) have an optimal productivity when the water table is shallow and peat height is low, i.e. high nutrient availability. Ombrotrophic hummock species, on the other hand, have an optimal productivity when water table is relatively deep (ca. 20 cm deep) and peat height is greater than ca. 1.5 m. These characteristics are represented with PFT specific parameters, describing the gradient of the optimum NPP (Net Primary Productivity) on each side of the optimal water table depth and optimal peat depth, along with a parameter specifying the belowground fraction of total NPP (Table 1.1). Trees are not yet represented in the model set of PFTs.

1.2.2.2 Water balance

Water balance is expected to play an important role in the system and thus in the model (Belyea and Baird, 2006 ; Waddington *et al.*, 2009). In HPM, the annual water

balance is based on precipitation, evapotranspiration, which is a function of water table depth, and runoff. Three parameters control the runoff: R_0 , a site-specific base rate for an inundated peatland with shallow peat; c_8 , which specifies the rate of increase of runoff with peat height (as a proxy for land slope); and T_0 , influencing runoff through peat effective transmissivity (Table 1.2). The annual net water input resulting from the net water balance calculation is added (subtracted) each year and the water table depth is determined by consideration of peat depth and bulk density.

1.2.2.3 Hydraulic properties

Hydraulic properties of peat (effective transmissivity and water-filled pore space in the unsaturated zone) depend on water table depth and on peat bulk density, and thus, indirectly, on vegetation properties (particularly on decomposition properties). Bulk density calculation includes four parameters (Table 1.2): two site specific parameters – minimum bulk density (ρ_{\min}) and maximum bulk density increase ($\Delta\rho$) – and two general parameters – c_3 and c_4 representing the value at which bulk density has increased half way from minimum to maximum and the steepness of the bulk density transition curve, respectively. The transition from minimum to maximum bulk density is a function of the degree of decomposition of the peat. Consequently, peat layers identified as well-decomposed have a higher bulk density and a lower hydraulic conductivity than fresh peat layers. Bulk density results from different interactions between productivity, accumulation, decomposition and water balance, which are not sufficiently understood to derive the calculation of bulk density from these processes. Bulk density of the peat thus depends on the litter types and their rates of decomposition.

1.2.2.4 Productivity

Productivity in HPM is based on two factors: annual water table depth and peat depth, which is used as a proxy for the accessibility to nutrients. Total productivity

depends on the assemblage of plant functional types (each of which has specific water table depth and peat depth values for optimum productivity and a specific relative productivity in order to represent vegetation composition, see Table 1.1) and on the maximum potential NPP, which is a site specific value (Table 1.2). This value is central in the productivity of HPM, since air temperature is not represented in the current version of the model. Depending on water table depth and peat depth, different PFTs dominate the vegetation assemblage. Peat accumulation thus takes into account NPP and the litter properties of each PFT with respect to its representation in the assemblage.

1.2.2.5 Peat decomposition

Peat decomposes year after year and follows different decomposition rates depending on the PFT (k values in Table 1.1). As a result, the accumulating peat includes a varying portion of decomposed peat stemming from the different PFTs of the former vegetation cover. Note that the influence of peat temperature on decomposition is ignored in the current version of HPM. At the end of each simulated year, a portion of the acrotelm peat moves to the catotelm, the amount depending of the change in water table depth. In HPM, the transition between these compartments is represented by a gradient of anoxia (described by the anoxia scale length, Table 1.2). Decomposition rates differ according to the position of the layer in the peat column. In the unsaturated zone, there is a maximum rate at an optimal water content (W_{opt} , Table 1.2), with the rate declining for drier and wetter peat. At the water table, the decomposition rate multiplier is set to W_{sat} , and below the water table the multiplier declines exponentially, with a scale length of c_2 (Table 1.2).

1.2.3 Calibration and spin-up

Values used for calibration are for the Mer-Bleue bog (Roulet *et al.*, 2007), located in Ontario, for sake of comparison with the previous study (Frolking *et al.*, 2010).

Inputs needed are maximum potential net primary productivity (NPP_{pot}), annual precipitation for the simulation period (P) as well as minimum bulk density (ρ_{min}) and magnitude of the bulk density increase ($\Delta\rho$) expected at the site.

Initialisation is set up by constraining the model to accumulate peat until peat depth reaches a certain level (here 15 cm accumulated peat). During this period, water balance is not dynamic and the water table depth is prescribed (here 7 cm). Once peat accumulations reaches this level, HPM calculates annual water and carbon balances. The water table depth during initialisation is shallow since peat height is limited to small amounts.

1.2.4 Evaluation

Up to now, evaluation of HPM has been achieved by a comparison with paleodata from the Mer-Bleue bog and sensitivity analysis of certain parameters (Frolking *et al.*, 2010) and by a comparison with paleodata from several bogs and fens located in the eastern coast of the Gulf of Bothnia, in Finland (Tuittila *et al.*, 2013). The results generally showed a good agreement with the observations, except for very young peatlands. It is to be noted that the influence of precipitation regime on the simulation was important and that a coarse precipitation reconstruction based on lake levels was used in Frolking *et al.* (2010).

1.3 Methods

For the sake of comparison, we investigated three different methodologies for the sensitivity study. All of them surveyed the response of the model to changes in parameter values. In this paper, is defined as a parameter, any value that can cause a variation in the output of the model. The first two sets of experiments were local sensitivity analyses. The results of the first local sensitivity analysis can be compared

to the results of Frolking *et al.* (2010). The second set of experiments aimed at comparing three different local sensitivity analyses with different parameter settings: three precipitation scenarios were performed. The method used for the third set of experiments was a screening method enabling the exploration of multiple parameter settings.

1.3.1 Output of interest

HPM generates several outputs, including peat accumulation, peat height, peat composition, water table depth. In this paper, we focused on one output: the total quantity of carbon sequestered (in kg) after 5000 years simulation. Carbon sequestration processes are one of the most important issues bringing peatlands into global change science. Carbon mass is the net result of productivity and decomposition of the peat. Since it results from different interactions, this output is a single measure of aggregate model behaviour that is comparable to observations.

1.3.2 Local sensitivity analysis

Local sensitivity analysis owes its wide use to its great simplicity. The method is characterized as 'local' because a very limited area of the model space is represented.

1.3.2.1 'One-factor-at-a-time' analysis

Within all possible combinations of parameters, each of which can vary over a range, only one combination is represented and only values of one parameter vary in the 'one-factor-at a time' or 'one-at a time' design (OAT) method, while all others remain constant. This method, chosen in Frolking *et al.* (2010), gives an insight into the impact of changing parameter values on the output.

For sake of comparison with the subsequent sets of experiments, we performed here a similar analysis to the one performed by Frolking *et al.* (2010). The chosen

parameters were based on their study, where 11 parameters were analyzed. These parameters were chosen because they intuitively represent important elements of the model. We arbitrarily chose 4 of those parameters – maximum potential NPP (NPP_{pot}), minimum bulk density (ρ_{min}), anoxia scale length (c_2), and annual precipitation (P) – and examined their influence on the total carbon mass after 5000 simulation years (see Table 1.2 for details). In Frolking *et al.* (2010), parameters were varied using 2 to 5 different values. However, a wide range of values needs to be analyzed for each parameter in order to observe possible shifts in the model response. Seven values for each parameter were chosen from a range (Table 1.2) that appeared realistic to the modeller / ecologist to represent the potential natural variability of the parameter. The total computing cost of the analysis was 28 model runs.

1.3.2.2 Two-parameter combinations

This second approach is very similar to the previous one and aimed at identifying the influence of the combination of two parameters on the output. Thus, here again, only a limited portion of the model space was explored. Three combinations of precipitation and another parameter (maximum potential NPP, minimum bulk density or anoxia scale length) were chosen, and for each combination two additional precipitation scenarios were performed. Precipitation was chosen because it gives a simple representation of a change in environmental conditions. Overall, for this exercise, three precipitation values were used: one equivalent to the ‘Mer Bleue simulation’ (0.9 m yr^{-1}), a wetter and a dryer scenario (0.7 and 1.1 m yr^{-1}). This exercise shows how the sensitivity analysis might be affected by interaction effects between parameters.

1.3.3 Screening method

Given the large number of parameters in HPM, it would be helpful to identify the parameters that have the greatest influence on the model output, as well as those that

are not influential, in order to improve the model (e.g. by removing the non-influential parameters) and to conduct studies toward specific regions of model parameter space. This can be achieved with help of a screening method. The chosen screening method was the elementary effects method from Morris (1991) as it provides an estimate of importance of each parameter and yields the identification of non-influential parameters. We chose not to group the PFT-related parameters in order to highlight the differences among them, even if they might individually have a limited influence (each of them influencing only a small portion of the vegetation or peat composition).

In contrast to an OAT analysis, this method is composed of a series of randomised OAT experiments, i.e. each parameter varies one after the other. The accumulation of randomly chosen OAT (i.e. local) experiments allows the exploration of the whole model space at relatively low computer cost. For each parameter, a limited number of values were chosen within a prescribed range and distribution. When the distribution of the parameter was unknown, a uniform distribution was assumed (Table 1.2). The number of model simulations (N) needed for this experiment is calculated as follows:

$$N = r(k + 1) \quad (1)$$

where r is the number of trajectories (i.e. number of randomly sampled points for each parameter) and k the number of model parameters (Morris, 1991). Here, 127 parameters were taken into account and the number of trajectories was set to 10. Thus, 1280 model executions were needed. Each parameter was represented by 8 levels (corresponding to quantiles of the parameter distribution).

1.3.3.1 Sampling

The choice of the sampling method is an important step for the sensitivity analysis, since it does have a strong influence on the results of the experiment (Beven, 2009 ; Saltelli *et al.*, 2008). We chose a sample that represents the model space in its best

possible way without requiring too many values (Beven, 2009). The classic Monte-Carlo method requires choosing a lot of parameter values to efficiently represent the model space, whereas a quasi-random sample allows a better representation with a limited number of discrete values. However, the variable spaces are not homogeneously represented and there are gaps in the sample distribution. As a result, for a given parameter, some values might occur very often in the sampling while other values might occur rarely and are represented in few simulations only. We used SimLab, version 3.2.6 (Joint Research Centre of the European Commission, 2011), to generate a quasi-random sample.

The experiment was designed so that each simulation had the same initialisation period (i.e. spin-up). In the current setting, the spin-up lasted 8 simulation years. Parameters values changed when the simulation became dynamic, i.e. as soon as the accumulated peat reached 15 cm thickness.

1.3.3.2 Elementary effects (EE)

Sensitivity measures were also calculated with SimLab 3.2.6 (Joint Research Centre of the European Commission, 2011). Elementary effects of a parameter are defined as the ratio between the output response change and the difference in parameter value. A series of elementary effects was obtained for each parameter. The sensitivity measures μ and σ describe the mean and standard deviation of the distribution of the elementary effects of each parameter. The μ value describes the overall influence of a parameter on the output, whereas σ assesses the influence on the output of interactions and nonlinearity associated with this parameter. Parameters having large μ and σ values have a stronger impact on the variance of the output than parameters having μ and σ values close to zero.

1.4 Results

1.4.1 Local sensitivity analysis

1.4.1.1 One-at-a-time analysis

Relationships between parameter values and the output, i.e. the total mass of carbon accumulated during 5000 simulation years, are presented in Figure 1.1. As the value of NPP_{pot} increased, the total amount of carbon stored in the peatland after 5000 years of simulation increased, as expected (Figure 1.1a, filled circles). The shape of the curve, however, was nonlinear. When NPP_{pot} lay between 0.5 and 2 $kg\ m^{-2}\cdot yr^{-1}$, the slope of the response curve reached its maximum. Thus, the total mass of carbon was more sensitive to NPP_{pot} when its values are low. The results also suggest that the effect of increasing NPP_{pot} was limited after a certain level: in the current configuration of the model, beyond 3 $kg\ m^{-2}\cdot yr^{-1}$ other processes limited carbon mass. Overall the influence of NPP_{pot} was important since the carbon mass varied nearly by a factor of 10 for values between 0.5 and 2 $kg\ m^{-2}\cdot yr^{-1}$.

An increase in ρ_{min} was expected to have a positive influence on the total carbon mass since it contributes to decreased peat porosity and thus slows the rate of peat height growth for a given mass increment. This could cause the water table to be closer to the peat surface, limiting decomposition (Figure 1.1b, filled circles). Indeed, the results showed an increase in total carbon mass. However, the relationship between this parameter and total carbon mass was not linear. The graph suggests that minimum bulk density had a limited influence on total carbon mass since a large increase in its value only led to a limited variation of the output (factor of 1.5).

A different behaviour can be seen in the graph relating the anoxia scale length parameter to total carbon mass (Figure 1.1c, filled circles). As in Froelking *et al.* (2010) a decrease in total carbon mass with an increase in anoxia scale length was

expected. This expectation came true in our experiment when anoxia scale length was longer than 0.5 m but not when values lay between 0.1 and 0.5 m. There was thus an optimal value for which the total carbon mass was maximal. At first, this result seems questionable but a further investigation provided a logical explanation for this behaviour. A short anoxia scale length favoured high peat accumulation. This high peat accumulation led to a drop in the water table depth and thus to a larger aerobic zone and more decomposition, which slowed accumulation. Total carbon accumulation was thus limited. In turn, when the anoxia scale was longer, the water table depth remained at an intermediate level for a longer period of time; this limited decomposition and allowed a greater peat accumulation. At the end of the simulation, more carbon had accumulated and the water table depth did not end up very deep. However, as the anoxia scale length became greater than 0.5 m, decomposition increased in the saturated zone, so water table depth had a diminished influence on total decomposition. This led to a decrease in total carbon mass. Overall, anoxia scale length had an impact similar to the one of minimum bulk density on total carbon mass, allowing carbon mass to double when the value of anoxia scale length was optimal.

A change in annual precipitation (with constant precipitation throughout the simulation) could lead to different responses of the output (Figure 1.1d). These responses did not follow the modeller's intuition. In order to understand the response of the model to precipitation increase it is important to note that the potential evapotranspiration parameter (which is site specific) remained constant to a level of 0.55 m yr^{-1} . Thus the different precipitation regimes applied to the model actually acted as different precipitation-evapotranspiration ratios (there is no run-on in the simulations). Figure 1.1d shows that for $P < 0.55 \text{ m yr}^{-1}$ (the potential evapotranspiration level), very little carbon accumulated. Above this level though, total carbon mass increased as precipitation increased. The slope of this increase was high and precipitation had a strong influence on total carbon mass. However, for an

amount of precipitation of 1.2 m yr^{-1} , total carbon mass after 5000 years of simulation was significantly smaller than for lower precipitation regimes. Again, this result was not anticipated and corresponds to a feedback effect in the model. Indeed, with 1.2 m yr^{-1} of precipitation, the system obtained 0.65 m water in excess each year. In the first fifty simulation years, the simulated water table was close to the surface or even slightly above the surface. This allowed a close-to-optimum productivity of minerotrophic PFTs and a very low decomposition rate. Even though precipitation remained constant, high peat accumulation was followed by a rapid water table drop down, and an increase in decomposition causing a slower carbon accumulation. Overall, a modification of the precipitation regime induced a very wide range of responses in total carbon mass (between essentially zero and 392 kg) and in different directions.

1.4.1.2 Two-parameter combinations

A second part of the local sensitivity analysis was carried out using the same parameters, with two of them varying simultaneously. This allowed observing interactions between two parameters and their common influence on the output. To illustrate this phenomenon, we chose three different precipitation scenarios that vary simultaneously with each of the three parameters studied in the previous section (maximum potential NPP, minimum bulk density and anoxia scale length).

Figure 1.1a shows the plots of two other series of simulations with varying NPP_{pot} . When the precipitation regime was low (here 0.7 m yr^{-1} , represented by hollow squares), the shape drawn was similar to the results with 0.9 m yr^{-1} of precipitation (filled circles). However, total carbon mass varied with less amplitude, i.e. the parameter had less influence on total carbon mass than when $P = 0.9 \text{ m yr}^{-1}$. The response of total carbon mass when variations in NPP_{pot} were associated with higher precipitation (1.1 m yr^{-1} , represented by hollow triangles) differed from the other responses. When NPP_{pot} increased from 0.5 to $2 \text{ kg m}^{-2} \text{ yr}^{-1}$, total carbon mass

increased rapidly. With a further increase in NPP_{pot} however, total carbon mass decreased. This pattern resembles Figure 1.1d where only precipitation varied. When NPP_{pot} was greater than $2 \text{ kg m}^{-2} \text{ yr}^{-1}$ total carbon mass was no longer limited by this parameter but by the amount of precipitation. These results shows that when a second parameter varied (here precipitation), the responses of the output to variation in another parameter could be manifold. Thus it is difficult to assess the influence of a parameter on an output with the local OAT method.

Changes in ρ_{min} caused a slow increase in total carbon mass when precipitation regime was 0.9 m yr^{-1} (filled circles). Changes in precipitation regimes (Figure 1.1b) generated different responses of the output. With a precipitation regime of 0.7 m yr^{-1} (hollow squares), total carbon mass was optimal for ρ_{min} values located in the middle of the range. Indeed, bulk density influenced the variation of the water table depth. If minimum bulk density and precipitation were low, the water table, as well as the peat accumulation, dropped rapidly and carbon accumulation was low. On the other hand, if ρ_{min} was high and precipitation was low, peat accumulation was very limited and carbon accumulation remained low. Overall, ρ_{min} showed low influence on the output in this case. When precipitation was higher than the nominal value (in the 1.1 m yr^{-1} scenario represented by hollow triangles), total carbon mass was more influenced by ρ_{min} . Total carbon mass varied between 150 and more than 450 kg depending on the ρ_{min} value. Interestingly, when ρ_{min} was set at 20 kg m^{-3} , total carbon mass was higher when precipitation equalled 0.9 m yr^{-1} than when precipitation was set to 1.1 m yr^{-1} . Actually, at the beginning of the simulation, peat accumulation was higher when precipitation was higher because water table depth was at the surface and enhanced productivity. Nevertheless, high productivity here again caused a rapid drop in water table leading to less production and more decomposition. This feedback effect did not occur when precipitation was lower than 1.1 m yr^{-1} . In addition, there was a feedback effect between bulk density and water table depth. When bulk density was high, porosity was low and an excess in precipitation led the water table depth at the

surface of the peatland for a long time and, as a result, productivity increased. For this reason total carbon mass was higher when precipitation was higher.

The interaction between anoxia scale length and precipitation was more straightforward. The general pattern of an increase in carbon mass when precipitation increases happened as expected here. However, it was noticeable that the optimum pattern observed when precipitation was 0.9 m yr^{-1} (filled circles) was amplified for precipitation of 1.1 m yr^{-1} (hollow triangles). A greater amount of water available to system favoured higher water tables and thus slower decomposition. Inversely, this pattern did not appear when precipitation was 0.7 m yr^{-1} (hollow squares), because water tables were lower and high decomposition in the thicker oxic zone limited carbon accumulation.

1.4.2 Morris' screening method

Similarly to the previous diagrams, Figure 1.2 represents the relationship between the different parameters and total carbon mass. In the first panel (Figure 1.2a), a general increasing trend was observed. Here again, as NPP_{pot} increased, total carbon mass got higher. However, several simulations showed small carbon mass when NPP_{pot} was high. In those cases, other parameters constrained carbon accumulation. Another interesting pattern of this panel is that response ranges of total mass generally increased when NPP_{pot} increased. Moreover, the mean response of total carbon mass essentially stopped increasing when NPP_{pot} was greater than $3 \text{ kg m}^{-2} \text{ yr}^{-1}$. Above this level, NPP_{pot} was no longer a limiting factor, while below this level NPP_{pot} could limit total peat accumulation.

The relationship between ρ_{min} and total carbon mass showed a generally increasing trend (Figure 1.2b). Very low values of ρ_{min} limited carbon mass and very high values, on the contrary, allowed the accumulation of very high carbon masses. However, for a ρ_{min} value of 60 kg m^{-3} , we noted that the total carbon mass remained

low compared to the results of the previous experiment (compare Figure 1.1b and 1.2b). This is due to the random sampling distribution, which did not include the combination of parameters chosen in the first experiment.

The relationship between anoxia scale length and total carbon mass (Figure 1.2c) did not show any clear trend but showed wide response ranges for specific values (e.g. 0.1 or 1.2 m). Thus, in those cases, anoxia scale length was not a limiting factor. These values described very different systems where anoxia scale length and water table depth interact (see section 4.1 for details on the interaction). Therefore, the wide range of response for one anoxia scale length could be linked to the amount of water available to the system (depending itself on precipitation and evapotranspiration values).

The response pattern of total carbon mass to precipitation was very different from what was observed in Figure 1.1, where higher precipitation tended to increase total carbon mass. Here, on Figure 1.2d, increasing precipitation caused an overall decrease in carbon mass. It is important to remember that in the current experiment, all parameters may take varying values. Thus evapotranspiration might have compensated for precipitation or, on the contrary, might have been so limited that the simulated peatland was actually flooded. A very wide range of carbon masses were obtained from simulations with very low precipitation (ca. 0.2 m yr^{-1}). These results were partly due to an artefact of the sampling method. When looking in more detail at the way samples (i.e. combination of parameters) were distributed, we observed that a very large number of the simulations with 0.2 m yr^{-1} of precipitation had a precipitation-evaporation rate close to 1 and potential maximum NPP around $5 \text{ kg m}^2 \cdot \text{yr}^{-1}$. This led to several 'optimal simulations' with very high carbon masses and represent extreme conditions for a northern peatland. However, this result highlights the non-intuitive fact that various responses can arise with low precipitation values. On the other hand, Figure 1.2d also shows that high precipitation

regimes constrained carbon mass. The balance of water availability had a strong influence on the result, and both high and low precipitation could limit carbon mass.

1.4.2.1 Morris Elementary Effects (EE)

Figure 1.3 presents the Morris elementary effects for the total carbon mass after 5000 simulation years. μ and σ , respectively, describe the mean and standard deviation of the distribution of the elementary effects of each of the 127 parameters. μ gives an insight of the overall influence of a parameter on the total carbon mass. σ is an indicator of nonlinearity and interactions. Parameters showing large μ values but low σ have a direct influence on the output, whereas parameters showing both large μ and σ values have a significant effect involving interactions or nonlinearity. On the contrary, when μ and σ values are low, the associated parameters have no significant effect on the output. Here NPP_{pot} and the decomposition rate multiplier at the water table (W_{sat}) both had large μ values, indicating that they had a particularly strong influence on total carbon mass. However, W_{sat} 's μ value was negative. This parameter thus had a negative influence on total carbon mass: when W_{sat} value increased, total carbon mass decreased. W_{sat} is a parameter linked to the calculation of the decomposition rate, so that this result was not unexpected. NPP_{pot} , on the other hand, had a positive influence on total carbon mass. This result suggests that the model would benefit from an accurate representation of the decomposition factor and of potential maximum NPP.

Several parameters having lower μ values could be identified as groups of parameters associated to common processes. The evapotranspiration factor ET_f , the water table depth threshold for minimal evapotranspiration z_1 , the runoff increase with peat height c_8 , the annual runoff adjustment factor R_0 , and the minimum relative transmissivity T_0 are parameters related to the water outflow in the system by the mean of runoff or evapotranspiration (triangles in Figure 1.3). With the exception of z_1 showing a slightly positive influence, all of these parameters had a negative influence on total

carbon mass. They affected the water balance and therefore favoured deeper water table depths, which in turn, favoured decomposition. However, evapotranspiration, and even more so runoff, depend on site specific conditions and are usually poorly described by field data.

A second group of parameters included ρ_{\min} , maximum potential increase in bulk density ($\Delta\rho$) and another parameter affecting the shape of the bulk density curve (c_3 , squares in Figure 1.3). μ values for these parameters were relatively low (especially for ρ_{\min} and c_3) indicating that the overall influence of the parameters was limited. However their σ values were relatively high. Their influence on total carbon mass might thus be related to interactions between parameters or associated to nonlinear behaviours in the model.

A third group of PFT specific parameters was identified, including h_{PD7}^{opt} (peat depth for optimal productivity of lawn *Sphagnum*), $NPP_{\text{rel}7}$ and $NPP_{\text{rel}5}$ (maximum relative NPP of lawn *Sphagnum* and brown mosses, hollow circles in Figure 1.3). These parameters are related to major changes in the system. The conditions under which PFTs occurred influenced the equilibrium of the system by controlling the accumulation and decomposition rate of the peat layers.

Precipitation (P) was expected to have a strong impact on the result. Even though P appears influential in Figure 1.3, it could not be considered as one of the most influential parameter because its μ and σ values were low compared to the groups of influential parameters.

It is also important to note that many parameters had limited influence on the variance of the model outputs. Among them were parameters describing: root input, the above-ground fraction of NPP, and the water level for optimal productivity of each PFT (with exception of σ_{WT4}). Constant values could thus be attributed to these

parameters, with minimal impact on the results when HPM is used to simulate carbon mass.

Figure 1.3 also shows a large variability in σ values. Parameters with high σ values have high interactions with other parameters or have a nonlinear influence on total carbon mass. Thus, it is difficult to summarize, in a simple way, how those parameters influenced the output.

1.5 Discussion

Sensitivity analysis explores the manner in which parameters influence the results of a simulation. However, when working with a complex model taking feedbacks into account, and depending on the sensitivity analysis method chosen, the results can be extremely diverse and thus their interpretation uncertain.

For example, the results of the local OAT experiments on selected parameters show that some parameters have more influence than others on the output and that the response of the model is nonlinear and cannot always be intuitively foreseen. When using this method, local optima and threshold effects might show up under specific circumstances but are not necessarily representative of the model behaviour. Among the tested parameters, precipitation and NPP_{pot} had the strongest impact on total carbon mass.

However, the relationship between carbon mass and the different parameters, presented in the two-parameter combinations sets of experiments, were obviously different from the patterns observed in the OAT experiments. Looking at a large variety of possible combinations of parameters gives more insight into the behaviour of the model, but also introduces extreme conditions scenarios or parameter combinations. The amplitude of the responses in carbon mass for a single parameter

value indicated that interactions between parameters play an important role in model dynamics and thus on the model results. As an example, very high values of carbon mass seemed to be caused by the combination of high NPP_{pot} , low precipitation, high ρ_{min} and $\Delta\rho$, as well as an optimal anoxia scale length, though this combination might be rare in nature. Though sampling is expected not to be homogeneously distributed in the screening experiment, this can also lead to a shift in the general trends of the results because of the large number of simulations having extreme conditions, as this is the case in the precipitation experiment (Figure 1.2d, with 0.2m yr^{-1} precipitation, a precipitation-evaporation rate close to 1 and potential maximum NPP around $5\text{ kg m}^{-2}\text{ yr}^{-1}$).

A screening method is helpful to perform a first exploration of the model behaviour with limited computational costs, particularly when the number of parameters is high. This method gives a first approximation of the sensitivity of the model to its parameters. Though it also gives an insight into the degree of interaction in which the parameters are involved, it does not allow any further conclusions on how these interactions operate. When the parameter ranks do not match with the modeller's intuition, as in our case, it is recommended to further explore the model behaviour by the means of a global sensitivity analysis allowing the identification of the influence of parameter interactions on the outputs. This is the purpose of a subsequent study analysing the role of interactions on carbon accumulation in HPM by the calculation of Sobol' indices (Quillet, Garneau and Froking, *in press*).

The elementary effects highlighted the role of several parameters that were not considered as important (e.g. W_{sat} , c_8 , z_1 , ET_f , T_0 , etc.). The influential parameters should be better constrained in order to improve the model. The potential maximum NPP (expressed with NPP_{pot}) formulation could, for example, include a more detailed description of temperature and sunlight, which, along with water availability, influence NPP (Churkina and Running, 1998 ; Nemani *et al.*, 2003). Nevertheless,

this model component is site specific and needs to be estimated from global datasets or data from the studied site.

The same constraints apply to the representation of evapotranspiration (z_1 , ET_f) or runoff (c_8 , T_0 , R_0). Whereas an evapotranspiration estimate could be obtained from global data sets, the water table depth threshold for maximal evapotranspiration is likely to be site-specific. Regarding runoff, R_0 could be roughly estimated from a global land surface model, but minimum profile relative transmissivity, for example, requires on-site measurements to be better constrained.

For some parameters, however, improvement would not be straightforward. For example, improving the way W_{sat} (decomposition rate multiplier at annual mean water table depth) or c_8 (increase in runoff with peat height) are represented in the model would be challenging as it would require more depth-resolved knowledge and data on decomposition and ecohydrological processes in peat.

Overall, an improvement of the HPM NPP formulation is expected to greatly reduce uncertainty in the model results. Moreover, linking HPM to global climate or earth system models would lead to a linkage between climatic variables and peatland productivity. Thus, we suggest enhancing the representation of productivity by including several climatic variables such as temperature or sunlight, which are available in global models. Likewise, baseline evapotranspiration and runoff estimates could also be taken from the global model outputs. Regarding decomposition, one could use simulated soil temperature from global models to improve its representation. Some hydraulic properties or runoff parameters, however, remain a source of uncertainty, suggesting that further research is needed in these areas.

The different experiments also point out that a complex model accounting for interactions between the sub-models has nonlinear behaviour and its simulations can

migrate from one equilibrium to another depending on the parameter setting. The reaction of the model to a difference in precipitation or in anoxia scale length is one example of this behaviour. Both parameters interact with water table depth so that two different equilibria are possible. In one case, peat accumulates rapidly after initiation. However, this rapid accumulation induces a water table decline, which is responsible for the following decrease in accumulation and increase in decomposition. As a result, the simulation final peat profile has a thick layer of minerotrophic species at the base of the peat column followed by a sharp transition to an ombrotrophic PFTs-dominated assemblage – an abrupt fen-bog transition. Once the ombrotrophic vegetation is in place, low accumulation lasts until the end of the simulation. In a second case, the simulation begins with a slow peat accumulation and the water table deepens slowly. The water table depth stays within ranges where plant productivity is maintained. Peat accumulation remains slow until the end of the simulation. In this case, ombrotrophic species NPP (and especially lawn *Sphagnum*) arise in more gradually – a gradual fen-bog transition. Overall, the total mass of accumulated carbon can be equivalent in both cases, depending on the parameter setting. HPM's processes and interactions are able to produce different scenarios of peatland development and dynamics that are plausible in nature. This suggests that, under specific conditions, (e.g. high water availability, low porosity of the peat) the minerotrophic phase (or fen phase) can be very wet and productive or, on the contrary, relatively dry and influenced by *Sphagnum* species. An additional sensitivity analysis accounting for interactions between parameters, needed to explore the causes of this behaviour, is presented in Quillet, Garneau and Froelking (*in press*). Yet, observations corroborate the empirical results of Hughes and Dumayne-Peaty (2002) and Hughes and Barber (2004). Their studies focused on the paleoecological analysis of several raised bogs in Ireland and in UK during the Holocene. Both studies aimed at identifying the different pathways of fen-bog transition in different sites (Hughes and Barber, 2004) and within a site (Hughes and Dumayne-Peaty, 2002). They showed that similar climatic conditions can lead to at least two different

pathways to ombrotrophy: one wet and a drier one relying on the presence of *Sphagnum* species. Moreover, our experiment results concur with Hughes and Dumayne-Peaty's statement that both allogenic and autogenic processes can control fen-bog transition patterns.

Overall, the screening method allowed, by the exploration of different model responses, the assessment of the peatland processes dynamics, that cannot be achieved by a local sensitivity analysis nor by the comparison between results and observations.

In general, if the role of some processes in the development of peatlands is counterintuitive or unknown, some processes may not be incorporated into a model, e.g., the a priori idea that they will not be important, but they may indeed have a significant influence (direct or indirect) on the system. Not representing them might be an important omission. In HPM, several processes are ignored, such as microtopography, trees or permafrost, though these processes might have a greater influence on the system than expected. This kind of limitations represents an additional source of uncertainty that cannot be assessed. It is thus advised to take these limitations into account when drawing conclusions on the dynamic model results. Moreover, results showed that the evaluation methodology impacts the assessment of model outputs from dynamic models. Nonlinearity, interactions and feedbacks between processes impact outputs in an unanticipated manner. We thus suggest that system dynamics models evaluation should always take all parameters into account in order to avoid misinterpretation of the influence of certain parameters.

1.6 Conclusions

With help of three different sensitivity experiments, we aimed at identifying the influence of the a priori choice of parameters when evaluating a model. We observed

that the conclusions drawn by the different methods are very different and moreover that it is not advised to draw any general conclusion from a local OAT experiment because the model space represented is very limited. This limitation raises the question of how the modeled parameters and processes are chosen.

The screening method appears to be efficient to investigate system behaviour at relatively low computational costs. This method leads the model toward its limits by imposing extreme scenarios. Nonetheless, we observed that response patterns can follow field data. It gives us confidence that HPM represents processes of carbon mass accumulation in a plausible manner. For the purpose of its integration in global climate models, the results showed that, in particular, parameters controlling decomposition, water balance and hydraulic properties strongly influence carbon mass accumulation and should be carefully incorporated into a global version. We think it is likely that globally generalizable rules of peat decomposition peat hydraulic properties can be developed, but that water balance will always be strongly dependent on the local setting.

The exploration of different scenarios performed here also highlighted the potentiality of the model to arrive at different equilibria. Different minerotrophic phase and fen-bog transitions pathways were identified, however both led to ombrotrophic raised bogs after five millennia. HPM thus is an efficient tool for examination of processes dynamics of northern peatlands.

Moreover, the calculation of the elementary effects allowed us to identify the parameters that have a strong influence on the total carbon mass. This information is important for further improvement and simplification of the model. These results also indicate that some parameters strongly interact with each other; it would thus be useful to further investigate the interactions between parameters to capture the behaviour of the model.

Acknowledgments

The authors are grateful to the anonymous reviewers for their constructive comments, which helped improve this manuscript. AQ was supported by funds from the Canadian Foundation for Climate and Atmospheric Sciences, by funds supporting the Chaire Déclique at GEOTOP-UQAM (MG) and by NSERC (Natural Sciences and Engineering Research Council of Canada) discover grant (CP). SF and JT were supported by NSF grants ATM-0628399 and ARC-1021300.

References

- Baird, A. J., P. J. Morris and L. R. Belyea. 2012. «The DigiBog peatland development model 1: rationale, conceptual model, and hydrological basis». *Ecohydrology*, vol. 5, no 3, p. 242-255.
- Belyea, L. R., and A. J. Baird. 2006. «Beyond "the limits to peat bog growth": Cross-scale feedback in peatland development». *Ecological Monographs*, vol. 76, no 3, p. 299-322.
- Beven, K. J. 2009. *Environmental Modelling: An Uncertain Future?* Abingdon, England: Routledge, 310 p.
- Borren, W., and W. Bleuten. 2006. «Simulating Holocene carbon accumulation in a western Siberian watershed mire using a three-dimensional dynamic modeling approach». *Water Resources Research*, vol. 42, no 12.
- Churkina, G., and S. W. Running. 1998. «Contrasting climatic controls on the estimated productivity of global terrestrial biomes». *Ecosystems*, vol. 1, no 2, p. 206-215.
- Clymo, R. S. 1984. «*Sphagnum*-dominated peat bog: a naturally acid ecosystem». *Ecological effects of deposited sulphur and nitrogen compounds. Discussion meeting, London, 1983*, p. 487-499.
- , 1992. «Models of peat growth». *Suo*, vol. 43, no 4-5, p. 127-136.
- Frolking, S., and N. T. Roulet. 2007. «Holocene radiative forcing impact of northern peatland carbon accumulation and methane emissions». *Global Change Biology*, vol. 13, no 5, p. 1079-1088.

- Frolking, S., N. T. Roulet and D. Lawrence. 2009. «Issues related to incorporating northern peatlands into global climate models». In Carbon cycling in northern peatlands, A. J. Baird, L. R. Belyea, X. Comas, A.S. Reeve et L. D Slater, p. 19-35. Washington : American Geophysical Union.
- Frolking, S., N. T. Roulet, T. R. Moore, P. J. H. Richard, M. Lavoie and S. D. Muller. 2001. «Modeling northern peatland decomposition and peat accumulation». *Ecosystems*, vol. 4, no spring, p. 479-498.
- Frolking, S., N. T. Roulet, E. Tuittila, J. L. Bubier, A. Quillet, J. Talbot and P. J. H. Richard. 2010. «A new model of Holocene peatland net primary production, decomposition, water balance, and peat accumulation». *Earth System Dynamics*, vol. 1, no 1, p. 1-21.
- Gorham, E. 1991. «Northern peatlands: role in the carbon cycle and probable response to climatic warming». *Ecological applications*, vol. 1, no 2, p. 182-195.
- Heinemeyer, A., S. Croft, M. H. Garnett, E. Gloor, J. Holden, M. R. Lomas and P. Ineson. 2010. «The MILLENNIA peat cohort model: Predicting past, present and future soil carbon budgets and fluxes under changing climates in peatlands». *Climate Research*, vol. 45, no 1, p. 207-226.
- Helton, J. C., J. D. Johnson, C. J. Sallaberry and C. B. Storlie. 2006. «Survey of sampling-based methods for uncertainty and sensitivity analysis». *Reliability Engineering and System Safety*, vol. 91, no 10-11, p. 1175-1209.
- Hilbert, D. W., N. T. Roulet and T. R. Moore. 2000. «Modelling and Analysis of Peatlands as Dynamical Systems». *Journal of Ecology*, vol. 88, no 2, p. 230-242.
- Hughes, P. D. M., and K. E. Barber. 2004. «Contrasting pathways to ombrotrophy in three raised bogs from Ireland and Cumbria, England». *The Holocene*, vol. 14, no 1, p. 65-77.
- Hughes, P. D. M., and L. Dumayne-Peaty. 2002. «Testing theories of mire development using multiple successions at Crymlyn Bog, West Glamorgan, South Wales, UK». *Journal of Ecology*, vol. 90, no 3, p. 456-471.
- Joint Research Centre of the European Commission (2011). SimLab: Software package for uncertainty and sensitivity analysis: Downloadable for free at: <http://simlab.jrc.ec.europa.eu>.

- Kleinen, T., V. Brovkin and R. J. Schuldt. 2012. «A dynamic model of wetland extent and peat accumulation: Results for the Holocene». *Biogeosciences*, vol. 9, no 1, p. 235-248.
- Korhola, A., J. Alm, K. Tolonen, J. Turunen and H. Jungner. 1996. «Three-dimensional reconstruction of carbon accumulation and CH₄ emission during nine millennia in a raised mire». *Journal of Quaternary Science*, vol. 11, no 2, p. 161-165.
- Li, T., Y. Huang, W. Zhang and C. Song. 2010. «CH₄MODwetland: A biogeophysical model for simulating methane emissions from natural wetlands». *Ecological Modelling*, vol. 221, no 4, p. 666-680.
- Morris, M. D. 1991. «Factorial sampling plans for preliminary computational experiments». *Technometrics*, vol. 33, no 2, p. 161-174.
- Morris, P. J., A. J. Baird and L. R. Belyea. 2012. «The DigiBog peatland development model 2: ecohydrological simulations in 2D». *Ecohydrology*, vol. 5, no 3, p. 256-268.
- Nemani, R. R., C. D. Keeling, H. Hashimoto, W. M. Jolly, S. C. Piper, C. J. Tucker, R. B. Myneni and S. W. Running. 2003. «Climate-driven increases in global terrestrial net primary production from 1982 to 1999». *Science*, vol. 300, no 5625, p. 1560-1563.
- Quillet, A., M. Garneau and S. Frolking. in press. «What drives carbon accumulation in peatlands? A global sensitivity analysis of the Holocene Peat Model». *Journal of Geophysical Research G: Biogeosciences*.
- Roulet, N. T., P. M. Lafleur, P. J. H. Richard, T. R. Moore, E. R. Humphreys and J. Bubier. 2007. «Contemporary carbon balance and late Holocene carbon accumulation in a northern peatland». *Global Change Biology*, vol. 13, no 2, p. 397-411.
- Saltelli, A., M. Ratto, T. Andres, F. Campolongo, J. Carboni, D. Gatelli, M. Saisana and S. Tarantola. 2008. *Global sensitivity analysis. The primer*. Chichester, England: John Wiley & Sons Ltd, 292 p.
- Saltelli, A., S. Tarantola, F. Campolongo and M. Ratto. 2004. *Sensitivity analysis in practice: a guide to assessing scientific models*. Chichester, England: John Wiley & Sons Ltd, 219 p.

- St-Hilaire, F., J. Wu, N. T. Roulet, S. Frohking, P. M. Lafleur, E. R. Humphreys and V. Arora. 2010. «McGill wetland model: Evaluation of a peatland carbon simulator developed for global assessments». *Biogeosciences*, vol. 7, no 11, p. 3517-3530.
- Tang, J., Q. Zhuang, R. D. Shannon and J. R. White. 2010. «Quantifying wetland methane emissions with process-based models of different complexities». *Biogeosciences*, vol. 7, no 11, p. 3817-3837.
- Tuittila, E. S., S. Juutinen, S. Frohking, M. Väiranta, A. Laine, A. Miettinen, M.-L. Seväkivi, A. Quillet and P. Merilä. 2013. «Wetland chronosequence as a model of peatland development: Vegetation succession, peat and carbon accumulation». *The Holocene*, vol. 23, p. 23-33.
- Tuittila, E. S., M. Väiranta, J. Laine and A. Korhola. 2007. «Quantifying patterns and controls of mire vegetation succession in a southern boreal bog in Finland using partial ordinations». *Journal of Vegetation Science*, vol. 18, no 6, p. 891-902.
- Turunen, J., E. Tomppo, K. Tolonen and A. Reinikainen. 2002. «Estimating carbon accumulation rates of undrained mires in Finland - application to boreal and subarctic regions». *The Holocene*, vol. 12, no 1, p. 69-80.
- Väiranta, M., A. Korhola, H. Seppä, E. S. Tuittila, K. Sarmaja-Korjonen, J. Laine and J. Alm. 2007. «High-resolution reconstruction of wetness dynamics in a southern boreal raised bog, Finland, during the late Holocene: A quantitative approach». *The Holocene*, vol. 17, no 8, p. 1093-1107.
- Waddington, J. M., W. L. Quinton, J. S. Price and P. M. Lafleur. 2009. «Advances in canadian peatland hydrology, 2003-2007». *Canadian Water Resources Journal*, vol. 34, no 2, p. 139-148.
- Wania, R., L. Ross and I. C. Prentice. 2009. «Integrating peatlands and permafrost into a dynamic global vegetation model: 1. Evaluation and sensitivity of physical land surface processes». *Global Biogeochemical Cycles*, vol. 23, no 3, p. GB3014.
- Yu, Z., I. D. Campbell, D. H. Vitt and M. J. Apps. 2001. «Modelling long-term peatland dynamics. I. Concepts, review, and proposed design». *Ecological Modelling*, vol. 145, no 2-3, p. 197-210.
- Yu, Z., J. Loisel, D. P. Brosseau, D. W. Beilman and S. J. Hunt. 2010. «Global peatland dynamics since the Last Glacial Maximum». *Geophysical Research Letters*, vol. 37, no 13, p. L13402.

Table 1.1: Nominal values of plant functional types (PFTs), after Frohking et al. (2010)

| PFT | PFT ID | $Z^{\text{opt}}_{\text{WTI}}$ | σ^-_{WTI} | σ^+_{WTI} | $h^{\text{opt}}_{\text{PDI}}$ | σ^-_{PDI} | σ^+_{PDI} | NPP_{rel} | AG_{frac} | k_0 |
|-------------------------|--------|-------------------------------|-------------------------|-------------------------|-------------------------------|-------------------------|-------------------------|---------------------------|---------------------------|--------------------|
| | [-] | [m] | [m] | [m] | [m] | [m] | [m] | [-] | [-] | [y ⁻¹] |
| Grass | 1 | 0.40 | 0.40 | 0.40 | 0.01 | 1.00 | 1.00 | 0.75 | 0.50 | 0.20 |
| Minerotrophic herb | 2 | 0.10 | 0.30 | 0.30 | 0.30 | 1.00 | 1.00 | 0.75 | 0.50 | 0.30 |
| Minerotrophic sedge | 3 | 0.10 | 0.40 | 0.40 | 0.10 | 2.00 | 2.00 | 1.00 | 0.20 | 0.30 |
| Minerotrophic shrub | 4 | 0.20 | 0.20 | 1.00 | 1.00 | 2.00 | 2.00 | 0.50 | 0.50 | 0.20 |
| Brown moss | 5 | 0.01 | 0.20 | 0.05 | 0.10 | 1.50 | 1.50 | 0.50 | 1.00 | 0.10 |
| Hollow <i>Sphagnum</i> | 6 | 0.01 | 0.20 | 0.05 | 2.00 | 1.00 | 19.00 | 0.50 | 1.00 | 0.10 |
| Lawn <i>Sphagnum</i> | 7 | 0.10 | 0.30 | 0.40 | 2.00 | 1.00 | 19.00 | 0.50 | 1.00 | 0.07 |
| Hummock <i>Sphagnum</i> | 8 | 0.20 | 0.10 | 0.50 | 2.00 | 1.00 | 19.00 | 0.50 | 1.00 | 0.05 |
| Feathermoss | 9 | 0.40 | 0.40 | 0.60 | 4.00 | 6.00 | 19.00 | 0.25 | 1.00 | 0.10 |
| Ombrotrophic herb | 10 | 0.20 | 0.20 | 0.20 | 4.00 | 2.00 | 19.00 | 0.25 | 0.50 | 0.25 |
| Ombrotrophic sedge | 11 | 0.20 | 0.30 | 0.30 | 4.00 | 2.00 | 19.00 | 0.50 | 0.20 | 0.15 |
| Ombrotrophic shrub | 12 | 0.30 | 0.30 | 1.00 | 4.00 | 2.00 | 19.00 | 0.50 | 0.50 | 0.15 |

Table 1.2: Model parameters characteristics and associated range and distribution for the sensitivity analysis

| Parameter description | Abbreviation | Units | Range | | PDF | |
|--|--|--|------------------|-------------------|--------------------|---------|
| | | | Min. | Max. | | |
| Annual precipitation | P | [m yr ⁻¹] | 0.30 | 1.20 | Normal | |
| Factor for annual potential evapotranspiration | ET _f | [-] | 0.10 | 1.00 | Normal | |
| WTD threshold for maximal ET | z ₁ | [m] | 0.01 | 0.40 | Uniform | |
| Factor for WTD threshold for minimal ET | z _r | [m] | 0.04 | 0.69 | Uniform | |
| Potential ET/ Minimal ET | c ₆ | [-] | 1.20 | 1.70 | Uniform | |
| Annual runoff adjustment factor | R ₀ | [m yr ⁻¹] | -0.01 | 0.10 | Uniform | |
| Increase in runoff with peat height | c ₈ | [m ⁻¹] | 0.05 | 0.30 | Uniform | |
| Minimum profile relative transmissivity | T ₀ | [-] | 0.05 | 0.80 | Normal | |
| Maximum potential net primary productivity | NPP _{pot} | [kg m ⁻² yr ⁻¹] | 0.50 | 5.00 | Uniform | |
| Maximum root depth for non-sedge vascular plants | Rt ₁ | [m] | 0.15 | 0.35 | Uniform | |
| Depth to 80% of the sedge roots | Rt ₂ | [m] | 0.20 | 0.40 | Uniform | |
| Maximum root depth for sedges | Rt ₃ | [m] | 1.50 | 2.50 | Uniform | |
| Scale length for the anaerobic effect on decomposition rate | c ₂ | [m] | 0.10 | 2.00 | Uniform | |
| Optimal WFPS for decomposition | W _{opt} | [-] | 0.30 | 0.50 | Uniform | |
| Decomposition rate multiplier at annual mean water table depth | W _{at} | [-] | 0.15 | 0.45 | Uniform | |
| Minimal decomposition rate multiplier | f _{min} | [-] | 0.0001 | 0.01 | Uniform | |
| Minimum litter/peat degree of saturation | W _{min} | [-] | 0.01 | 0.05 | Uniform | |
| Controls litter/peat unsaturated water content function | c ₉ | [-] | 0.35 | 0.65 | Uniform | |
| Controls litter/peat unsaturated water content function | c ₁₀ | [kg m ⁻³] | 10.00 | 30.00 | Uniform | |
| M/M ₀ at which bulk density reaches half of its amplitude | c ₃ | [-] | 0.10 | 0.30 | Uniform | |
| Controls steepness of the bulk density curve | c ₄ | [-] | 0.05 | 0.20 | Uniform | |
| Minimum peat bulk density | ρ _{min} | [kg m ⁻³] | 20.00 | 70.00 | Normal | |
| Maximum potential increase in peat bulk density | Δρ | [kg m ⁻³] | 55.00 | 140.00 | Uniform | |
| Organic matter particle bulk density | ρ _{om} | [kg m ⁻³] | 1000.00 | 1600.00 | Uniform | |
| For each PFT | Peat depth for optimum productivity | h ^{opt} _{PDi} | [m] | 50% ^a | 150% ^a | Normal |
| | Productivity range around the optimum | σ ⁺ _{PDi} | [m] | 50% ^a | 150% ^a | Normal |
| | | σ ⁻ _{PDi} | [m] | 50% ^a | 150% ^a | Normal |
| | Water table depth for optimum productivity | Z ^{opt} _{WTi} | [m] | 75% ^a | 125% ^a | Normal |
| | Productivity range around the optimum | σ ⁺ _{WTi} | [m] | 75% ^a | 125% ^a | Normal |
| | | σ ⁻ _{WTi} | [m] | 75% ^a | 125% ^a | Normal |
| | Relative net primary productivity | NPP _{rel i} | [-] | 50% ^a | 200% ^a | Uniform |
| | Above-ground net primary productivity | AG _{net i} | [-] | 75% ^{ab} | 125% ^{ab} | Uniform |
| Decomposition rates | k _{d j} | [yr ⁻¹] | 75% ^a | 125% ^a | Normal | |

^aof the nominal values, ^bexcept for *Sphagnum* PFTs

N.B: examples of notation for PFT parameters: h^{opt}_{PD1} is peat depth optimum productivity for PFT 1, σ⁺_{WT8} parameter is the productivity range below the optimum for PFT 8

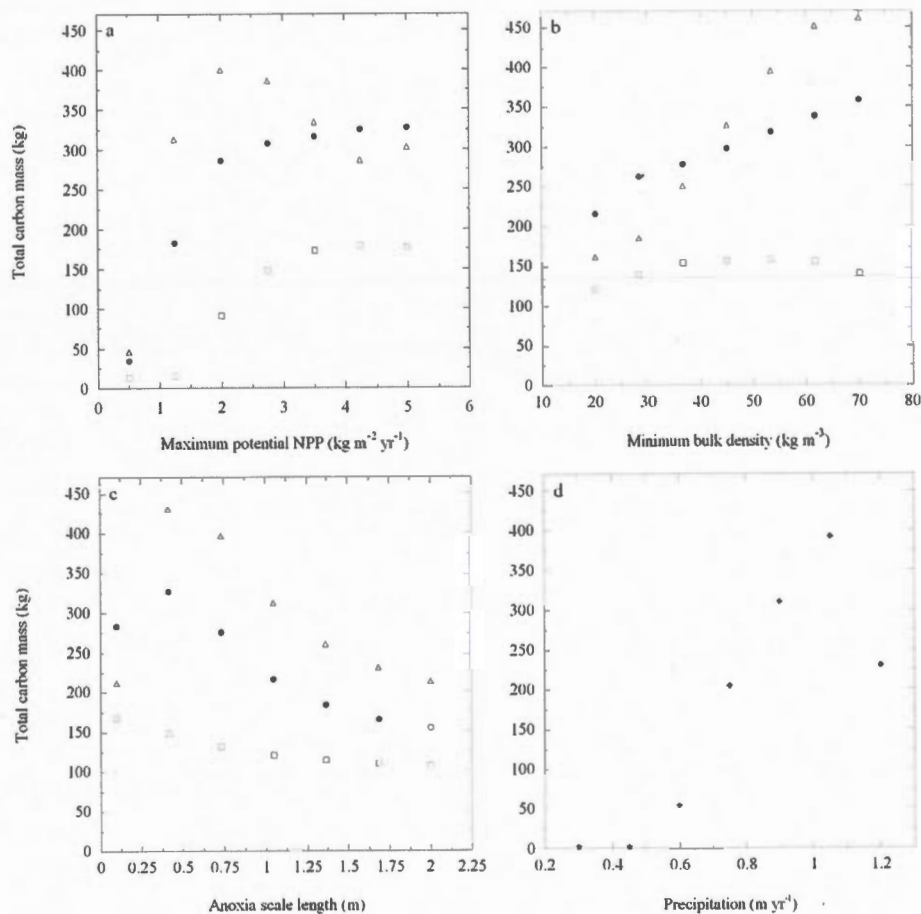


Figure 1.1: Total carbon mass after 5000 simulation years for different parameter values of (a) maximum potential NPP (NPP_{pot}), (b) minimum bulk density (ρ_{min}), (c) anoxia scale length (c_2) and (d) annual precipitation (P). In these one-at-a-time (OAT) sensitivity analyses one parameter changes at a time and all other parameters remain constant at nominal values. In (a)–(c), filled circles represent simulations with precipitation nominal value 0.9 m yr^{-1} , hollow squares and triangles represent simulations with precipitation scenarios of 0.7 m yr^{-1} and 1.1 m yr^{-1} respectively (all other parameters remain constant).

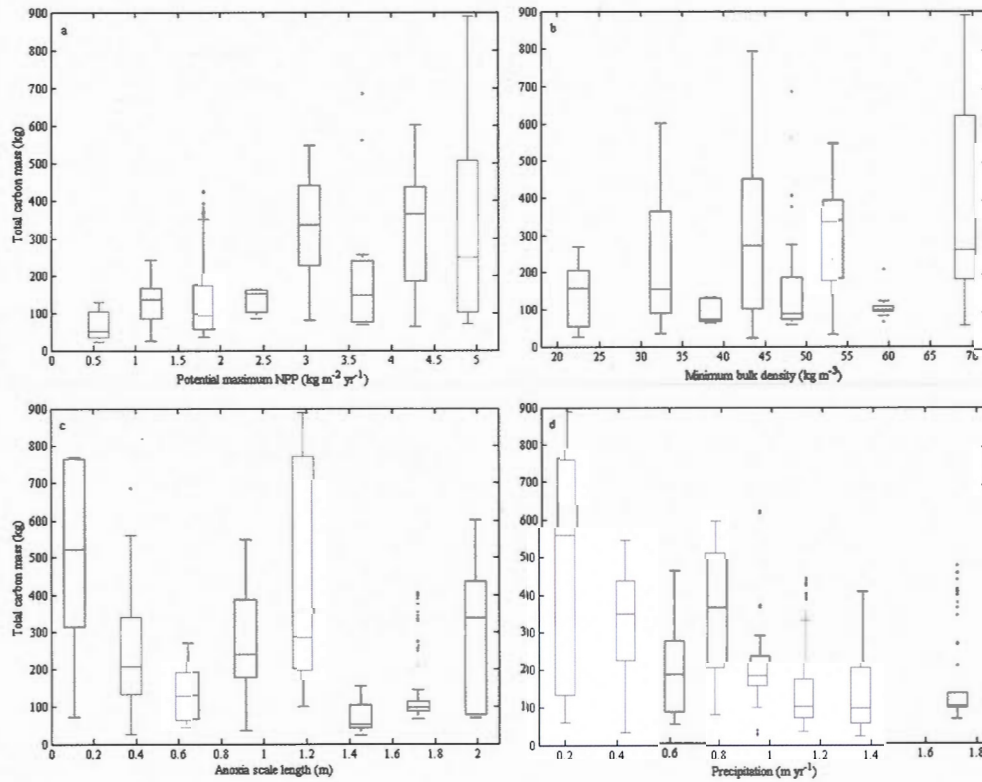


Figure 1.2: Total carbon mass after 5000 simulation years for different combination of parameters according to the random sampling method applied for the elementary effects calculation. Here 1280 simulations are performed with parameters combinations based on all the model parameters (127); each parameter may take a different value within its range (Table 1.2). The central mark of the box is the median, the bottom and the top of the box represent the 25th and 75th percentiles, the whiskers extend to the most extreme data points not considered outliers, and outliers are plotted individually.

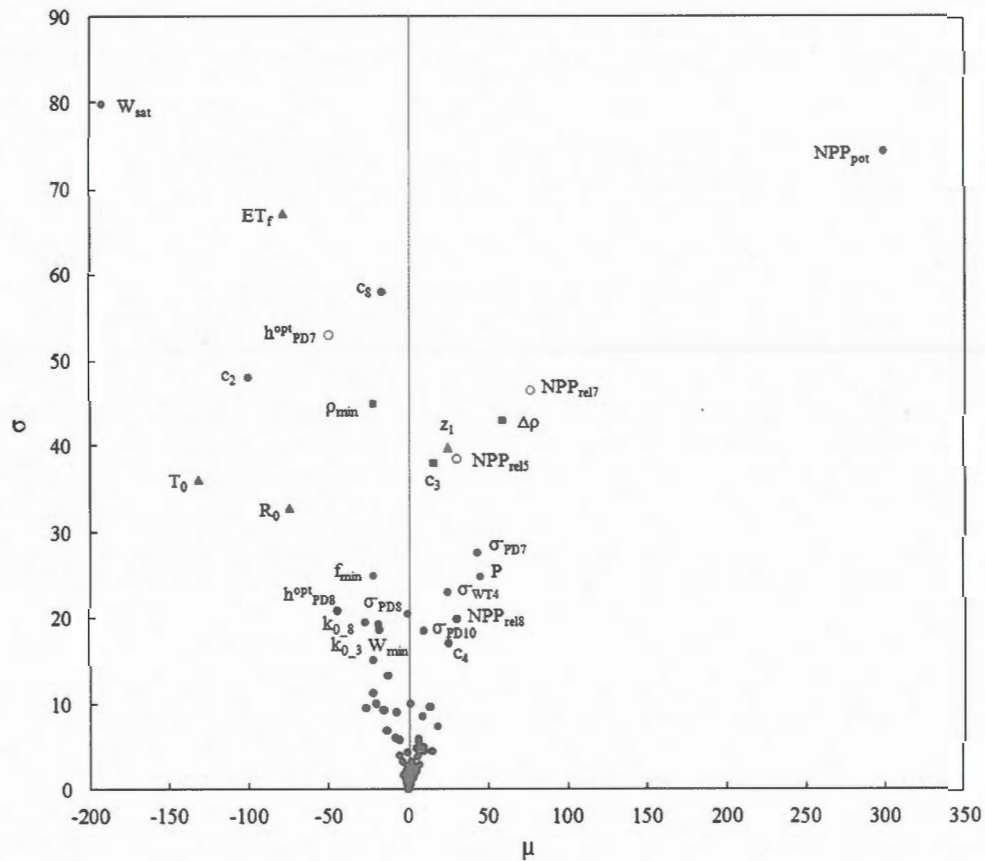


Figure 1.3: Mean (μ) and standard deviation (σ) of the distribution of elementary effects of each model parameter for total carbon mass after 5000 simulation years. Triangles, squares and hollow circles represent groups of parameters related to water outflows, bulk density and PFTs respectively. All other parameters are represented by filled circles. μ gives an insight of the overall influence of a parameter on the total carbon mass. σ is an indicator of non-linearity and interactions with other parameters.

CHAPITRE II

SOBOL' SENSITIVITY ANALYSIS OF THE HOLOCENE PEAT MODEL: WHAT DRIVES CARBON ACCUMULATION IN PEATLANDS?

Anne Quillet¹, Michelle Garneau², Steve Frolking³

¹ GÉOTOP et Chaire DÉCLIQUE-Hydro-Québec, Université du Québec à Montréal, succ. centre-ville, CP 8888, Montréal QC. H3C 3P8, Canada.

² GÉOTOP, Chaire DÉCLIQUE-Hydro-Québec & Département de Géographie, Université du Québec à Montréal, succ. centre-ville, CP 8888, Montréal QC. H3C 3P8, Canada.

³ Institute for the Study of Earth, Oceans, and Space, University of New Hampshire, 8 College Road, Durham, NH 03824-3525, USA.

Article sous presse dans le *Journal of Geophysical Research : Biogeosciences*

Résumé

La compréhension des processus de développement et d'accumulation de carbone des tourbières nordiques est cruciale pour leur intégration dans les modèles globaux du cycle du carbone. Afin d'y parvenir, les modèles de tourbières nordiques sont de plus en plus complexes et comprennent maintenant des processus de rétroaction entre l'accumulation, la décomposition, l'hydrologie et la végétation. Nous présentons ici les résultats d'une analyse globale de sensibilité, effectuée dans le but d'évaluer le comportement et les interactions entre paramètres d'un modèle de simulation des tourbières. Une série de simulations du Holocene Peat Model utilisant différentes combinaisons de paramètres a été réalisée en vue d'estimer l'influence des interactions entre paramètres sur la masse totale de carbone après simulation de 5000 années de développement d'une tourbière. L'impact de l'incertitude associée aux paramètres est souligné, de même que l'importance des interactions entre paramètres multiples. La sensibilité du modèle indique que les propriétés physiques de la tourbe jouent un rôle important dans l'accumulation de la tourbe et que ces paramètres étant mal contraints par des observations, ils devraient être le sujet de plus amples recherches. De plus, les résultats montrent que les processus autogènes sont en mesure de produire une grande variété de comportements de développement de tourbière, sans que des changements environnementaux aient été intégrés dans les simulations.

Abstract

Understanding development of northern peatlands and their carbon accumulation dynamics is crucial in order to confidently integrate northern peatlands into global carbon cycle models. To achieve this, northern peatland models are becoming increasingly complex and now include feedback processes between peat depth, decomposition, hydrology and vegetation composition and productivity. Here we present results from a global sensitivity analysis performed to assess the behavior and parameter interaction of a peatland simulation model. A series of simulations of the Holocene Peat Model were performed with different parameter combinations in order to assess the role of parameter interactions on the simulated total carbon mass after 5000 years of peatland development. The impact of parameter uncertainty on the simulation results is highlighted, as is the importance of multiple parameter interactions. The model sensitivity indicates that peat physical properties play an important role in peat accumulation; these parameters are poorly constrained by observations, and should be a focus of future research. Furthermore, results show that autogenic processes are able to produce a wide range of peatland development behaviors independently from any external environmental changes.

2.1 Introduction

Decomposition of organic matter in peatlands is less than production. This allowed the buildup of a northern peatland carbon stock estimated at 273 – 547 Pg during the Holocene (Gorham, 1991 ; Turunen *et al.*, 2002 ; Yu *et al.*, 2010), which places peatlands among the major components of the global carbon cycle. However, carbon storage in peatlands is linked to several processes, which are the foundation of the complexity of these ecosystems. Indeed productivity and decomposition of peatlands are a function of hydroclimatic and geomorphic conditions. Physical and hydraulic properties of peat create specific conditions for decomposition and influence the ecosystem water balance. Moreover, nutrient availability affects vegetation composition, which in turn affects productivity, decomposition, hydrology, and thus carbon storage. Therefore, peatlands are described as complex adaptive systems and present a large variety of properties that make the detection of the leading processes difficult (Belyea, 2009 ; Belyea and Baird, 2006).

Several modelling studies have attempted to represent the processes of accumulation in peatland development (Clymo, 1984, 1992). Following Clymo, models have been developed that included the different feedbacks between production, decomposition and water balance (Baird, Morris and Belyea, 2012 ; Froelking *et al.*, 2001 ; Hilbert, Roulet and Moore, 2000 ; Morris, Baird and Belyea, 2012 ; Yu *et al.*, 2001a ; Yu *et al.*, 2001b). Inclusion of a description of species-specific characteristics and their influence on peatland development is more recent (Froelking *et al.*, 2010 ; Heijmans *et al.*, 2008 ; Heinemeyer *et al.*, 2010).

However, in order to assess the validity of postulates underlying these models, their capacity to reproduce processes, as they are observed in the field, has to be evaluated. In case the modeler focuses on understanding the processes rather than aiming to reproduce the state of a system at a specific location, sensitivity analysis appears to be

an interesting tool. Sensitivity analysis explores the variability of the model response when different parameter values are applied, quantifying the influence of the various parameters on the model results. Sensitivity analyses can be grouped into two types: local and global sensitivity analyses. Whereas local sensitivity analysis focuses on a limited number of parameter values and tests their influence on the model output, global sensitivity analysis has the advantage of accounting for interactions between parameters in the model. This is particularly valuable when non-linear behaviors are expected. Saltelli *et al.* (2004, 2008) reviewed the various sensitivity analysis methods and their application potential in great detail.

Although in many studies model evaluation is limited to local sensitivity analyses (e.g. Frohking *et al.*, 2010 ; Hilbert, Roulet and Moore, 2000 ; St-Hilaire *et al.*, 2010 ; Wania, Ross and Prentice, 2009), Quillet *et al.* (2013) gained additional insight into the sensitivity of the Holocene Peat Model (HPM, Frohking *et al.*, 2010) by using a screening method in addition to the local sensitivity analysis and comparing the results of the two methods. The authors ranked the model parameters according to their influence on the total carbon mass. Moreover, they pointed out that some parameters might be involved more or less strongly in interactions with other parameters. In the current paper, we propose to investigate the role of the interactions in more detail. We postulate that the analysis of the influence of parameter interactions on carbon accumulation simulated by the Holocene Peat Model will enable the exploration of the processes controlling carbon accumulation in the field and more specifically highlight the role of the different groups of plant functional types (PFTs) in the carbon accumulation process. For this purpose, we propose to perform a global sensitivity analysis and a calculation of sensitivity indices after Sobol' (1993), and to examine the influential interactions in more detail.

2.2 The Holocene Peat Model

The main processes within the Holocene Peat Model are described by Quillet *et al.* (2013), in the following sub-sections and a more detailed description is given by Frohking *et al.* (2010). The model simulates the development of an ombrotrophic peatland in one dimension, i.e. at one point. It reproduces the development of a peatland at its center and delivers a year-by-year reconstruction of production, decomposition, hydraulic properties and vegetation assemblages over several millennia. Outputs include annual peat thickness, peat composition, carbon accumulation and water table depth. The Holocene Peat Model, in its original version, is parameterized to represent specific peatlands: located in northern latitudes, reflecting a fen-bog transition, with negligible trees and soil mineral effects. The model is a semi-empirical model based on laboratory and field data (e.g. decomposition rates of different species) as well as on numerical representations (e.g. hydraulic properties derived from known functions).

2.2.1 Vegetation representation and productivity

The model is based on the assumption that water table depth and nutrient status influence vegetation composition at the surface (e.g. Rydin and Jeglum, 2006). A particularity of the Holocene Peat Model is the inclusion of 12 plant functional types differentiated through their ability to grow at different water table depths and under different conditions of nutrient availability, with the use of peat depth as a proxy for nutrient status (based on observations by Tuittila *et al.* (2007, 2012) and Väiranta *et al.* (2007)). For example, certain PFTs have an optimal productivity when the water table is high and peat height is low, i.e. when nutrient availability is high. Other PFTs have optimal productivity when water table is lower and peat height is large enough to isolate the surface from groundwater-derived nutrients. Trees are not represented yet in the model. These characteristics are represented with PFT-specific parameters

describing the impact on productivity for conditions on each side of the optimal mean annual water table depth and optimal peat depth (Table 2.1). Moreover, the different PFTs also have different litter properties (above- vs. below-ground litter production, and litter quality or decomposability).

2.2.2 Water balance and hydraulic properties

In the Holocene Peat Model, an annual water balance is estimated from the precipitation regime, potential evapotranspiration reduced as a function of water table depth, and estimated runoff based on both a site-specific component and peatland slope. Three parameters control the runoff: R_0 controlling the net amount of water exiting the system (similar to an outlet), c_8 controlling the amount of water loss due to the general slope of the peatland (this slope is calculated by the model as proportional to total peat height when peat height reaches a certain level) and T_0 influencing runoff through transmissivity (Table 2.1). The amount of water resulting from this water balance calculation is added (subtracted) each year and the water table depth can be inferred when different peat properties are taken into account.

Hydraulic properties of peat depend on both water table depth and peat bulk density and thus on vegetation properties (particularly on decomposition properties). Peat layers identified as 'well decomposed' have lower hydraulic conductivity than fresh peat layers. Several parameters (W_{opt} , W_{sat} , W_{min}) characterize of the water-filled pore space and their link to saturation effect (Table 2.1).

2.2.3 Peat decomposition

Peat decomposes continuously (i.e. year after year) and follows different decomposition rates depending on the PFT (k values in Table 2.2 are initial decomposition rates; these rates decline linearly with fraction of total mass lost as the peat decomposes; e.g. Frohking *et al.* (2001)). As a result, the formed peat includes a

portion of decomposed peat originating from the different PFTs portions of a former vegetation cover. At the end of each simulated year, a new water table depth is calculated and so some peat can transition from unsaturated to saturated. The impact of this transition on decomposition is represented by a gradient of anoxia below the mean annual water table (described by the anoxia scale length, Table 2.1). Decomposition rates differ according to the position of the layer in the peat column. Peat bulk density is calculated for each annual cohort, and it increases non-linearly by a maximum of Δ_p from a prescribed minimum value (ρ_{\min}) as the cohort decomposes and mass is lost. The increase in bulk density is a function of cohort mass lost, and is controlled by two parameters, c_3 and c_4 (Table 2.1).

2.2.4 Peat accumulation

Peat accumulates when productivity exceeds decomposition. Productivity depends on the plant functional types (each of which has a specific relative productivity in order to represent vegetation composition according to realistic distribution values, see Table 2.2) and on the total maximum potential NPP (NPP_{pot}), which is a site-specific parameter (Table 2.1). Depending on water table depth and peat depth, different PFTs dominate the vegetation assemblages. Peat accumulation thus takes into account the litter properties of each PFT with respect to its representation in the assemblage.

2.2.5 Model calibration and initiation

Inputs needed are maximum potential net primary productivity (NPP_{pot}), precipitation regime (P) as well as minimum bulk density (ρ_{\min}) and magnitude of the bulk density (Δ_p) expected at the site.

Initialization is set up by constraining the model to accumulate peat until total peat height reaches a certain level (here 0.15 m). During this period, the water balance is

not dynamic and the water table depth is prescribed. Water table depth during initialization is shallow (i.e. 0.07 m).

2.3 Global sensitivity analysis

In order to assess the influence of parameters, a common method is the analysis of the influence of the parameters on one output of the simulation one-by-one, i.e. a local sensitivity analysis. While one parameter value changes, all others remain constant. This method gives an insight into the impact of changing parameter values on the value of the output. However, this method does not take account of interactions between model parameters or the potential nonlinearity of the model results. This drawback is highlighted in several studies (e.g. Campolongo, Saltelli and Cariboni, 2011 ; Saltelli *et al.*, 2008) as well as in the study of Quillet *et al.* (2013) also dealing with the Holocene Peat Model. Moreover, interactions between parameters are not taken into account in the local sensitivity analysis. Global sensitivity analysis aims to fill this gap by considering the entire model space as well as higher order interactions (i.e. n-way interactions between parameters for n greater than 1). The chosen variance-based method has the advantage of being model-independent; i.e. non-linearity or non-monotonicity in the model does not have an impact on the results of the sensitivity calculation, since the results are based on the relationship between the parameters and the output only (Saltelli *et al.*, 2004). The method consists of comparing the largest possible set of distinct simulation runs. Each simulation is run with a unique parameter combination. A very high number of runs is needed to cover the model space and the possible interactions among all parameters present in the model. Analyzing high-order interactions between parameters is very computationally expensive. The number of runs is calculated as follows:

$$C = (2 + \sum_{i=1}^n \binom{k}{i}) \times 2^{J+4} \quad (1)$$

with C is the number of runs, n is the maximum order of the sensitivity indices (e.g. 2 for 2-way interactions) to be computed, k is the number of parameters, and j is called 'base sample', which can assume values of 0,1,2,3 etc. depending on the computing resources available.

2.3.1 Screening method

In order to fulfill a global sensitivity analysis with the Holocene Peat Model, 127 parameters had to be considered. Since the global sensitivity analysis is far too expensive to be performed on so many parameters (i.e. more than 5 million runs would be required), a screening method allowing the sorting of parameters according to their influence on the simulation results had to be applied first. The method chosen is the Morris Elementary Effects (Morris, 1991) that consists in randomly choosing a series of parameter combinations that best represent the model space. The calculation of the influence of each parameter on the output enables the filtering of non-influential parameters. Morris elementary effects for total carbon mass are presented by Quillet *et al.* (2013). After screening, the number of relevant parameters was reduced to a group of 26 parameters described in Table 2.1.

2.3.2 Sobol' indices

At this stage, it is possible to complete the experiment by an estimation of the influence of these parameters, as well as of interactions between them, on the variance of the output. To assess the role of each parameter or interaction between parameters, sensitivity measures are needed. The chosen measures are based on Sobol' (1993) and therefore known as 'Sobol' indices'. Sobol' indices aim at representing the bias in the variance of the output (here total carbon mass) that can be attributed to a parameter or a combination of parameters (in the case of interactions). The measure of the influence S_i of the parameter P_i on the variance V of the output Y is called 'first-order-effect' and is defined as follows:

$$S_i = \frac{V(E(Y|P_i))}{V_y} \quad (2)$$

This measure represents the main effect contribution of the parameter P_i to the variance of the output. Thus, if the model is additive, the sum of the S_i of all parameters equals 1.

An interaction is defined as the combined effect of two parameters that exceeds the sum of their individual effects. This effect is called “second-order effect” of two parameters P_1 and P_2 and can be computed as

$$S_{P_1P_2} = \frac{V(E(Y|P_1,P_2))}{V_y} - \frac{V(E(Y|P_1))}{V_y} - \frac{V(E(Y|P_2))}{V_y} \quad (3)$$

Even though the number of parameters has been restricted to 26 through the screening method, the number of computations necessary to assess the second-order interactions of all model space with confidence is still high (ca. 45 000 runs with a j value of 4 in eq.1). We thus limited our analysis to the second-order interactions.

2.3.3 Experimental setting

For this study, the experiment follows the setting presented for the screening experiment performed by Quillet *et al.* (2013). The calculation of the Sobol’ indices is based on the results of the simulation runs. Nevertheless, the manner in which parameter values are sampled matters. A quasi-random sampling is chosen because it is more adequate to represent the model space than the traditional Monte-Carlo sampling (Beven, 2009 ; Saltelli *et al.*, 2008). The quasi-random sample contains parameter values following a specific range and probability distribution that are assigned to each parameter individually. When the distribution of the parameter is unknown, a uniform distribution was assumed (Table 2.1). The quasi-random sample

as well as the calculation of the Sobol' indices were performed with the SimLab software, version 3.2.6 (Joint Research Centre of the European Commission, 2011).

In addition, the experiment was designed so that each simulation had the same initialization period. During initialization, the parameters are represented by nominal values from Mer Bleue bog located in Ontario (Tables 2.1 and 2.2) (Roulet *et al.*, 2007). In the current setting, the initialization lasts 8 years. Parameters values change when the simulation becomes dynamic, i.e. as soon as the accumulating peat reaches 15 cm thickness.

Regarding the output, we focus here on the total quantity of carbon sequestered (kg C) after 5000 simulation years. This value can be compared to data sets, and carbon sequestration processes are now very important topics in peatland science. Since it is the net result of several different processes, this output is a useful metric to evaluate the overall model.

2.4 Results

With help of a screening method Quillet *et al.* (2013) identified the 26 parameters having a significant influence on total carbon mass in the Holocene Peat Model. In addition, they showed that slightly different parameter values could lead the model simulations on different peatland development trajectories. Indeed, different fen-bog transition pathways could be identified, while simulations showed comparable output responses.

Among the 26 influential parameter identified by Quillet *et al.* (2013), both maximum potential NPP (NPP_{pot}) and the decomposition rate multiplier W_{sat} had a strong influence on total carbon mass. The authors could also identify three groups of parameters that are potential sources of uncertainty in peat accumulation: a group of

parameters related to the peatland water balance, a group of PFT-specific parameters and a group of parameters controlling the shape of the bulk density curve. These are identified as parameters involved in interactions with other parameters and associated with non-linearity. The global sensitivity analysis performed here is based on these 26 parameters. A description of parameters and their value ranges can be found in Table 2.1.

2.4.1 Main processes affecting carbon mass

2.4.1.1 Maximum potential productivity

First-order effects highlight the direct influence of a parameter on the total carbon mass. Figure 2.1a shows that maximum potential NPP, NPP_{pot} , has a high influence on the total carbon mass. This direct link between the quantity of carbon and the potential productivity is straightforward since enhancing productivity potential allows the system to accumulate more carbon.

The sum of the second-order effects of each parameter gives an indication on the influence of the interactions involved for each parameter (Figure 2.1b). Maximum potential NPP (NPP_{pot}) also has the first rank here. The influence of interactions of this parameter with other parameters is very high. The variability of total peat mass is thus linked to the potential NPP available. The total effects of each parameter (Figure 2.1c) give an estimate of the overall influence of the parameter on total peat mass. More details on the nature of interactions are presented in Figure 2.2. For example, panel f shows the second-order effects of NPP_{pot} . Only six parameters interact significantly with NPP_{pot} , all other non-positive values are not shown because they are not significant. A strong interaction between NPP_{pot} and the minimum profile relative transmissivity (T_0) influences total carbon mass. Indeed, NPP_{pot} has an impact on the overall thickness of the peatland in the Holocene Peat Model and T_0 influences the total runoff. The combination of both parameters influences the water

table depth of the peatland, which in turn controls productivity (Figure 2.3). As a result, total carbon mass is sensitive to these parameters, which should thus be better constrained to improve the simulation.

2.4.1.2 Physical peat properties

The anoxia scale length, minimum and maximum increase in peat bulk density (ρ_{\min} and $\Delta\rho$) and parameters controlling the shape of the bulk density curve c_3 and c_4 (Table 2.1), show both direct (Figure 2.1a) and indirect impacts (Figure 2.1b) on the total carbon mass. These parameters influence peat hydraulic properties, water balance and decomposition and thus the bulk density profile. Apart from ρ_{\min} and $\Delta\rho$, these parameters are difficult to constrain with field data. They can therefore be considered as parameters inducing uncertainty in the simulations.

Similarly to the anoxia scale length, the decomposition rate multiplier W_{sat} is a parameter for the anoxia impact on decomposition of the peat located below the mean annual water table. Though this parameter has a low direct effect on carbon mass (Figure 2.1a), it is involved in a series of interactions (Figure 2.2i). Besides its interaction with bulk density-associated parameters ($\Delta\rho$ and c_4), W_{sat} also interacts with the maximum potential NPP (NPP_{pot}) and several parameters related to the description of the PFT productivity.

2.4.1.3 Water balance

Several parameters influencing the water balance calculation have an impact on total carbon mass. These parameters are annual precipitation (P), the factor for annual potential evapotranspiration (ET_f), the annual runoff adjustment factor (R_0), the increase in runoff with peat height (c_8), the minimum profile relative transmissivity (T_0) and the water table depth threshold for maximal evapotranspiration (z_1). Among them, c_8 and T_0 show a strong influence on the output, while c_8 impacts mostly

through its first-order effect and T_0 through its second-order effect, where it interacts with NPP_{pot} , as described earlier. While P can be relatively well constrained if palaeo-reconstructions of precipitation are available for the site studied, it is challenging to estimate other parameters values, and thus difficult to reduce the uncertainty in the simulation.

To conclude this section, two major shortcomings hinder the improvement of the representation of system processes: bulk density and water balance. In the model, the representation of the transition from low to high bulk density is not very realistic and water balance is poorly represented at a yearly timescale.

2.4.2 Relationships between PFTs and accumulated carbon mass

2.4.2.1 Influence of various PFTs on carbon mass

Several PFT parameters showed low first-order effects and substantial second-order effects (Figures 2.1a and b). These included parameters describing the decomposition capacity of minerotrophic sedges (k_{0_3}) and hummock-*Sphagnum* (k_{0_8}), parameters describing productivity potential for brown mosses, lawn- and hummock-*Sphagnum* (NPP_{rel5} , NPP_{rel7} and NPP_{rel8}), others describing the optimal peat depth and NPP sensitivity on the shallow side of this optimum for lawn-, hummock-*Sphagnum* and ombrotrophic herbs productivity (h_{PD7}^{opt} , h_{PD8}^{opt} , σ_{PD7} , σ_{PD8} and σ_{PD10}). An additional parameter describes NPP sensitivity of minerotrophic shrubs to water table depth on the shallow side of the optimum: σ_{WTD4} . However, this is the only parameter showing the influence of the water table depth as a proxy for productivity. Parameterization of productivity through water table depth constraints thus seems to have limited impact on the simulation results. Overall, it is noteworthy that among the 12 PFTs competing in the model, the characteristics of only 5 PFTs appear to have an impact on total carbon mass. From this observation, we can conclude that the

other PFTs have limited impact on the response of the model. However, several characteristics of PFTs 7 (lawn-*Sphagnum*) and 8 (hummock-*Sphagnum*) appear to have a particular impact on the output, showing high second order interactions (Figure 2.1b). This result raises the question of the function of these PFTs in the model.

2.4.2.2 The role of lawn-*Sphagnum* (PFT #7)

Two lawn-*Sphagnum*'s parameters describing peat depth conditions for optimum productivity (peat depth optimum h_{PD7}^{opt} and variance of the productivity curve for the shallow side of this optimum σ_{PD7}) were selected after the screening (Quillet *et al.*, 2013). They both show negligible first-order effects (Figure 2.1a) but important sums of second-order effects (above 0.08, Figure 2.1b). Figure 2.2v and 2.2w show that h_{PD7}^{opt} and σ_{PD7} interact respectively with different parameters: h_{PD7}^{opt} interacts strongly with anoxia scale length (c_2) and the decomposition rate multiplier W_{sat} , two parameters controlling decomposition of saturated peat underlying the water table depth (Figure 2.2v), whereas σ_{PD7} interacts with the annual runoff adjustment parameter R_0 , and bulk density parameters (minimum peat bulk density (ρ_{min}), parameters controlling the shape of the bulk density curve c_3 and c_4 ; Figure 2.2w). Their respective influence on total carbon mass thus takes different pathways. We hypothesize that interactions between these parameters and precipitation (P) or R_0 represent also the combinations of environmental conditions in the model that are most favorable to impact total carbon mass. Overall, maximum carbon mass occurs when P ranges from ca. 0.6 to ca. 1.1 m.yr⁻¹ and R_0 is low because it limits water outflow and thus favors anaerobic conditions with low decomposition. Lower precipitation leads to deeper water tables and to an increase in decomposition. Very high precipitation, on the contrary, favors a high productivity at first, but leads to a rapid increase in peat height and a dropping of the water table. With a deep water table, decomposition is high and productivity is limited. When P and R_0 are in their

optimal ranges, lawn-*Sphagnum* can maximize the carbon mass accumulated if they establish at relatively low peat depths. This can be achieved with large values of σ_{PD7}^- , h_{PD7}^{opt} or a combination of both. Indeed lawn-*Sphagnum* decomposes relatively slowly (Table 2.2) and thus accumulates rapidly. Again this rapid accumulation is followed by a deepening of the water table to a level at which lawn-*Sphagnum* spp. are better competitors. This allows the build-up of maximized carbon masses at the end of the simulation.

σ_{PD7}^- and h_{PD7}^{opt} also interact with other PFTs' characteristics and we hypothesize that interactions between different parameters related to PFTs characteristics describe the conditions for which PFTs characteristics combinations are the most influential, i.e. optimal conditions leading to variance in total carbon mass.

2.4.2.3 Feedbacks between lawn- and hummock-*Sphagnum*

The parameter representing the decomposition rate of hummock-*Sphagnum* (k_{0_8}) shows a sum of second-order effects lying around 0.06 (Figure 2.1b) and is the most influential when compared with the other parameters (relative NPP, NPP_{rel8} , peat depth productivity optimum h_{PD8}^{opt} and variance of the productivity curve for the shallow side of this optimum σ_{PD8}^- for hummock-*Sphagnum*). It interacts with a series of parameters (Figure 2.2q) related to all model processes, suggesting that it is involved in several feedbacks. For example, k_{0_8} interacts with NPP_{rel7} (Figure 2.4). As decomposition of hummock-*Sphagnum* is low, the average total carbon mass reaches high levels. However, total carbon mass can also reach high levels when the decomposition factor of hummock-*Sphagnum* is high. This is due to a feedback effect: an increased decomposition of hummock-*Sphagnum* causes an increase of peat bulk density while the water table rises. This, in turn, shrinks the thickness of the acrotelm and enables a decrease in decomposition and an increase in net accumulation. After 5000 simulation years, more carbon remains in the peatland.

Overall, NPP_{rel7} values above 0.5 are necessary to optimize total carbon mass. Below this level, hummock-*Sphagnum* benefits from the low productivity of lawn-*Sphagnum* and occupies a larger portion of the plant assemblage. In this case, high decomposition of hummock-*Sphagnum* no longer favors carbon accumulation and total carbon mass show relatively low values at the end of the simulation.

The anoxia scale length (c_2) shows a relatively important interaction with the productivity optimal peat depth for lawn-*Sphagnum* (h_{PD7}^{opt} , Figure 2.2u). The impact of this combination of parameters on the average total carbon mass is presented in Figure 2.5. It is obvious that for short anoxia scale length (a stronger limit on decomposition below the water table), decomposition is lower and simulation results show high carbon mass values. However, Figure 2.5 also shows that it is possible to reach high carbon mass when the anoxia scale is long under certain values of h_{PD7}^{opt} . Indeed, this is possible if the maximum potential productivity (NPP_{pot}) is high and compensates for decomposition and because highly decomposed peat prevents a decline of the water table as bulk density increases. However, this case only occurs for specific values of h_{PD7}^{opt} . Having a relatively low productivity compared to minerotrophic species, but also being relatively resistant to decomposition (Table 2.1), lawn-*Sphagnum* is not an efficient carbon accumulator when settling at low peat thicknesses but favors carbon accumulation by the means of its low decomposition rate when a certain amount of peat has already accumulated. A late onset of lawn-*Sphagnum* productivity does not lead to high carbon accumulation, given that simulation time is limited to 5000 years.

The parameters having the most powerful influence on the variance of total carbon mass have been identified as NPP_{pot} , the anoxia scale length (c_2) and parameters related to peatland hydrology (minimum profile relative transmissivity T_0 , increase in runoff with peat height c_8). Overall, the influence of PFT parameters is not important compared to the influence of other parameters such as NPP_{pot} or the anoxia scale

length c_2 . However, the sensitivity to the different lawn and hummock-*Sphagnum* parameters suggest the importance of these PFTs to peat accumulation.

2.5 Discussion

Maximum potential NPP (NPP_{pot}) causes a large variability in the results, with direct influence on carbon accumulation in peatlands. Moreover, NPP_{pot} interacts with minimum profile relative transmissivity (T_0) and influences runoff, so that uncertainty in NPP_{pot} leads to variability of different processes and feedbacks. However, for the Holocene Peat Model to be effective in case studies, it is necessary to have a better constraint on these parameters, since the response can vary widely. The response of total carbon mass can vary for a single NPP_{pot} value, though total NPP depends on changes in water table depth and nutrient availability (by the means of vegetation changes with peat depth). We thus argue that NPP should probably be influenced by temperature, or other climatic variables such as photosynthetically active radiation (PAR) or growing season length, since these factors are not included in the NPP_{pot} parameter. Loisel, Gallego-Sala and Yu (2012) performed a meta-analysis to investigate the response of *Sphagnum* to a series of climatic variables and showed that *Sphagnum* growth is sensitive to PAR integrated over the growing season. Moreover, Ise *et al.* (2008) found that the feedback between water table and peat depth leads to an increased sensitivity of peat decomposition to temperature. Therefore isolating the effect of temperature on productivity might improve the representation of this feedback in the model.

Other parameters influence the water balance calculation, such as annual precipitation (P), the factor for annual potential evapotranspiration (ET_f), the annual runoff adjustment factor (R_0), the increase in runoff with peat height (c_8), the minimum profile relative transmissivity (T_0) and the water table depth threshold for maximal evapotranspiration (z_1). While precipitation data may be obtained or derived from

reconstruction, data on both evapotranspiration and runoff/run-on characteristics are rarely available. Usually, the outflows of a peatland are not known unless specific instrumental field measurements are made. Since hydrological changes and lateral expansion also affect water balance (Belyea and Clymo, 2001 ; Belyea and Malmer, 2004 ; Glaser *et al.*, 2004) additional information is needed to properly reconstruct early peatland development. A better representation of the amount of water available in the peatland, based on the physical properties of peat, would help limit uncertainty. Another avenue, circumventing the improvement of the physical peat properties representation, would be the use of a proxy, such as testate amoebae, allowing water table depth reconstructions (Booth, 2008 ; Charman *et al.*, 2007) and thus limiting the uncertainty associated with the water balance calculation. Such proxies could also be used to test model water table depth simulations.

Sobol' indices highlight the influence of several parameters related to bulk density (c_3 and c_4 controlling the shape of the curve and ρ_{\min} and Δ_p describing the minimum and the maximum increase in bulk density). These parameters are involved in multiple interactions with NPP_{pot} , water balance or PFT parameters. In the Holocene Peat Model, bulk density is represented as a distinct function, since little is known quantitatively about the relationship between hydraulic properties, decomposition, water table depth, and bulk density. Nevertheless, the results show that bulk density plays an important role when studying total carbon mass in the model. We thus advise to choose the different parameters values with care and when possible to try to fit the curve to the bulk density records from several cores sampled at the study site. Processes underlying hydraulic properties or decomposition are identified as weakly known and should be integrated in upcoming research. Overall, as noted by Belyea and Baird (2006) and Morris, Baird and Belyea (2012), this study points out that there is a lack of data and understanding of the anoxia gradient, peat bulk density as well as hydraulic properties in the peat column and how they are linked with decomposition and water balance.

This study shows that a great variability of results can be obtained when various parameter combinations are used. It appears possible to simulate different peatlands characterized by either a small or a large amount of carbon and following different development pathways. This is an important result since this experiment did not take any environmental changes into account. Values of maximum potential NPP (NPP_{pot}), annual precipitation (P), annual potential evapotranspiration (ET_f) or runoff (R_0 , c_8) were constant during the simulations. Although behavior could change if environmental changes were included, internal (i.e. autogenic) processes by themselves are sufficiently influent to induce a large variety of peatland development patterns and, as stated by several authors (e.g. Almquist-Jacobson and Foster, 1995 ; Anderson, Foster and Motzkin, 2003 ; Belyea and Baird, 2006), can affect peatland development and carbon accumulation.

The results of the sensitivity analysis highlighted the dominance of certain PFTs (particularly lawn- and hummock-*Sphagnum*) over the others, with respect to long-term carbon accumulation. *Sphagnum* is identified as an important builder able to outcompete other species (Van Breemen, 1995) and specifically *Sphagnum Sphagnum* and *Sphagnum Acutifolia* sections (lawn- and hummock-*Sphagnum* in the Holocene Peat Model) influence peat formation (Malmer and Wallén, 2004 ; Rydin and Jeglum, 2006). We hypothesize that this bias between PFTs emphasizes the complexity and adaptability of carbon accumulation processes in peatlands. This delicate balance is thus more affected by transitional species, tolerant of a wide range of conditions, than by species that have only a narrow niche. Robroek *et al.* (2007) studied the competition between *Sphagnum* species in a greenhouse by intermingling 6 different *Sphagnum* species collected in Ireland and growing them under different water-level treatments. Their results show that species growing higher above the water table (e.g. *Sphagnum magellanicum*, *S. rubellum* or *S. fuscum*) outcompete others having a preferred habitat close to the water table (e.g. *S. cuspidatum*). This indicates that not all *Sphagnum* species have the same competitive abilities and

resilience and this is consistent with the sensitivity finding: lawn and hummock species play an important role in the system by outcompeting other groups of species.

Although the representation of competition between PFTs in the Holocene Peat Model does not capture the true complexity of the role of PFTs in peat accumulation, the simulation results show that lawn- and hummock-*Sphagnum* interact in a complex way in the model. Combinations of their parameters can create optimal conditions for carbon accumulation or on the contrary limit carbon accumulation. Furthermore, nutrient limitation properties of these PFTs, simplistically represented by the peat height gradient for optimum productivity, seem to have a stronger impact on total carbon mass than their water table optima. The PFTs' nutrient tolerance interacts with other parameters and through other processes (e.g. anoxia gradient or runoff) on the water table depth but this is not the case for the water table optima. Robroek *et al.* (2007) pointed out that inter-specific competition occurred independently from water table depth, supporting the result of limited influence of parameters describing water table optima for the different PFTs. Moreover, the sensitivity of carbon mass to nutrient limitations of *Sphagnum* might also be representative for competition between *Sphagnum* and vascular plants. Malmer *et al.* (2003) conducted fertilization experiments on different *Sphagnum* and vascular species in southern Sweden and found that an increasing proportion of *Sphagnum* species in the vegetation biomass tended to increase peat accumulation rates. Moreover, the effects of nutrient transport on peatland patterning also suggest that the distribution of nutrients influences vegetation cover and thus peat accumulation rates (Eppinga *et al.*, 2009b). Thus, the different vegetation PFTs characteristics, although described in the Holocene Peat Model in one dimension, are useful for the representation of complex feedbacks in peatland development processes.

2.6 Conclusions

Carbon accumulation in peatlands is the result of complex interactions between productivity, decomposition and hydrology. Therefore, accurate modelling of these processes requires representing many aspects of the system. We performed a global sensitivity analysis on the Holocene Peat Model in order to assess its representation of the feedback processes influencing carbon accumulation. Moreover, attention was paid to the specific influence of the different PFTs, which is a distinctive feature of this model.

Results highlight several processes that should be better characterized (such as maximum potential productivity) or subject to further research (such as vertical gradients in anoxia, bulk density and peat hydraulic properties) in order to constrain uncertainty in the model. Furthermore, without any external environmental variability through time, the autogenic processes in the Holocene Peat Model are able to produce a variety of peatland development patterns. Lawn- and hummock-*Sphagnum* species come out as 'effective ecosystem engineers', following the terminology of Van Breemen (1995), that compete with other plants (non-vascular and vascular) to potentially shift the carbon accumulation pattern of the system.

Acknowledgments

The authors are grateful to Stefano Tarantola for his help with statistical analyses and with the use of the Simlab software. AQ was supported by funds from the Canadian Foundation for Climate and Atmospheric Sciences, by funds supporting the Chaire Déclique at GEOTOP-UQAM (MG). SF was supported by NSF grants ATM-0628399 and DEB-1019523.

References

- Almquist-Jacobson, H., and D. R. Foster. 1995. «Toward an integrated model for raised-bog development: theory and field evidence». *Ecology*, vol. 76, no 8, p. 2503-2516.
- Anderson, R. L., D. R. Foster and G. Motzkin. 2003. «Integrating lateral expansion into models of peatland development in temperate New England». *Journal of Ecology*, vol. 91, no 1, p. 68-76.
- Baird, A. J., P. J. Morris and L. R. Belyea. 2012. «The DigiBog peatland development model 1: Rationale, conceptual model, and hydrological basis». *Ecohydrology*, vol. 5, no 3, p. 242-255.
- Belyea, L. R. 2009. «Nonlinear dynamics of peatlands and potential feedbacks on the climate system». In *Carbon cycling in northern peatlands*, A. J. Baird, L. R. Belyea et X. Comas, p. 5-18. Washington, D.C.: AGU.
- Belyea, L. R., and A. J. Baird. 2006. «Beyond "the limits to peat bog growth": Cross-scale feedback in peatland development». *Ecological Monographs*, vol. 76, no 3, p. 299-322.
- Belyea, L. R., and R. S. Clymo. 2001. «Feedback control of the rate of peat formation». *Proceedings of the Royal Society B: Biological Sciences*, vol. 268, no 1473, p. 1315-1321.
- Belyea, L. R., and N. Malmer. 2004. «Carbon sequestration in peatland: patterns and mechanisms of response to climate change». *Global Change Biology*, vol. 10, no 7, p. 1043-1052.
- Beven, K. J. 2009. *Environmental modelling: an uncertain future?* Abingdon, England: Routledge, 310 p.
- Booth, R. K. 2008. «Testate amoebae as proxies for mean annual water-table depth in *Sphagnum*-dominated peatlands of North America». *Journal of Quaternary Science*, vol. 23, no 1, p. 43-57.
- Campolongo, F., A. Saltelli and J. Cariboni. 2011. «From screening to quantitative sensitivity analysis. A unified approach». *Computer Physics Communications*, vol. 182, no 4, p. 978-988.

- Charman, D. J., A. Blundell, J. Alm, S. Bartlett, C. Begeot, M. Blaauw, F. Chambers, J. Daniell, R. Evershed, J. Hunt, E. Karofeld, A. Korhola, H. Kuester, J. Laine, M. Magny, D. Mauquoy, E. McClymont, F. Mitchell, P. Oksanen, R. Pancost, K. Sarmaja-Korjonen, H. Seppä, Ü. Sillasoo, B. Stefanini, M. Steffens, E. S. Tuittila, M. Väliranta, J. van der Plicht, B. van Geel and D. Yeloff. 2007. «A new European testate amoebae transfer function for palaeohydrological reconstruction on ombrotrophic peatlands». *Journal of Quaternary Science*, vol. 22, no 3, p. 209-221.
- Clymo, R. S. 1984. «*Sphagnum*-dominated peat bog: a naturally acid ecosystem». Ecological effects of deposited sulphur and nitrogen compounds. Discussion meeting, London, 1983, p. 487-499.
- 1992. «Models of peat growth». *Suo*, vol. 43, no 4-5, p. 127-136.
- Eppinga, M. B., M. Rietkerk, M. J. Wassen and P. C. De Ruiter. 2009. «Linking habitat modification to catastrophic shifts and vegetation patterns in bogs». *Plant Ecology*, vol. 200, no 1, p. 53-68.
- Frolking, S., N. T. Roulet, T. R. Moore, P. J. H. Richard, M. Lavoie and S. D. Muller. 2001. «Modeling northern peatland decomposition and peat accumulation». *Ecosystems*, vol. 4, no spring, p. 479-498.
- Frolking, S., N. T. Roulet, E. Tuittila, J. L. Bubier, A. Quillet, J. Talbot and P. J. H. Richard. 2010. «A new model of Holocene peatland net primary production, decomposition, water balance, and peat accumulation». *Earth System Dynamics*, vol. 1, no 1, p. 1-21.
- Glaser, P. H., B. C. S. Hansen, D. I. Siegel, A. S. Reeve and P. J. Morin. 2004. «Rates, pathways and drivers for peatland development in the Hudson Bay Lowlands, northern Ontario, Canada». *Journal of Ecology*, vol. 92, no 6, p. 1036-1053.
- Gorham, E. 1991. «Northern peatlands: role in the carbon cycle and probable response to climatic warming». *Ecological applications*, vol. 1, no 2, p. 182-195.
- Heijmans, M., D. Mauquoy, B. Van Geel and F. Berendse. 2008. «Long-term effects of climate change on vegetation and carbon dynamics in peat bogs». *Journal of Vegetation Science*, vol. 19, no 3, p. 307-320.

- Heinemeyer, A., S. Croft, M. H. Garnett, E. Gloor, J. Holden, M. R. Lomas and P. Ineson. 2010. «The MILLENNIA peat cohort model: Predicting past, present and future soil carbon budgets and fluxes under changing climates in peatlands». *Climate Research*, vol. 45, no 1, p. 207-226.
- Hilbert, D. W., N. T. Roulet and T. R. Moore. 2000. «Modelling and analysis of peatlands as dynamical systems». *Journal of Ecology*, vol. 88, no 2, p. 230-242.
- Ise, T., A. L. Dunn, S. C. Wofsy and P. R. Moorcroft. 2008. «High sensitivity of peat decomposition to climate change through water-table feedback». *Nature Geoscience*, vol. 1, no 11, p. 763-766.
- Joint Research Centre of the European Commission (2011). SimLab: Software package for uncertainty and sensitivity analysis: Downloadable for free at: <http://simlab.jrc.ec.europa.eu>.
- Loisel, J., A. V. Gallego-Sala and Z. Yu. 2012. «Global-scale pattern of peatland *Sphagnum* growth driven by photosynthetically active radiation and growing season length». *Biogeosciences*, vol. 9, no 7, p. 2737-2746.
- Malmer, N., C. Albinsson, B. M. Svensson and B. Wallén. 2003. «Interferences between *Sphagnum* and vascular plants: Effects on plant community structure and peat formation». *Oikos*, vol. 100, no 3, p. 469-482.
- Malmer, N., and B. Wallén. 2004. «Input rates, decay losses and accumulation rates of carbon in bogs during the last millenium: internal processes and environmental changes». *The Holocene*, vol. 14, no 1, p. 111-117.
- Morris, M. D. 1991. «Factorial sampling plans for preliminary computational experiments». *Technometrics*, vol. 33, no 2, p. 161-174.
- Morris, P. J., A. J. Baird and L. R. Belyea. 2012. «The DigiBog peatland development model 2: Ecohydrological simulations in 2D». *Ecohydrology*, vol. 5, no 3, p. 256-268.
- Quillet, A., S. Frohking, M. Garneau, J. Talbot and C. Peng. 2013. «Assessing the role of parameter interactions in the sensitivity analysis of a model of peatland dynamics ». *Ecological Modelling*, vol. 248, p. 30-40.
- Robroek, B. J. M., J. Limpens, A. Breeuwer, P. H. Crushell and M. G. C. Schouten. 2007. «Interspecific competition between *Sphagnum* mosses at different water tables». *Functional Ecology*, vol. 21, no 4, p. 805-812.

- Roulet, N. T., P. M. Lafleur, P. J. H. Richard, T. R. Moore, E. R. Humphreys and J. Bubier. 2007. «Contemporary carbon balance and late Holocene carbon accumulation in a northern peatland». *Global Change Biology*, vol. 13, no 2, p. 397-411.
- Rydin, H., and J. K. Jeglum. 2006. *Biology of Peatlands*. Coll. «The Biology of Habitats Series»: Oxford University Press, 354 p.
- Saltelli, A., M. Ratto, T. Andres, F. Campolongo, J. Carboni, D. Gatelli, M. Saisana and S. Tarantola. 2008. *Global sensitivity analysis. The primer*. Chichester, England: John Wiley & Sons Ltd, 292 p.
- Saltelli, A., S. Tarantola, F. Campolongo and M. Ratto. 2004. *Sensitivity analysis in practice: a guide to assessing scientific models*. Chichester, England: John Wiley & Sons Ltd, 219 p.
- Sobol', I. M. 1993. «Sensitivity estimates for nonlinear mathematical models». *Mathematical Modelling and Computational Experiments*, vol. 1, no 4, p. 407-414.
- St-Hilaire, F., J. Wu, N. T. Roulet, S. Frolking, P. M. Lafleur, E. R. Humphreys and V. Arora. 2010. «McGill wetland model: Evaluation of a peatland carbon simulator developed for global assessments». *Biogeosciences*, vol. 7, no 11, p. 3517-3530.
- Tuittila, E. S., S. Juutinen, S. Frolking, M. Välranta, A. Laine, A. Miettinen, M.-L. Seväkivi, A. Quillet and P. Merilä. 2012. «Wetland chronosequence as a model of peatland development: Vegetation succession, peat and carbon accumulation». *The Holocene*, vol. 23, p.23-33.
- Tuittila, E. S., M. Välranta, J. Laine and A. Korhola. 2007. «Quantifying patterns and controls of mire vegetation succession in a southern boreal bog in Finland using partial ordinations». *Journal of Vegetation Science*, vol. 18, no 6, p. 891-902.
- Turunen, J., E. Tomppo, K. Tolonen and A. Reinikainen. 2002. «Estimating carbon accumulation rates of undrained mires in Finland - application to boreal and subarctic regions». *The Holocene*, vol. 12, no 1, p. 69-80.
- Välranta, M., A. Korhola, H. Seppä, E. S. Tuittila, K. Sarmaja-Korjonen, J. Laine and J. Alm. 2007. «High-resolution reconstruction of wetness dynamics in a southern boreal raised bog, Finland, during the late Holocene: A quantitative approach». *The Holocene*, vol. 17, no 8, p. 1093-1107.

- Van Breemen, N. 1995. «How *Sphagnum* bogs down other plants». Trends in Ecology and Evolution, vol. 10, no 7, p. 270-275.
- Wania, R., L. Ross and I. C. Prentice. 2009. «Integrating peatlands and permafrost into a dynamic global vegetation model: 1. Evaluation and sensitivity of physical land surface processes». Global Biogeochemical Cycles, vol. 23, no 3, p. GB3014.
- Yu, Z., I. D. Campbell, D. H. Vitt and M. J. Apps. 2001a. «Modelling long-term peatland dynamics. I. Concepts, review, and proposed design». Ecological Modelling, vol. 145, no 2-3, p. 197-210.
- Yu, Z., J. Loisel, D. P. Brosseau, D. W. Beilman and S. J. Hunt. 2010. «Global peatland dynamics since the Last Glacial Maximum». Geophysical Research Letters, vol. 37, no 13.
- Yu, Z., M. R. Turetsky, I. D. Campbell and D. H. Vitt. 2001b. «Modelling long-term peatland dynamics. II. Processes and rates as inferred from litter and peat-core data». Ecological Modelling, vol. 145, no 2-3, p. 159-173.

Table 2.1: Characteristics of the 26 selected model parameters and their associated range and distribution for the sensitivity analysis, after Quillet *et al.* (2013)

| Parameter description | Parameter abbreviation | Units | Range | | PDF |
|---|---------------------------------|---|------------------|-------------------|---------|
| | | | Min value | Max value | |
| Annual precipitation | P | [m.yr ⁻¹] | 0.30 | 1.20 | Normal |
| Factor for annual potential evoptranspiration | ET _f | [-] | 0.10 | 1.00 | Normal |
| Water table depth threshold for maximal evapotranspiration | z ₁ | [m] | 0.01 | 0.40 | Uniform |
| Annual runoff adjustment factor | R ₀ | [m.yr ⁻¹] | -0.01 | 0.10 | Uniform |
| Increase in runoff with peat height | c ₈ | [m ⁻¹] | 0.05 | 0.30 | Uniform |
| Minimum profile relative transmissivity | T ₀ | [-] | 0.05 | 0.80 | Normal |
| Maximum potential NPP | NPP _{pot} | [kg.m ⁻² .yr ⁻¹] | 0.50 | 5.00 | Uniform |
| Scale length for the anaerobic effect on decomposition rate | c ₂ | [m] | 0.10 | 2.00 | Uniform |
| Decomposition rate multiplier at annual mean water table depth | W _{sat} | [-] | 0.15 | 0.45 | Uniform |
| Minimal decomposition rate multiplier | f _{min} | [-] | 0.0001 | 0.01 | Uniform |
| Minimum litter/peat degree of saturation | W _{min} | [-] | 0.01 | 0.05 | Uniform |
| Fraction of initial mass input remaining at which bulk density reaches half of its amplitude | c ₃ | [-] | 0.10 | 0.30 | Uniform |
| Controls steepness of the bulk density curve | c ₄ | [-] | 0.05 | 0.20 | Uniform |
| Minimum peat bulk density | ρ _{min} | [kg.m ⁻³] | 20.00 | 70.00 | Normal |
| Maximum potential increase in peat bulk density | Δρ | [kg.m ⁻³] | 55.00 | 140.00 | Uniform |
| Peat depth for optimum productivity for PFTs 7 and 8 | h ^{opt} _{PDi} | [m] | 50% ^a | 150% ^a | Normal |
| Productivity curve variance for the shallow side of the optimum peat depth for PFTs 7, 8 and 10 | σ ² _{PDi} | [m] | 50% ^a | 150% ^a | Normal |
| Productivity curve variance for the shallow side of the optimum water table depth for PFT 4 | σ ² _{WT4} | [m] | 75% ^a | 125% ^a | Normal |
| Relative Net Primary Productivity for PFTs 5, 7 and 8 | NPP _{rel i} | [-] | 50% ^a | 200% ^a | Uniform |
| Decomposition rates for PFTs 3 and 8 | k _{0,i} | [yr ⁻¹] | 75% ^a | 125% ^a | Normal |

^aof the nominal values (Table 2).

Example of notation for PFT parameters: h^{opt}_{PDi} is peat depth optimum productivity for PFT 7, lawn *Sphagnum*

Table 2.2: Nominal values of plant functional types (PFTs), after Frohking *et al.* (2010)

| PFT | PFT ID | $Z^{\text{opt}}_{\text{WTi}}$ | σ_{WTi} | σ^+_{WTi} | $h^{\text{opt}}_{\text{PDi}}$ | σ_{PDi} | σ^+_{PDi} | NPP_{rel} | k_0 |
|-------------------------|--------|-------------------------------|-----------------------|-------------------------|-------------------------------|-----------------------|-------------------------|---------------------------|---------------------|
| | [-] | [m] | [m] | [m] | [m] | [m] | [m] | [-] | [yr ⁻¹] |
| Grass | 1 | 0.40 | 0.40 | 0.40 | 0.01 | 1.00 | 1.00 | 0.75 | 0.20 |
| Minerotrophic herb | 2 | 0.10 | 0.30 | 0.30 | 0.30 | 1.00 | 1.00 | 0.75 | 0.30 |
| Minerotrophic sedge | 3 | 0.10 | 0.40 | 0.40 | 0.10 | 2.00 | 2.00 | 1.00 | 0.30 |
| Minerotrophic shrub | 4 | 0.20 | 0.20 | 1.00 | 1.00 | 2.00 | 2.00 | 0.50 | 0.20 |
| Brown moss | 5 | 0.01 | 0.20 | 0.05 | 0.10 | 1.50 | 1.50 | 0.50 | 0.10 |
| Hollow <i>Sphagnum</i> | 6 | 0.01 | 0.20 | 0.05 | 2.00 | 1.00 | 19.00 | 0.50 | 0.10 |
| Lawn <i>Sphagnum</i> | 7 | 0.10 | 0.30 | 0.40 | 2.00 | 1.00 | 19.00 | 0.50 | 0.07 |
| Hummock <i>Sphagnum</i> | 8 | 0.20 | 0.10 | 0.50 | 2.00 | 1.00 | 19.00 | 0.50 | 0.05 |
| Feathermoss | 9 | 0.40 | 0.40 | 0.60 | 4.00 | 6.00 | 19.00 | 0.25 | 0.10 |
| Ombrotrophic herb | 10 | 0.20 | 0.20 | 0.20 | 4.00 | 2.00 | 19.00 | 0.25 | 0.25 |
| Ombrotrophic sedge | 11 | 0.20 | 0.30 | 0.30 | 4.00 | 2.00 | 19.00 | 0.50 | 0.15 |
| Ombrotrophic shrub | 12 | 0.30 | 0.30 | 1.00 | 4.00 | 2.00 | 19.00 | 0.50 | 0.15 |

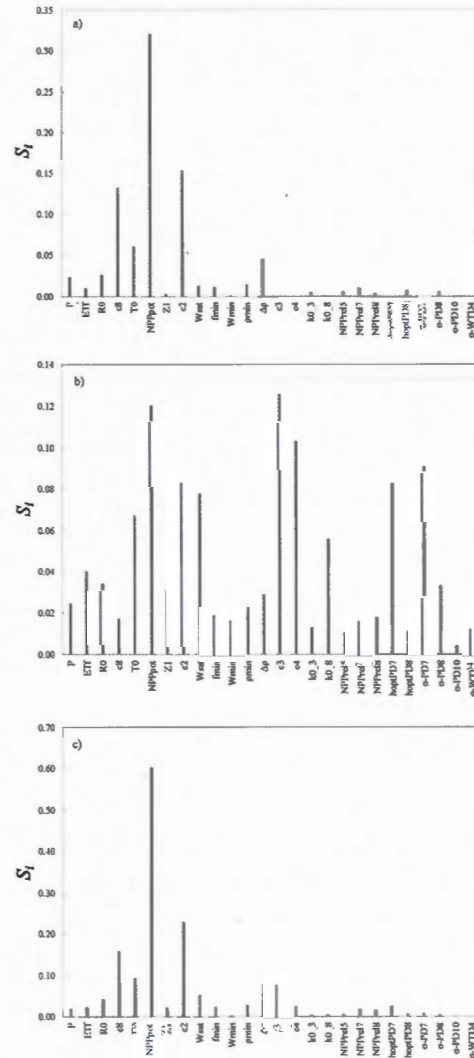


Figure 2.1: Sobol' indices (S_i) calculated for the total carbon mass after 5000 simulation years: a) first-order effect of each parameter, b) sum of the second-order effects for each parameter and c) total effect of each parameter. The magnitude of the first-order effect represents the direct influence of that parameter on the variance in model output assessed, i.e., total carbon mass; note that the first-order effect is very small for some parameters. The magnitude of the second-order effect represents the variance of the output related to a parameter's interactions with other parameters. The total effect includes first- and second-order effects as well as all the higher-order interactions (i.e. 3 or more parameters) and represents the variance in the output that would remain if only this parameter were to stay undetermined.

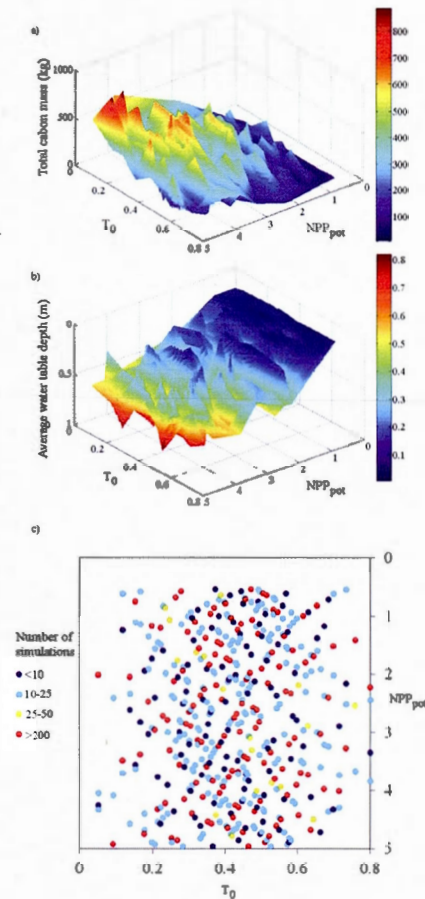


Figure 2.3: a) Average response of total carbon mass (kg) to different values of maximum potential NPP (NPP_{pot}) and minimum profile relative transmissivity (T_0), b) average response of water table depth (positive down) for different values of NPP_{pot} and T_0 , and c) number of simulation for each combination of parameter values. Note: panels (a) and (b) show the average response of the model for these specific combinations of parameter values.

Note that for a specific combination of parameters (here T_0 and NPP_{pot}) all other parameters may take different values within their range, so that large amplitudes in the model response can be observed (see Fig. 5b). Since a limited number of combinations of parameter values have been tested (relative to the 10^{26} possible combinations), the potential variation of the model response for some combinations of T_0 and NPP_{pot} might be poorly represented (especially if the number of simulations in panel (c) is low). So the ridge/valley character of the plot results from sampling the full parameter space, while the general trends in the figure are more representative of overall model behavior.

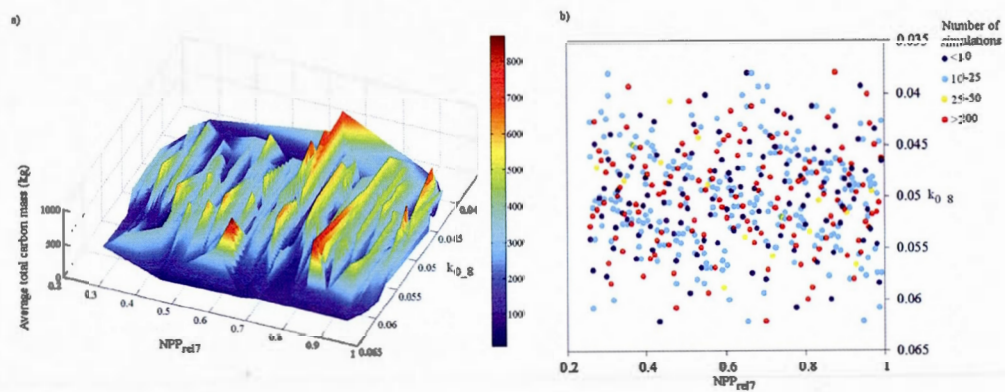


Figure 2.4: a) Average response of total carbon mass (kg) for different decomposition rates for hummock-*Sphagnum* (k_{0_g}) and different values of relative productivity of lawn-*Sphagnum* (NPP_{rel7}) and b) number of simulation for each combination of parameter values. See note in Figure 2.3 caption.

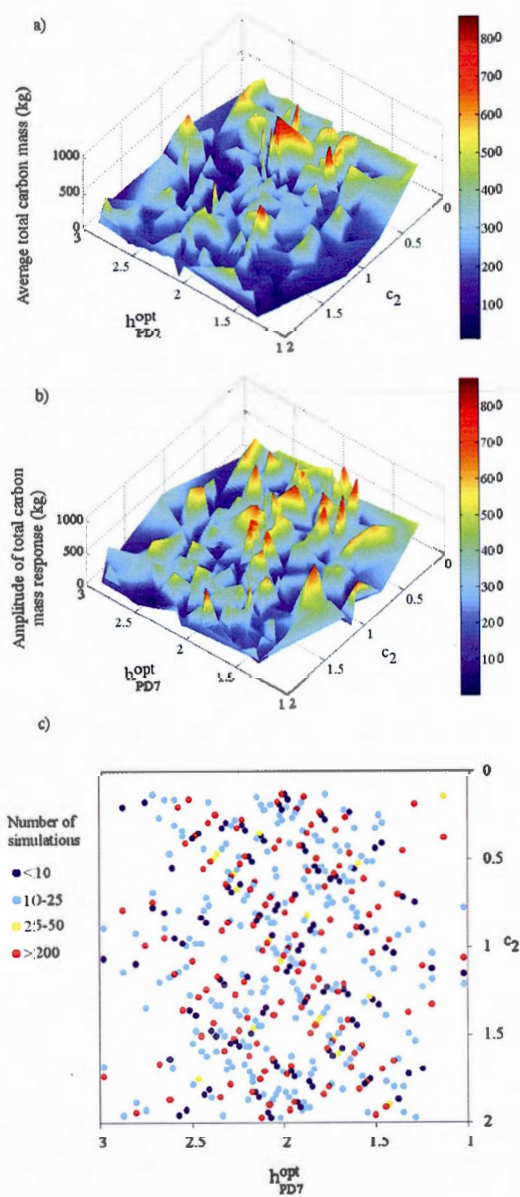


Figure 2.5: a) Average response of total carbon mass (kg) for different values of productivity optimum peat depth for lawn-*Sphagnum* (h_{PD7}^{opt}) and anoxia scale length (c_2), b) response amplitude of total carbon mass for different values of h_{PD7}^{opt} and c_2 and c) number of simulation for each combination of parameter values. See note in Figure 2.3 caption.

CHAPITRE III

INTEGRATION OF MULTI-PROXY DATASETS IN A PEATLAND MODELLING EXERCISE: A NEW TOOL FOR PALAEO- ECOLOGICAL STUDIES

Anne Quillet¹, Michelle Garneau², Simon van Bellen³ and Steve Frohking⁴, Eeva-Stinna Tuittila⁵

¹ GÉOTOP et Chaire DÉCLIQUE-Hydro-Québec, Université du Québec à Montréal, succ. centre-ville, CP 8888, Montréal QC. H3C 3P8, Canada.

² GÉOTOP, Chaire DÉCLIQUE-Hydro-Québec & Département de Géographie, Université du Québec à Montréal, succ. centre-ville, CP 8888, Montréal QC. H3C 3P8, Canada.

³ School of Geosciences, University of Aberdeen, Elphinstone Road, Aberdeen AB24 3UF, United Kingdom

⁴ Institute for the Study of Earth, Oceans, and Space, University of New Hampshire, 8 College Road, Durham, NH 03824-3525, USA.

⁵ School of Forest Sciences, University of Eastern Finland, Joensuu Campus, Yliopistokatu 2, P.O. Box 111, FI-80101 Joensuu, Finland.

Article soumis au *Journal of Ecology*

Résumé

Afin d'évaluer l'influence des changements hydrologiques sur les écosystèmes tourbeux, nous analysons la réponse du Holocene Peat Model, conçu pour simuler le développement d'une tourbière à l'échelle millénaire, à deux types de configurations hydrologiques. Les deux sites étudiés sont des tourbières ombrotrophes ouvertes situées dans la région des Basses-Terres de la Baie James dans le Nord-Est du Canada. Pour chacun des sites deux simulations sont réalisées : la première est basée sur une reconstruction des précipitations établie à partir de données polliniques qui sert d'entrée au modèle et la seconde est basée sur une reconstruction des niveaux de nappe phréatique dérivée des analyses de Thécambes et permet le forçage de la nappe phréatique du modèle.

Les taux d'accumulation de carbone (CAR) simulés ainsi que la composition de la végétation simulée sont comparés avec des données paléoécologiques. Dans les deux expériences et les deux sites, les taux d'accumulation de carbone simulés présentent des périodes de perte nette de carbone, qui, bien qu'elles ne puissent être identifiées dans les jeux de données paléoécologiques, coïncident avec des variations des taux d'accumulation de carbone observés. La comparaison des assemblages végétaux avec les résultats des simulations souligne des différences entre les deux configurations hydrologiques.

Cette étude montre que des périodes de perte nette de carbone peuvent se produire durant le développement d'une tourbière nordique. De plus, la méthodologie utilisée ici est considérée comme utile pour l'analyse des causes des variations de végétation dans les relevés de macrorestes.

Abstract

To assess the influence of hydrological changes on northern peatland ecosystems, we analysed the response of the Holocene Peat Model (HPM), designed to simulate peatland development at millennial timescale, to two hydrological settings. The studied sites are two open ombrotrophic peatlands located in the James Bay Lowlands in Northeastern Canada. For both sites, two simulations were realised: one based on a precipitation reconstruction from pollen data, used as input in the model, and a second using a water table depth reconstruction derived from testate amoebae to apply a water table forcing on the model.

Simulated variations in carbon accumulation rates (CAR) and vegetation composition were analysed against the palaeoecological datasets of carbon accumulation and vegetation composition. Results in CAR in both sites and hydrological settings showed periods of net carbon loss, which coincided with fluctuations in observed CAR, though they cannot be traced in palaeoecological datasets. The comparison between plant macrofossils records and simulated vegetation distributions highlighted differences between precipitation and water table depth driven simulations.

This study shows that periods of net carbon loss can occur during the development of northern peatlands. Additionally, the methodology used was found useful to analyse the origin of vegetation shifts in macrofossil datasets.

3.1 Introduction

Northern peatlands are wetland ecosystems, where anoxic conditions limit decomposition and enable these ecosystems to store large amounts of organic carbon as peat. The total amount of carbon stored in northern peatlands is estimated at ca. 547 Pg (Yu *et al.*, 2010), though they cover about 3% of the world's terrestrial area (Charman, 2002). Peatlands have an impact on the climate radiative forcing at a millennial time scale (Frolking and Roulet, 2007) and are therefore of particular interest for global carbon cycle studies.

On the millennial timescale, studying carbon accumulation patterns of peatlands relies on the analysis of peat composition and stratigraphy. Peat is composed of more or less preserved vegetation assemblages recording past ecohydrological changes (e.g. Tuittila *et al.*, 2007). Additionally, peatlands store fossils of testate amoebae assemblages that are used in quantitative reconstructions of peatland water table level and pH conditions (Mitchell, Charman and Warner, 2008) as well as other remnants that act as records of past local and regional conditions such as pollen and charcoal (Väliranta *et al.*, 2007). The analysis of peatlands can support the understanding of variations in carbon dynamics throughout the Holocene.

Net carbon accumulation is the balance between production and decomposition. Both allogenic and autogenic processes can influence this balance. These complex processes have been the focus of numerous modelling efforts, attempting to capture the nature of processes controlling carbon accumulation (Belyea and Baird, 2006 ; Clymo, 1984 ; Frolking *et al.*, 2001 ; Frolking *et al.*, 2010 ; Hilbert, Roulet and Moore, 2000 ; Ise *et al.*, 2008). Moreover, peatland ecohydrology, which is mainly influenced by regional climatic variations, local hydrological changes and autogenic successions in the peatland, involves different feedback processes that affect carbon accumulation. Over the last years, several modelling studies have aimed to take these

processes into account (Baird, Morris and Belyea, 2012 ; Eppinga *et al.*, 2009a ; Morris, Baird and Belyea, 2012 ; Morris, Belyea and Baird, 2011).

The evaluation of the capacity of an ecosystem model to capture the mechanisms and reproduce their outcomes in realistic rates can be achieved by testing it against measured data. This approach is still rather seldomly conducted in peat accumulation modelling due to the lack of complete data sets that cover processes or their outcomes in a comparable time scales with the model. Peatland development covers processes over a large variety of time scales that together leave a record on their net outcome in peat deposits. Recent development of quantitative palaeoecological methods and reconstruction of past environmental conditions (e.g. Birks and Seppä, 2010 ; Charman *et al.*, 2009 ; Seppä *et al.*, 2008 ; Välranta *et al.*, 2012) as well as the availability of multi-proxy data over a peatland history gives a novel opportunity for model evaluation.

The Holocene Peat Model (HPM) is a simple dynamic model simulating the transient evolution of a peatland since its early stages (Frolking *et al.*, 2010). The aim of HPM is to capture northern peatland ecosystem behaviour in order to quantify the amount of carbon sequestered in these ecosystems during the Holocene. HPM has so far been evaluated against site datasets (Mer Bleue Bog, Canada, Frolking *et al.*, 2010) and a chronosequence formed by several sites in Finland (Tuittila *et al.*, 2013). Moreover, sensitivity analyses have been performed on the model (Quillet *et al.*, 2013 ; Quillet, Garneau and Frolking, *in press*) highlighting its performance and limitations. These together identified water balance calculation as a limitation in HPM since it relies on several parameters with large uncertainty, such as the peatland outflows and the watershed inflows influencing nutrient availability.

In this study we aim to explore the manifold responses of peatland ecosystems to hydrological changes by analysing the response of the HPM, namely carbon accumulation and vegetation distribution, to different hydrological settings. The

settings are based on two palaeoecological proxies: precipitation reconstruction from pollen data (Viau and Gajewski, 2009) and water table depth reconstruction derived from testate amoebae (van Bellen, Garneau and Booth, 2011). Simulation results are analysed against palaeoecological datasets of carbon accumulation rates and plant macrofossils from two ombrotrophic peatlands located in Northeastern Canada. We hypothesise that the integration in the model of reconstructed hydrological changes from different proxies will help distinguish sources of variations in carbon accumulation and vegetation distribution during peatland development.

3.2 Palaeoecological analyses

3.2.1 Sites

The two ombrotrophic peatland complexes are located in the James Bay lowlands in Québec, Canada. The region is characterized by post-glacial environments and comprises a gradient of ecosystems from closed-crown boreal forest in the south to sub-arctic ecosystems in the north east. The studied peatlands are located in the Eastmain River watershed, close to the recently created Eastmain Reservoir (Figure 3.1). In this watershed, peatlands are estimated to cover about 8% of the area (Grenier *et al.*, 2008).

The two sampled peatlands, Lac Le Caron peatland (LLC, 52°17'15"N/75°50'21"W) and Mosaik peatland (MOS, 51°58'55"N/75°24'06"W) (Figure 3.1), are pristine open ombrotrophic raised bogs, dominated by *Sphagnum* and ericaceous shrubs. The development of these peatlands followed the retreat of the Laurentide ice sheet ca. 7500 cal BP and took place through depression infilling and through paludification at a later stage (van Bellen *et al.*, 2011). Current mean annual temperature for the region is -2°C and one third of the total annual precipitation (ca. 0.74 m.yr⁻¹) falls as snow (Hutchinson *et al.*, 2009). LLC peatland developed in a depression edged by an

escarpment and peat thickness reaches 5m in its deepest part. At its center, LLC presents an open area including few large pools and wet hollows and covers 2.24 km². MOS peatland developed on a relatively flat topographical basin. Its deepest point is found around 3m. Overall, this peatland is much wetter than LLC and is characterized by a series of large pools and wet hollows in its central area. MOS covers 2.67 km². A more detailed description of both sites can be found in van Bellen *et al.* (2011).

3.2.2 Material collected and analyses

Ecohydrological reconstructions were obtained from central cores located near the thickest section of each peatland using a Jeglum (Box) corer for the first top meter and below that a Russian corer down to the mineral soil. Dry bulk density and organic carbon content were calculated after drying and loss on ignition (LOI) of 1 cm³ contiguous subsamples. Plant macrofossil analyses and testate amoebae analyses were performed at a 4 cm resolution for each core. The cores were dated with radiocarbon (12 dates for LLC and 10 for MOS) and calibrated with the IntCal04 calibration curve (Reimer *et al.*, 2004). The detailed techniques of analysis and a comprehensive description of the results are presented in van Bellen, Garneau and Booth (2011).

3.2.3 Water table depth reconstruction

We applied testate amoebae for water table depths reconstruction. Testate amoebae are unicellular rhizopods characterised by both their species specific sensitivity to water table depth and their resistance to decomposition (Mitchell, Charman and Warner, 2008). Identifying amoebae from a peat core allows quantitative reconstructions of the past water table depths by use of a transfer function (Booth, 2008). The results of the transfer function provide a reconstruction of the peatland water table depth since its early development. Water table depths have been

reconstructed for LLC and MOS (van Bellen, Garneau and Booth, 2011), with MSE of ± 0.11 m and ± 0.09 m respectively (Figure 3.3b and c).

3.3 The forcing exercise

3.3.1 The Holocene Peat Model

The Holocene Peat Model (HPM) includes feedbacks between vegetation, peat properties, water table depth and climate (Figure 3.2). The model includes 12 plant functional types (PFTs, i.e. groups of species, see also Laine *et al.* (2012)) that together form vegetation as an assemblage of PFTs. Each PFT has its own relative NPP, rate of decomposition and responds in its own way to water table variations and nutrient status (see Appendix 3.1). Further details on the physical processes behind the model can be found in Frohking *et al.* (2010).

3.3.2 Methods

To evaluate the performance of the Holocene Peat Model and to explore the influence of water table depth on carbon accumulation and vegetation composition in the two boreal peatlands studied by (van Bellen *et al.*, 2011 ; van Bellen, Garneau and Booth, 2011) we took the following steps:

- HPM was calibrated to suit the local site specifics of the sites using data from van Bellen, Garneau and Booth (2011);
- HPM was provided with reconstructed precipitation from Viau and Gajewski (2009). One simulation per site was performed;
- HPM was forced with reconstructed water table depths (van Bellen, Garneau and Booth, 2011), i.e. all components of the water balance calculation (e.g.

precipitation, runoff, evapotranspiration) are ignored and reconstructed water table depth values replace the water balance calculation output in all other sections of the model. One simulation per site was performed.

3.3.2.1 Calibration

The calibration method chosen here focused on the reconstructed carbon accumulation and vegetation patterns. Therefore, we calibrated HPM against the shape of the accumulation curve of both peatlands that were obtained from loss on ignition analyses. Nonetheless, there are several millions of possible combinations of calibration parameters, since the model includes more than a hundred parameters, each potentially taking different values. The results of a sensitivity analysis performed on HPM helped constraining the number of parameters impacting carbon accumulation to a relatively small number (i.e. 26). In order to tally with the sensitivity analysis, each parameter value in this experiment lie within its range of plausible natural variations defined in Quillet *et al.* (2013) and Quillet, Garneau and Frolking (*in press*).

Some model parameters are directly related to peatland location and hence were estimated from available data. This was the case for annual precipitation (ca. 0.74 m.yr^{-1}) (Hutchinson *et al.*, 2009) annual potential evapotranspiration (ca. 0.4 m.yr^{-1}) (Canada Centre for Mapping and National Atlas Information Service, 1974) and maximum potential NPP estimated to ca. $0.7 \text{ kg.m}^{-2}.\text{yr}^{-1}$ (Del Grosso *et al.*, 2008). These values are kept constant during the simulation. In this study, the relative NPP of some PFTs responds to some regional characteristics but, similarly to a Finnish experiment (Tuittila *et al.*, 2013), the relative NPP of grasses, minerotrophic herbs and minerotrophic sedges have been lowered in comparison to the original setting used to simulate the Mer Bleue bog, located at a lower latitude

(45.40°N) (Frolking *et al.*, 2010). The different parameter values used to calibrate the model to our study sites are detailed in Appendix 3.1.

Other parameters are 'peatland-specific' and depend on both local peatland development and how it is influenced by its adjacent environment (e.g. basin shape, nutrient input or hydrology). For the two bogs, we used different simulation lengths based on their basal ages (7562 years for LLC and 6984 years for MOS) and different parameter values for minimum bulk density and maximum bulk density increase (Appendix 3.1). The two sites present differences in peat thickness at their center and also different long-term carbon accumulation patterns influenced by both allogenic and autogenic processes (Figure 3.4). LLC has a concave accumulation curve, i.e. carbon accumulation is rapid during the early development stages and slows down thereafter, whereas carbon accumulation at MOS is nearly linear. Carbon accumulation patterns at both sites have been further analysed by van Bellen, Garneau and Booth (2011). The parameter controlling the decomposition rate of the anoxic compartment, i.e. the length of the anoxia gradient, as well as parameters controlling the shape of the NPP curve have a strong influence on carbon accumulation (Quillet *et al.*, 2013 ; Quillet, Garneau and Frolking, *in press*). They have thus been adjusted for both sites (Appendix 3.1).

In HPM, each simulation begins with an initiation phase, during which peat builds up until it reaches a certain thickness (Frolking *et al.*, 2010). Once this peat height is reached, the water balance and the other feedbacks between the different processes are activated for the rest of the simulation. During the initiation phase, the water table depth is kept constant (to insure that peat accumulates) at a level of 0.07 m below the surface (Frolking *et al.*, 2010). In this study, 0.1 m of peat thickness was required to activate the dynamical processes and the water balance calculation. This 0.1 m can be compared to the bottom section of the core, in which organic matter is mixed with

other sediments and cannot be considered as peat. The peat produced during the initiation phase was thus not included in the final results.

3.3.2.2 Addition of precipitation time series to the simulation setting

HPM offers the possibility to create a random series for precipitation derived from the current climatic precipitation average. This allows the simulation to be more realistic than constant precipitation but does not enhance the quality of the simulation in term of its historical reconstruction. Moreover, the different evaluations of HPM have shown that precipitation is, among all model parameters, one of the most influential (Frolking *et al.*, 2010 ; Quillet *et al.*, 2013 ; Quillet, Garneau and Frolking, *in press*).

We used the Holocene precipitation reconstruction for the boreal and low arctic regions of Canada from Viau and Gajewski (2009). This reconstruction has been achieved with the help of multiple pollen diagrams and the modern analogue technique. The obtained time series gives precipitation anomalies (i.e. deviations from the present average value) for northern Québec at a centennial resolution for the last 9000 years BP. It was applied to both sites.

We built the reconstructed precipitation time series as input in the model by adding the present annual precipitation value (here 0.74 m.yr^{-1}) to these anomalies (Figure 3.3a). This precipitation time series is based on 100-yr reconstruction values. The combination of this series with the calibration settings completes the baseline simulation frame of our two sites, which are hereafter named P_{LLC} and P_{MOS} .

3.3.2.3 Water table depth forcing

In order to highlight the role of the water balance in the simulation results, we also forced the model with water table depth reconstructions from testate amoeba assemblages (van Bellen, Garneau and Booth, 2011). The water table depths have

been interpolated according to the age-depth profiles, so that the series have a yearly resolution (Figure 3.3b and c). In these simulations, we deactivated the different components of HPM linked to the water balance calculation, so that neither precipitation, nor evapotranspiration, nor runoff and runoff influenced the results (Figure 3.2). Reconstructed water table depths from testate amoebae thus replaced the water table depth values calculated by the water balance module in the original version of the model. These simulations are designated as W_{LLC} and W_{MOS} in the following sections.

3.4 Results

3.4.1 Precipitation and water table depth

Reconstructed precipitation based on the study from Viau and Gajewski (2009) and used as input in the simulations, is presented in Figure 3.3a. This dataset does not present error bars, though error might be important on reconstructed precipitation. However, for the purpose of this study, trends and variations in precipitation are needed, rather than actual precipitation amounts. We thus argue that this dataset can be used as an estimate for our study region during the Holocene. Figure 3b and c respectively present reconstructed water table depths for Lac Le Caron and Mosaik peatlands derived from testate amoebae analyses (van Bellen, Garneau and Booth, 2011) along with simulated water table depths. The error for these reconstructions varies depending on species composition and on the degree of decomposition of the peat. Although the water table depths and precipitation time series do not follow the same trends, there were correspondences between them (e.g. around 7000 cal BP, where precipitation decreases and water table depths in both records tend to increase). Other periods show dissimilar behaviour such as the period of high precipitation around 3750 cal BP (Figure 3.3a) that were not reflected in the water table reconstructions (Figure 3.3b and c). Comparison between the simulated water table

depths in the P_{LLC} and P_{MOS} simulations and reconstructed water table depths from testate amoebae (Figure 3.3b and c) showed comparable ranges, amplitudes and also general trends during the past 7000 years, suggesting that the water balance calculation of the model gives reasonable results. Furthermore, these comparable trends point out the response of testate amoebae to precipitation on a millennial scale. On shorter time scales however, some periods show clear discrepancies between the curves, for example around 6000 cal BP at MOS and between ca. 2000 and 1000 cal BP at both sites. During these periods, testate amoebae may be responding to other signals; perhaps linked to the fen-bog transition at MOS around 6000 cal BP, and to some changes in the regional climatic conditions between 2000 and 1000 cal BP, as identified in other studies (Lamarre, Garneau and Asnong, 2012 ; van Bellen *et al.*, submitted), or the model may be misrepresenting climate impacts on water table dynamics.

3.4.2 Carbon accumulation

Accumulated carbon masses resulting from the simulation including reconstructed precipitation and from the water table depth-forced simulation are presented in Figure 3.4. For comparison, this figure also presents the accumulated carbon obtained from the LOI analyses of peat cores. Overall, carbon accumulation at LLC (Figure 3.4a) showed a concave shape with two periods of higher accumulation between 5500 and 4500 cal BP and during the last millennium, in the uppermost section of the core. Although the model was calibrated on carbon accumulation (i.e. total mass of carbon and basic shape of the carbon accumulation curve), these phases were not reproduced in the simulations, suggesting that they might be associated to other environmental variables or to autogenic processes not represented in HPM. Figure 3.5 allows the comparison of the annual carbon accumulation rates (CAR) in more detail. For simplification, these results are identified as CAR_{LLC} and CAR_{MOS} in the next sections. CAR_{LLC} and CAR_{MOS} are compared with the carbon content of each cohort

(i.e. simulated year) at the end of the simulation on panels a and b, and with the net annual carbon balance on panels c and d. On all four panels, simulation results showed extreme rates of accumulation at the beginning of the simulations. These values were probably artefacts of the initiation phase in HPM, which is less constrained. During the first development phase in LLC (Figure 3.5a and c), i.e. from ca. 7500 to 5600 cal BP, both empirical data analyses and simulations showed similar trends. However, between 5600 and 2500 cal BP, simulations showed rather constant carbon accumulation rates and the carbon accumulation slowdown is only replicated in the W_{LLC} simulation in panel a. Indeed, CAR_{LLC} presented large fluctuations during this period. Only the water table-forced simulation W_{LLC} showed similar fluctuations suggesting that the calculation of water balance in HPM could not induce these variations in the P_{LLC} simulation. For the last 1000 simulation years, accumulated carbon followed again a trend similar to the palaeo-reconstructions (Figure 3.4a) and also similar fluctuation patterns of the net annual carbon balance are observed for both P_{LLC} and W_{LLC} (Figure 3.5c). However, the simulated remaining carbon mass was much lower than the observation during this period (Figure 3.5a). This suggests that peat decomposition in the acrotelm might be overestimated in the model simulations.

The shape of the MOS cumulated carbon curve (Figure 3.4b) was very different from the LLC one, since carbon accumulated almost linearly over time during the development of this peatland. Still, several periods of slight slowdown between 5500 and 4800 cal BP and between 1900 and 400 cal BP and a short period of faster carbon accumulation around 2000 cal BP were observed. The simulated accumulated carbon curves, on the contrary, presented a lot of fluctuations between 7000 and 4000 cal BP indicating that the simulated initial phase of development was not representative of the original reconstructed conditions on the site. Indeed, CARs for MOS were low and relatively stable between 7000 cal BP and 5600 cal BP, whereas P_{MOS} and W_{MOS} net annual carbon balance values varied much during the same period (Figure 3.5d).

The short phase identified around 2000 cal BP and characterised by high carbon accumulation rates was poorly reproduced in the simulations. At the top of the MOS core (i.e. during the past 500 years AD), carbon accumulation rates fluctuated again. Similarly to the LLC results, these variations were reproduced in the net annual carbon balance from the W_{MOS} simulation (Figure 3.5d).

Periods during which decomposition exceeded production resulting in a net loss of carbon, can only be identified in the simulation results; losses through decomposition leave no trace in the cores. However, long periods of net carbon loss result in lower carbon accumulation rates seen in peat cores. Unfortunately, if carbon accumulation rates fluctuate rapidly (interannual to decadal fluctuations), LOI analyses result in low apparent carbon accumulation rates rather than fluctuations because of the low time resolution of the analyses. P_{LLC} and P_{MOS} simulations presented large periods of carbon loss: e.g. between 2000 and 1000 cal BP for LLC and between 5800 and 5200 cal BP for MOS (Figure 3.4). Carbon accumulation rates in Figure 3.5c and d suggested several shorter carbon loss periods. In LLC (Figure 3.5c), several severe decreases in CAR_{LLC} were characterised by a loss of carbon in the simulations. This was the case at ca. 7000 cal BP for both P_{LLC} and W_{LLC} and at ca. 5300 cal BP, ca. 2800 cal BP and ca. 800 cal BP for W_{LLC} . The P_{LLC} simulation generated other carbon loss events between 2000 cal BP and 500 cal BP, which coincided with fluctuations in CAR_{LLC} . Interestingly, around 5400 cal BP, there was a drastic increase in CAR_{LLC} , which was linked to high bulk density, and translating into a drastic carbon loss in the W_{LLC} simulation. This suggests that the higher bulk density during this period could be associated with a carbon loss. A decrease appeared in CAR_{MOS} around the same period and important carbon losses were simulated in both P_{MOS} and W_{MOS} . HPM's configuration for MOS might thus have been less resilient than for LLC simulations, even when the same precipitation reconstructions were used.

For MOS, simulated carbon accumulation rates showed a greater carbon loss frequency (Figure 3.5d). The W_{MOS} simulation showed carbon loss during periods where fluctuations were observed in CAR_{MOS} (e.g. at ca. 6400 cal BP and 100 cal BP). Nevertheless, P_{MOS} records important carbon losses at ca. 3600 cal BP and 3100 cal BP that match with CAR_{MOS} but are less severe in the W_{MOS} simulation. Around 2500 cal BP, the loss of carbon in the W_{MOS} simulation coincided with a large increase in CAR_{MOS} . W_{MOS} followed here a water table dropdown imposed by the water table reconstruction. However, the processes that drove carbon accumulation at MOS during this period were obviously different from the ones included in the model. This could hypothetically be related to a strong and/or periodic influence of runoff and associated increase in nutrient input at the site that cannot be taken into account in the model, since it considers that nutrient availability gradually vanishes with peat thickness.

3.4.3 Vegetation distribution

Plant macrofossils offer another independent dataset that can enhance our system comprehension. A condensed version of the plant macrofossil diagrams is presented in Figures 3.6a and 3.7a for LLC and MOS respectively. Detailed plant macrofossil analyses can be found in van Bellen, Garneau and Booth (2011). Here the chosen vegetation classes aim at matching the different PFTs of the model for the sake of comparison. Yet vegetation classes were only merged when macrofossil identification was not sufficiently specific to correspond to the different PFTs.

However simulation results in Figures 3.6 and 3.7 highlight a strong resilience of PFTs relative to the macrofossil diagrams. For example, though feather mosses occur sporadically and with small percentages in the macrofossil diagrams, they are overrepresented in the simulations.

In LLC (Figure 3.6a), after the peatland initiation with an abundance of brown mosses, the fen phase was dominated by a combination of Cyperaceae and ligneous species. This fen phase lasted less than 400 years. At ca. 7200 cal BP, the very sharp fen to bog transition was completed and *Sphagnum* species (mainly section *Acutifolia*) dominated the profile. In general, *Sphagnum* section *Acutifolia* remained dominant through time, although wetter *Sphagnum* species along with Cyperaceae occurred episodically.

In MOS (Figure 3.7a), the fen phase was largely dominated by Cyperaceae and lasted more than 1500 years. The fen to bog transition was gradual until *Sphagnum* section *Acutifolia* finally dominated the profile around 4700 cal BP. Contrasting with the general stability of the LLC sequence, the MOS profile showed a periodic changeover of wet and dry vegetation assemblages, representative of the responsiveness to hydrological changes of this site.

The P_{LLC} and W_{LLC} simulation results (Figure 3.6b and c) start with a peatland initiation phase dominated by herbs and sedges more than by brown mosses. The simulated fen to bog transition was very gradual and not representative of the observed step wise development at LLC. In the later phases, the vegetation was composed of both lawn and hummock *Sphagnum* species, which include *Sphagnum* section *Sphagnum* that are relatively unimportant in the LLC macrofossil record (Figure 3.6a). In general, the simulated vegetation was wetter and the dry species (such as ligneous plants) were more resistant to changes than the macrofossil dataset would suggest. However, the general vegetation distribution pattern was well reproduced.

Looking in more detail at the vegetation sequence, some differences between P_{LLC} and W_{LLC} could be detected. In the W_{LLC} simulation, hollow *Sphagnum* increased between 5200 and 4500 cal BP characterising wetter conditions. However, no important change in vegetation occurred in the P_{LLC} simulation as well as in the plant

macrofossils. This suggests again the important resilience of *Sphagnum* section *Acutifolia* species to changes in water table depth which is captured well in the model. On the other hand, at ca. 5800 cal BP, around 2500 cal BP, and 1500 cal BP, the W_{LLC} simulation captured the wet phases detected in the macrofossil assemblages while P_{LLC} only recorded a very wet phase between 2000 and 1000 cal BP. The wetter phases at ca. 4000 cal BP and 500 cal BP were better represented in the P_{LLC} simulation than in the W_{LLC} simulation.

Similarly to the LLC results, the initiation phase in the P_{MOS} and W_{MOS} simulations showed a dominance of herbs and sedges. In the W_{MOS} simulation, wet mosses occurred at levels where brown mosses were found in the macrofossils records. However, their simulated abundance was exaggerated in the simulation, on the contrary to LLC results. During the bog phase (since ca. 5500 cal BP), the alternation of wet and dry phases was replaced by smooth wiggles in the *Acutifolia* versus *Sphagnum* sections in the vegetation assemblage. In both simulations, variations affected hollow *Sphagnum* and occasionally wet mosses. The simulated vegetation for the MOS site was strongly resilient to changes.

In the P_{MOS} simulation, the appearance of hollow *Sphagnum* was in agreement with the macrofossil assemblages at e.g. 3300 cal BP and 2500 cal BP and matches also with several periods where *Sphagnum* section *Sphagnum* arise in the profile (e.g. around 3700 cal BP, between 1800 and 1300 cal BP). In the W_{MOS} simulation, the small increases in the abundance of hollow *Sphagnum* and wet mosses also coincided with wetter periods in the macrofossils dataset (e.g. around 4700 cal BP, between 3000 and 3500 cal BP, at ca. 400 cal BP and at the top of the core). Here again, though some humid or wet phases were recorded simultaneously between 3900 and 2500 cal BP, P_{MOS} and W_{MOS} showed many asynchronous features along the profile.

3.5 Discussion

Our results showed that, when calibration is carefully performed, peatland development is reasonably reproduced by HPM. The water balance calculation of HPM delivered a water table depth in agreement with the testate amoeba reconstructions and carbon accumulation rates showed comparable ranges to those resulting from the LOI analyses. Variations in the macrofossil records were better represented in the P_{LLC} and W_{LLC} simulations than in the P_{MOS} and W_{MOS} simulations. The comparison between the results of the two sites presenting different geomorphic and hydrological conditions highlighted the capacity of the model to follow different behaviours. Differences in simulation representativeness however might be linked to the limitations of both the model and the experiment calibration.

3.5.1 Model limitations

Peatland initiation, as highlighted in the previous section, was not well reproduced in the simulations. Several factors limit its reproducibility. The geomorphic specifics of the sites and regions are not taken into account in HPM. Moreover, fen to bog transition in HPM is gradual and minerotrophic species such as grasses or herbs remain present in the assemblage for several thousand years after the *Sphagnum* establishment. This behaviour is not recorded in the macrofossil assemblages. In HPM, the transition is driven by peat accumulation solely and thus cannot be abrupt. We observed this inability of HPM to produce abrupt transitions also in a chronosequence of several mires (Tuittila *et al.*, 2013).

When looking at the carbon accumulation results, the variability of the P_{LLC} and W_{LLC} simulations was reduced in comparison to the simulations for the MOS site, which showed large variability (Figure 3.5d). The opposite was observed in the simulated vegetation distributions, where the P_{LLC} and W_{LLC} simulation showed a much greater variability than the P_{MOS} and W_{MOS} simulations (Figures 3.6 and 3.7). These

behaviours are probably related to the differences in anoxia gradient parameterisation in both sites (Appendix 3.1). In the current version of HPM, the representation of the anoxia gradient highly depends on the decision of the user, i.e. parameter values have to be chosen and no comparable site data is so far available to estimate these values. This creates an important source of uncertainty in the simulations.

Additionally, differences in the parameter estimating the minimum profile relative transmissivity probably impacted the results (Appendix 3.1). At MOS this value was high and hence water table depth fluctuated rapidly in comparison to LLC (Figure 3.3b and c). Rapid changes in the water table depth of the P_{MOS} simulation also affected carbon accumulation rates, which also showed rapid shifts in MOS (Figure 3.5b). Unfortunately, the minimum profile relative transmissivity value had to be kept high in order to limit the total carbon mass and to insure that the simulation remained representative of the MOS site. This parameter was already identified as causing uncertainty in the results from a sensitivity analysis of HPM (Quillet *et al.*, 2013 ; Quillet, Garneau and Froelking, *in press*).

The limitations presented here collectively suggest that ecohydrological processes are the weak area in our understanding of peatland dynamics and its representation on process-based models. Knowledge of the anoxia gradient, the relative transmissivity and the fen to bog transition need to be enhanced in order to improve calibration and most probably also the representativeness of the model results.

3.5.2 The role of water table depth forcing in the simulation results

In the case of carbon accumulation, simulations with reconstructed precipitation tended to be smooth or to show isolated peaks that lasted only a couple of years (Figure 3.5). This is probably due to the proxy itself. The comparison between reconstructed precipitation and reconstructed water table depths from testate amoebae (Figure 3.3) highlights both the independence of the two records and the complexity

of their response. The relationship between water table depth and precipitation at this time scale appeared to be non-linear. Indeed, changes in water table depth in a peatland can occur for several reasons independently from precipitation: other climatic changes (e.g. temperature, evapotranspiration), autogenic changes (e.g. fen-bog transition, lateral expansion etc.) and hydrological changes. Water table depth forcing thus provided better simulations of carbon accumulation in peatland than precipitation alone.

Contrary to our expectations, the forcing experiment did not indubitably improve the representation of the vegetation distribution. While W_{LLC} results seem to be in greater agreement than P_{LLC} with macrofossil data, W_{MOS} clearly failed to represent the major variations in macrofossils. In fact, MOS peatland presents a great variability in macrofossil records but presents also a flatter topographical basin than LLC and is thus subject to less effective drainage (van Bellen *et al.*, 2011). Vegetation macrofossils showed that MOS site has been very sensitive to hydrological variations. Additionally, the lack of representation of the variability in the model results might be related to the poor resolution of the testate amoeba dataset. Indeed, a 4-cm resolution is coarse and cannot capture rapid (i.e. decadal to centennial) changes in testate amoeba assemblages, which are known to respond to water table fluctuations within seasons (Mitchell, Charman and Warner, 2008 ; Warner, Asada and Quinn, 2007). Water table reconstructions based on testate amoeba analyses at a higher resolution would be necessary to verify the role of the water table forcing on the model results. Moreover, the resilience to changes varies between proxies e.g. vegetation assemblages respond with a lag of decades and appear generally buffered to changes in water table via self-regulation of moisture content and the competition between species (Väliranta *et al.*, 2012). Nonetheless, HPM will not simulate rapid and large shifts in vegetation composition without equivalently rapid and large shifts in water table depth. The causes of variability in the simulation results should be

further investigated in order to assess the role of calibration and of site specificities in these processes.

3.5.3 Long-term net carbon loss

One major finding of this study, the loss of carbon during the peatlands history was emphasized by the several periods of long-term carbon loss occurring in the simulation results. Some of these periods occurred in the simulations run with precipitation reconstructions, others in the simulations forced with water table reconstructions and they appeared in the simulations of both sites. Several studies focusing on the contemporary net carbon balance of peatlands highlight the great interannual variability of the carbon balance that can result into a change from a net sink to a net source (e.g. Alm *et al.*, 1999 ; Koehler, Sottocornola and Kiely, 2011 ; Nilsson *et al.*, 2008 ; Roulet *et al.*, 2007). For example Roulet *et al.* (2007) measured the carbon balance at Mer Bleue Bog in Canada during 6 years and estimated that the annual carbon balance can vary between a carbon gain of $105 \text{ g.m}^{-2}.\text{yr}^{-1}$ and a carbon loss of $50 \text{ g.m}^{-2}.\text{yr}^{-1}$. Though these values are only available for relatively short time periods (less than a decade), these results are in the same range of amplitudes as our simulation results (Figure 3.5c and d). This gives us confidence that the representation of carbon loss phases in the HPM simulation, although they cannot be validated against field data, were plausible. Other processes may have an impact on the net carbon balance on millennial time scale such as vegetation shifts but lacking data makes it difficult to evaluate this behaviour in the model. Yu (2011) interpreted carbon fluxes of peatlands from different regions all over the globe using the available basal dates and carbon accumulation profiles. He found that the net carbon balance in the northern peatlands show large fluctuations during the Holocene and periods of long term net carbon loss occurring in tropical peatlands.

3.5.4 Tracing vegetation history in relation to climate and other forcing

Considering that the HPM simulations have limitations and that the model is designed to reproduce large-scale patterns of peatland development, we argue that the proper reproduction of a vegetation shift in a simulation implies that the processes responsible for this shift are included in the model. As a corollary, simulation results can be helpful at identifying the causes of shifts and variations in the macrofossil dataset. However, caution is advised in the historical interpretation of the results since the chronology of our sites is coarse and because the results are also compared with the pollen reconstruction from Viau and Gajewski (2009) based on a different chronology and including some error.

For example, between 4100 and 3900 cal BP, both macrofossil sequences (Figures 3.6a and 3.7a) indicated change in vegetation towards wetter plant associations. Both present a decline in *Sphagnum* section *Acutifolia* in LLC with an increase in Cyperaceae, ligneous fragment and wetter *Sphagnum* species. During this period, both LLC and MOS recorded decreasing trends in CAR (Figure 3.5), associated with decreases in bulk density, and a high amount of unidentified organic matter (Figures 3.6a and 3.7a). Moreover, during this period the carbon accumulation showed a slowdown for P_{MOS} and high carbon loss for W_{MOS} (Figure 3.5d). In agreement with our results, Beaulieu-Audy *et al.* (2009) report a decrease in CAR around 4000 cal BP in three peatlands in the La Grande river watershed, located north of the James Bay lowlands.

At that time, around 4000 cal BP, reconstructed water table depths were ~0.15 m at both sites, though the MOS water table was declining (Figure 3.3b and c). Additionally, a period of increased precipitation occurred slightly earlier (i.e. ca. 4200 cal BP) and reached its maximum around 3800 cal BP (Figure 3.3a). The results of the water table depth forcing (Figures 3.6c and 3.7c) did not record any major variation in the vegetation during this period. However, the P_{LLC} and P_{MOS}

simulations showed a clear decline of hummock *Sphagnum* to the favour of wetter PFTs (and of ombrotrophic herbs in the case of P_{LLC}). The increase in precipitation might thus be involved in the sudden vegetation change towards wetter associations in both LLC and MOS around 4000 cal BP. HPM was unable to capture these dynamics.

Between ca. 6000 and 5700 cal BP, MOS presented a shift in vegetation with increasing Cyperaceae to the detriment of ligneous species (Figure 3.7a). This wet shift coincides with the observed slight decrease in carbon accumulation reconstructed from the LOI analyses (Figure 3.5b). Simulated vegetation distributions showed a large presence of wet mosses and hollow *Sphagnum* in the W_{MOS} simulation (Figure 3.7c) but no drastic vegetation change is observed in the P_{MOS} simulation (Figure 3.7b). Since only water table-forced simulations could reproduce this vegetation shift, we argue that precipitation was probably not a major control on vegetation dynamics during this period. Moreover, a fire-induced change resulting in a wet shift (Morris *et al.*, submitted ; Sillasoo, Väiliranta and Tuittila, 2011) can probably be dismissed since no fire has been recorded at MOS during this period and fire frequencies were low in the region (van Bellen *et al.*, 2012). This event could thus be related to autogenic changes in the MOS peatland such as a local change in hydrology.

3.5.5 Multiple proxies

Regarding both carbon accumulation and vegetation distribution results, we observe that certain events (i.e. periods of carbon loss and dry or wet periods in the vegetation assemblages) are replicated in the simulations with reconstructed precipitation and others are rather replicated when HPM's water table depth is forced. This suggests that the two simulation experiments supplement each other. As usually highlighted in palaeoecological studies, we observe that the use of multiple proxies, each of them characterized by a specific sensitivity to allogenic and autogenic changes, can be

useful in modelling studies to reproduce the historical changes in a peatland. Moreover, using multiple proxies from the same peat core (and thus following the same age-depth model) as input in the model eliminate errors associated with tuning (Blaauw, 2012). This exercise facilitates comparison between results from different proxies.

3.6 Conclusion

The dynamic response of peatlands to ecohydrological changes has been assessed by the comparison of two simulation experiments on the development of two peat bogs located in the James Bay lowlands in Northeastern Canada, with the help of a reconstructed precipitation time series and with a forcing of the water table depth reconstructed from testate amoebae analyses.

In this study, HPM simulated phases of carbon loss corresponding to periods of low or sharp decrease in carbon accumulation rates that are in level measured in contemporary studies measuring carbon gas fluxes. Moreover, the results highlighted the capacity of HPM to reproduce general patterns in two peatlands presenting different geomorphic and hydrological conditions influencing the ecological response while pointing out the weakness in the knowledge on peatland ecohydrological processes.

The differences in the model responses that we found between sites stress the important heterogeneity between peatlands located in the same region; this heterogeneity makes large scale modelling challenging. The successful simulation of variations observed in the palaeo-records indicates that the model comprehends the representation of processes driving these variations. Thus, we conclude that the methodology applied here can be used to help distinguish the various causes of carbon accumulation shifts in palaeoecological studies.

Acknowledgments

The authors acknowledge Alain Tremblay (Environment Production, Hydro-Québec) for logistic and financial support within the Eastmain-1 project. AQ was supported by funds from the Canadian Foundation for Climate and Atmospheric Sciences, by funds supporting the Chaire Déclique at GEOTOP-UQAM (MG, SvB). SF was supported by NSF grant ATM-0628399.

References

- Alm, J., L. Schulman, J. Walden, H. Nykänen, P. J. Martikainen and J. Silvola. 1999. «Carbon balance of a boreal bog during a year with an exceptionally dry summer». *Ecology*, vol. 80, no 1, p. 161-174.
- Baird, A. J., P. J. Morris and L. R. Belyea. 2012. «The DigiBog peatland development model 1: Rationale, conceptual model, and hydrological basis». *Ecohydrology*, vol. 5, no 3, p. 242-255.
- Beaulieu-Audy, V., M. Garneau, P. J. H. Richard and H. Asnong. 2009. «Holocene palaeoecological reconstruction of three boreal peatlands in the la Grande Riviere region, Québec, Canada». *Holocene*, vol. 19, no 3, p. 459-476.
- Belyea, L. R., and A. J. Baird. 2006. «Beyond "the limits to peat bog growth": Cross-scale feedback in peatland development». *Ecological Monographs*, vol. 76, no 3, p. 299-322.
- Birks, H. J. B., and H. Seppä. 2010. «Late-Quaternary palaeoclimatic research in Fennoscandia - A historical review». *Boreas*, vol. 39, no 4, p. 655-673.
- Blaauw, M. 2012. «Out of tune: The dangers of aligning proxy archives». *Quaternary Science Reviews*, vol. 36, p. 38-49.
- Booth, R. K. 2008. «Testate amoebae as proxies for mean annual water-table depth in Sphagnum-dominated peatlands of North America». *Journal of Quaternary Science*, vol. 23, no 1, p. 43-57.
- Canada Centre for Mapping, and National Atlas Information Service (1974). Average Annual Potential Evapotranspiration Map. National Atlas of Canada. Ottawa, Natural Resources Canada.

- Charman, D. J. 2002. *Peatlands and environmental change*. Chichester, 301p.
- Charman, D. J., K. E. Barber, M. Blaauw, P. G. Langdon, D. Mauquoy, T. J. Daley, P. D. M. Hughes and E. Karofeld. 2009. «Climate drivers for peatland palaeoclimate records». *Quaternary Science Reviews*, vol. 28, no 19-20, p. 1811-1819.
- Clymo, R. S. 1984. «Sphagnum-dominated peat bog: a naturally acid ecosystem». *Ecological effects of deposited sulphur and nitrogen compounds. Discussion meeting, London, 1983*, p. 487-499.
- Del Grosso, S., W. Parton, T. Stohlgren, D. Zheng, D. Bachelet, S. Prince, K. Hibbard and R. Olson. 2008. «Global potential net primary production predicted from vegetation class, precipitation, and temperature». *Ecology*, vol. 89, no 8, p. 2117-2126.
- Eppinga, M. B., P. C. De Ruiter, M. J. Wassen and M. Rietkerk. 2009. «Nutrients and hydrology indicate the driving mechanisms of peatland surface patterning». *American Naturalist*, vol. 173, no 6, p. 803-818.
- Frolking, S., and N. T. Roulet. 2007. «Holocene radiative forcing impact of northern peatland carbon accumulation and methane emissions». *Global Change Biology*, vol. 13, no 5, p. 1079-1088.
- Frolking, S., N. T. Roulet, T. R. Moore, P. J. H. Richard, M. Lavoie and S. D. Muller. 2001. «Modeling northern peatland decomposition and peat accumulation». *Ecosystems*, vol. 4, spring, p. 479-498.
- Frolking, S., N. T. Roulet, E. Tuittila, J. L. Bubier, A. Quillet, J. Talbot and P. J. H. Richard. 2010. «A new model of Holocene peatland net primary production, decomposition, water balance, and peat accumulation». *Earth System Dynamics*, vol. 1, no 1, p. 1-21.
- Grenier, M., S. Labrecque, M. Garneau and A. Tremblay. 2008. «Object-based classification of a SPOT-4 image for mapping wetlands in the context of greenhouse gases emissions: The case of the Eastmain region, Québec, Canada». *Canadian Journal of Remote Sensing*, vol. 34, no SUPPL. 2, p. S398-S413.
- Hilbert, D. W., N. T. Roulet and T. R. Moore. 2000. «Modelling and Analysis of Peatlands as Dynamical Systems». *Journal of Ecology*, vol. 88, no 2, p. 230-242.

- Hutchinson, M. F., D. W. McKenney, K. Lawrence, J. H. Pedlar, R. F. Hopkinson, E. Milewska and P. Papadopol. 2009. «Development and testing of Canada-wide interpolated spatial models of daily minimum-maximum temperature and precipitation for 1961-2003». *Journal of Applied Meteorology and Climatology*, vol. 48, no 4, p. 725-741.
- Ise, T., A. L. Dunn, S. C. Wofsy and P. R. Moorcroft. 2008. «High sensitivity of peat decomposition to climate change through water-table feedback». *Nature Geoscience*, vol. 1, no 11, p. 763-766.
- Koehler, A. K., M. Sottocornola and G. Kiely. 2011. «How strong is the current carbon sequestration of an Atlantic blanket bog?». *Global Change Biology*, vol. 17, no 1, p. 309-319.
- Laine, A. M., J. Bubier, T. Riutta, M. B. Nilsson, T. R. Moore, H. Vasander and E. S. Tuittila. 2012. «Abundance and composition of plant biomass as potential controls for mire net ecosystem CO₂ exchange». *Botany*, vol. 90, no 1, p. 63-74.
- Lamarre, A., M. Garneau and H. Asnong. 2012. «Holocene paleohydrological reconstruction and carbon accumulation of a permafrost peatland using testate amoeba and macrofossil analyses, Kuujjuarapik, subarctic Québec, Canada». *Review of Palaeobotany and Palynology*, vol. 186, p. 131-141.
- Mitchell, E. A. D., D. J. Charman and B. G. Warner. 2008. «Testate amoebae analysis in ecological and paleoecological studies of wetlands: Past, present and future». *Biodiversity and Conservation*, vol. 17, no 9, p. 2115-2137.
- Morris, J. L., M. Väiliranta, Ü. Sillasoo, E. S. Tuittila and A. Korhola. submitted. «Re-evaluation of fire histories of three boreal bogs reveals a clear link between bog fire and climate». *Mires and Peat*.
- Morris, P. J., A. J. Baird and L. R. Belyea. 2012. «The DigiBog peatland development model 2: Ecohydrological simulations in 2D». *Ecohydrology*, vol. 5, no 3, p. 256-268.
- Morris, P. J., L. R. Belyea and A. J. Baird. 2011. «Ecohydrological feedbacks in peatland development: A theoretical modelling study». *Journal of Ecology*, vol. 99, no 5, p. 1190-1201.

- Nilsson, M., J. Sagerfors, I. Buffam, H. Laudon, T. Eriksson, A. Grelle, L. Klemedtsson, P. Weslien and A. Lindroth. 2008. «Contemporary carbon accumulation in a boreal oligotrophic minerogenic mire - A significant sink after accounting for all C-fluxes». *Global Change Biology*, vol. 14, no 10, p. 2317-2332.
- Quillet, A., S. Frolking, M. Garneau, J. Talbot and C. Peng. 2013. «Assessing the role of parameter interactions in the sensitivity analysis of a model of peatland dynamics ». *Ecological Modelling*, vol. 248, p. 30-40.
- Quillet, A., M. Garneau and S. Frolking. in press. «What drives carbon accumulation in peatlands? A global sensitivity analysis of the Holocene Peat Model». *Journal of Geophysical Research G: Biogeosciences*.
- Reimer, P. J., M. G. L. Baillie, E. Bard, A. Bayliss, J. Warren Beck, C. J. H. Bertrand, P. G. Blackwell, C. E. Buck, G. S. Burr, K. B. Cutler, P. E. Damon, R. Lawrence Edwards, R. G. Fairbanks, M. Friedrich, T. P. Guilderson, A. G. Hogg, K. A. Hughen, B. Kromer, G. McCormac, S. Manning, C. B. Ramsey, R. W. Reimer, S. Remmele, J. R. Southon, M. Stuiver, S. Talamo, F. W. Taylor, J. van der Plicht and C. E. Weyhenmeyer. 2004. «IntCal04 terrestrial radiocarbon age calibration, 0-26 cal kyr BP». *Radiocarbon*, vol. 46, no 3, p. 1029-1058.
- Roulet, N. T., P. M. Lafleur, P. J. H. Richard, T. R. Moore, E. R. Humphreys and J. Bubier. 2007. «Contemporary carbon balance and late Holocene carbon accumulation in a northern peatland». *Global Change Biology*, vol. 13, no 2, p. 397-411.
- Seppä, H., G. M. MacDonald, H. J. B. Birks, B. R. Gervais and J. A. Snyder. 2008. «Late-Quaternary summer temperature changes in the northern-European tree-line region». *Quaternary Research*, vol. 69, no 3, p. 404-412.
- Sillasoo, U., M. Väliranta and E. S. Tuittila. 2011. «Fire history and vegetation recovery in two raised bogs at the Baltic Sea». *Journal of Vegetation Science*, vol. 22, no 6, p. 1084-1093.
- Tuittila, E. S., S. Juutinen, S. Frolking, M. Väliranta, A. Laine, A. Miettinen, M.-L. Seväkivi, A. Quillet and P. Merilä. 2013. «Wetland chronosequence as a model of peatland development: Vegetation succession, peat and carbon accumulation». *The Holocene*, vol. 23, 1 January 2013, p. 23-33.

- Tuittila, E. S., M. Väliranta, J. Laine and A. Korhola. 2007. «Quantifying patterns and controls of mire vegetation succession in a southern boreal bog in Finland using partial ordinations». *Journal of Vegetation Science*, vol. 18, no 6, p. 891-902.
- Väliranta, M., A. Blundell, D. J. Charman, E. Karofeld, A. Korhola, Ü. Sillasoo and E. S. Tuittila. 2012. «Reconstructing peatland water tables using transfer functions for plant macrofossils and testate amoebae: A methodological comparison». *Quaternary International*, vol. 268, p. 34-43.
- Väliranta, M., A. Korhola, H. Seppä, E. S. Tuittila, K. Sarmaja-Korjonen, J. Laine and J. Alm. 2007. «High-resolution reconstruction of wetness dynamics in a southern boreal raised bog, Finland, during the late Holocene: A quantitative approach». *The Holocene*, vol. 17, no 8, p. 1093-1107.
- van Bellen, S., P. L. Dallaire, M. Garneau and Y. Bergeron. 2011. «Quantifying spatial and temporal Holocene carbon accumulation in ombrotrophic peatlands of the Eastmain region, Quebec, Canada». *Global Biogeochemical Cycles*, vol. 25, no 2, p. GB2016.
- van Bellen, S., M. Garneau, A. A. Ali and Y. Bergeron. 2012. «Did fires drive Holocene carbon sequestration in boreal ombrotrophic peatlands of eastern Canada?». *Quaternary Research*, vol. 78, no 1, p. 50-59.
- van Bellen, S., M. Garneau, A. A. Ali, A. Lamarre, E. C. Robert, G. Magnan, H. Asnong and S. Pratte. submitted. «Poor fen succession over ombrotrophic peat related to late-Holocene increased surface wetness in subarctic Quebec, Canada». *Journal of Quaternary Science*.
- van Bellen, S., M. Garneau and R. K. Booth. 2011. «Holocene carbon accumulation rates from three ombrotrophic peatlands in boreal Quebec, Canada: Impact of climate-driven ecohydrological change». *Holocene*, vol. 21, no 8, p. 1217-1231.
- Viau, A. E., and K. Gajewski. 2009. «Reconstructing millennial-scale, regional paleoclimates of boreal Canada during the Holocene». *Journal of Climate*, vol. 22, no 2, p. 316-330.
- Warner, B. G., T. Asada and N. P. Quinn. 2007. «Seasonal influences on the ecology of testate amoebae (Protozoa) in a small Sphagnum peatland in Southern Ontario, Canada». *Microbial Ecology*, vol. 54, no 1, p. 91-100.
- Yu, Z. 2011. «Holocene carbon flux histories of the world's peatlands: Global carbon-cycle implications». *Holocene*, vol. 21, no 5, p. 761-774.

Yu, Z., J. Loisel, D. P. Brosseau, D. W. Beilman and S. J. Hunt. 2010. «Global peatland dynamics since the Last Glacial Maximum». *Geophysical Research Letters*, vol. 37, no 13, p. L13402.

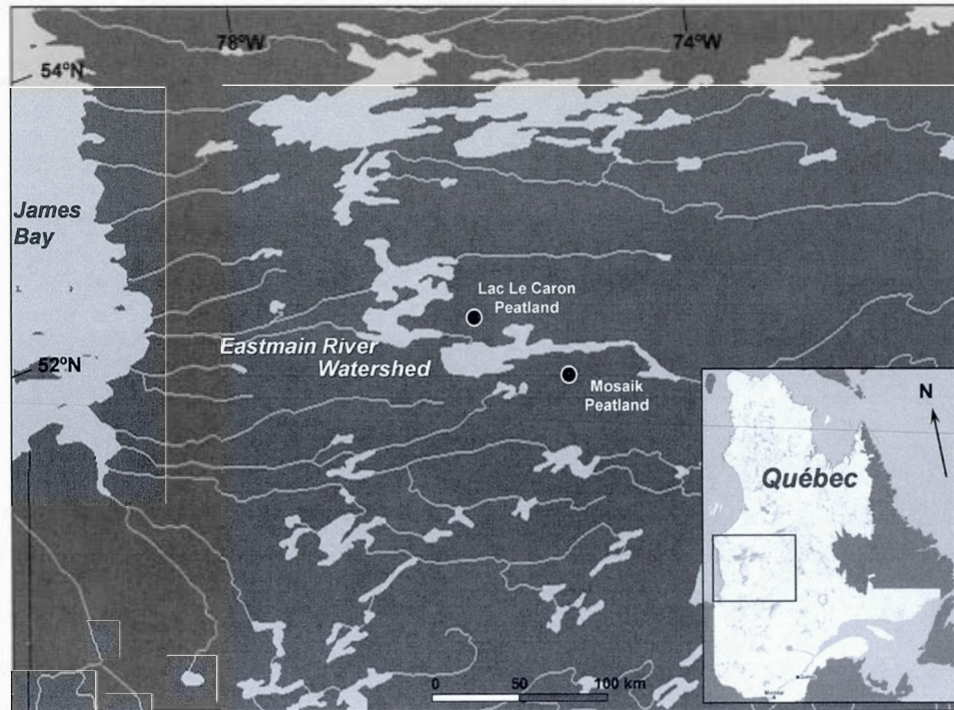


Figure 3.1: Location of the two peatlands

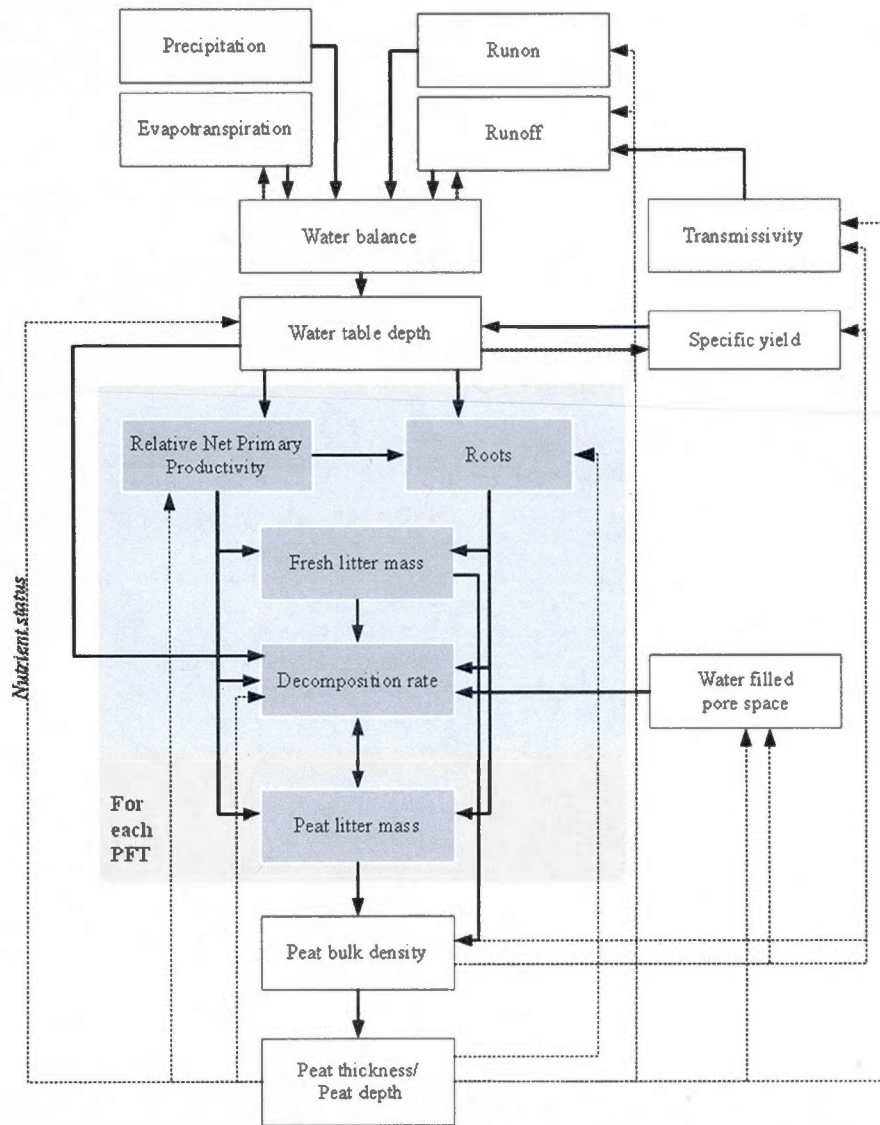


Figure 3.2: Conceptual diagram of HPM. Dashed-lines represent feedbacks.

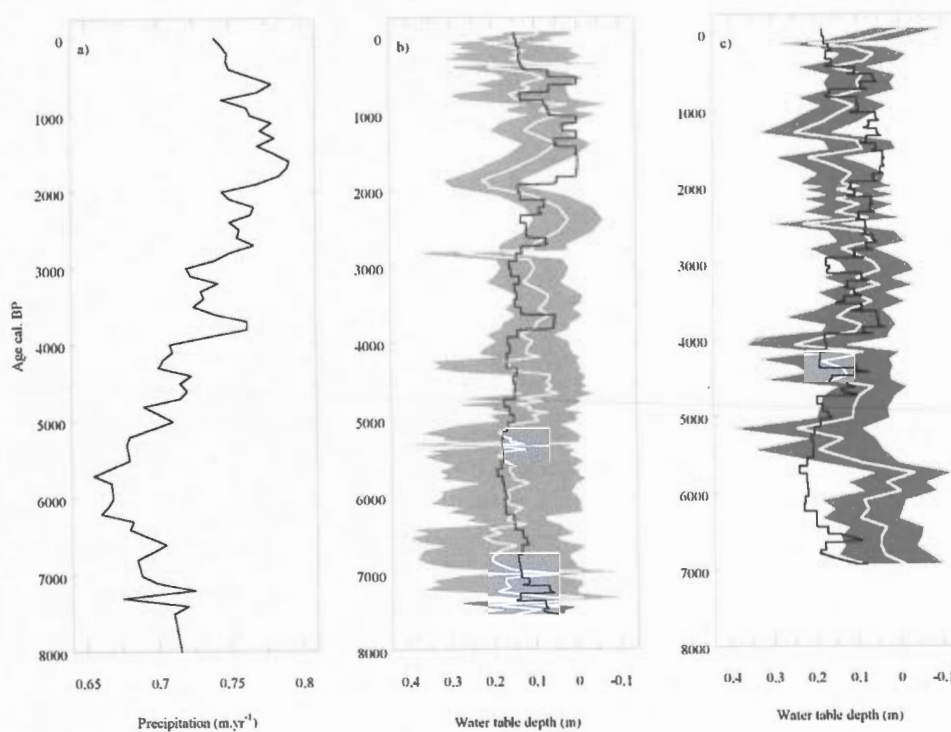


Figure 3.3: a) Precipitation in the Eastmain watershed reconstructed from pollen data (Viau and Gajewski, 2009). For b) LLC and c) MOS: water table reconstructions from testate amoebae (white solid line) with their standard errors (gray shade) (van Bellen, Garneau and Booth, 2011) and simulated water table depths from the simulation with reconstructed precipitation (black solid line). Water table depths are positive down.

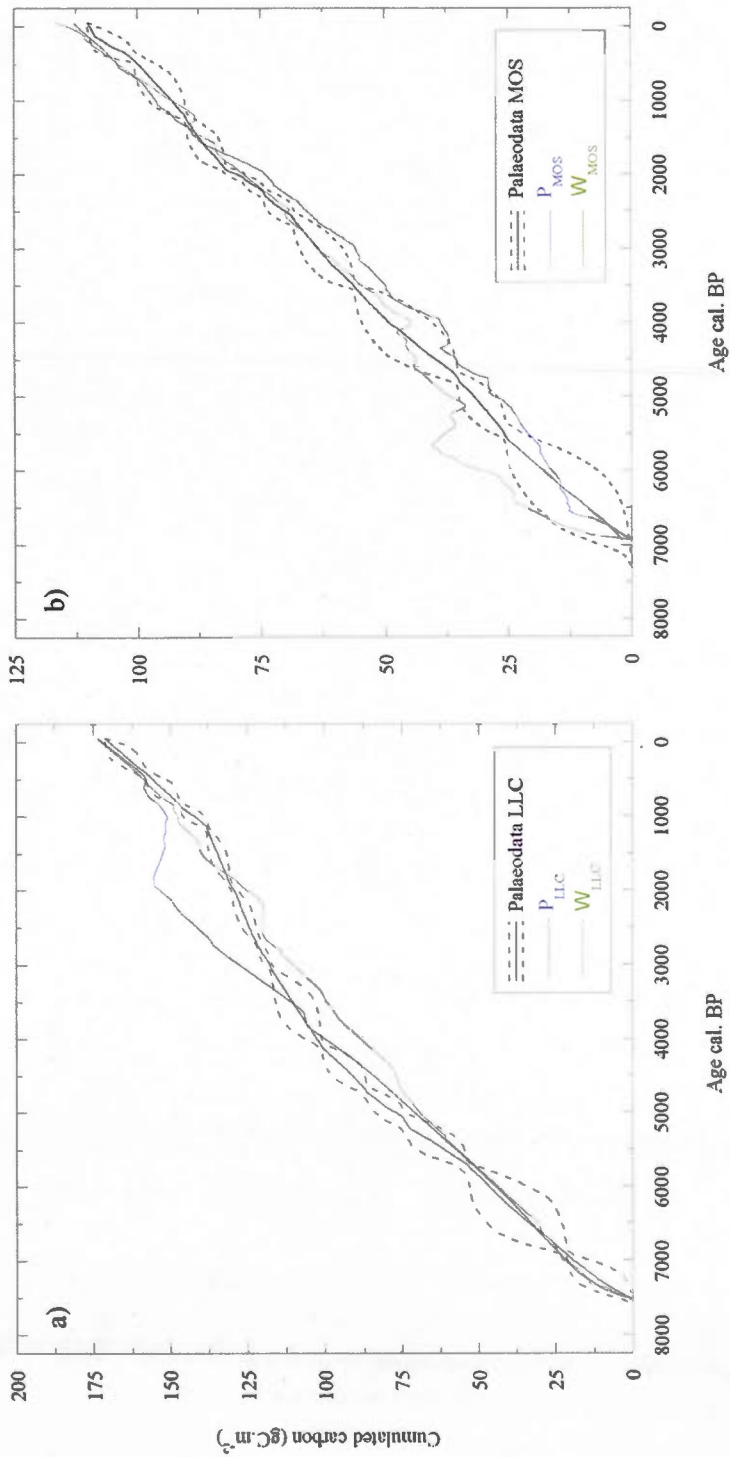


Figure 3.4: Accumulated carbon mass for a) LLC and b) MOS from loss on ignition results (black solid lines with 95% confidence interval in dashed lines), simulations with reconstructed precipitation (solid light gray) and with water table depth forcing (solid dark gray).

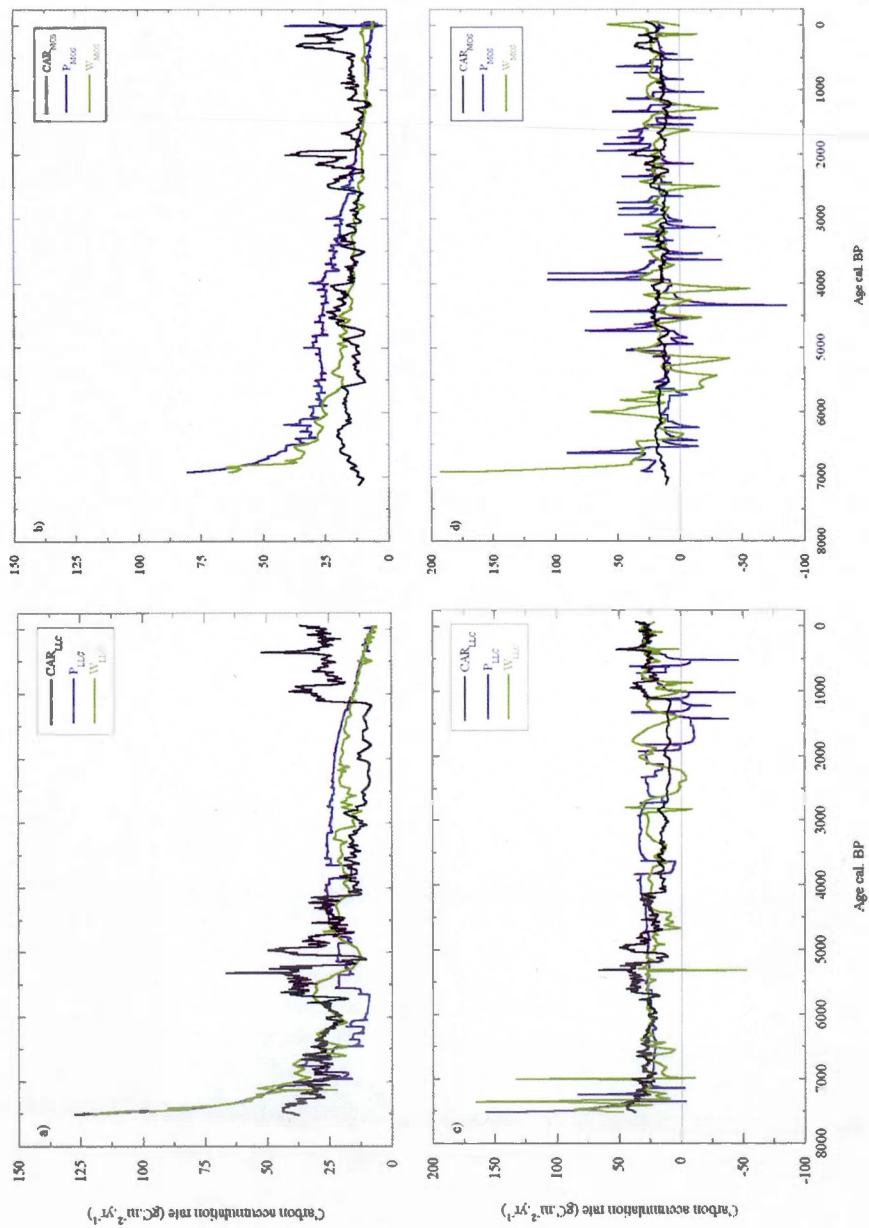


Figure 3.5: Carbon accumulation rates from loss on ignition analyses compared with simulated final core carbon content with reconstructed precipitation and with water table depth forcing for a) LLC and b) MOS and with simulated net annual carbon balance with reconstructed precipitation and with water table depth forcing for c) LLC and d) MOS.

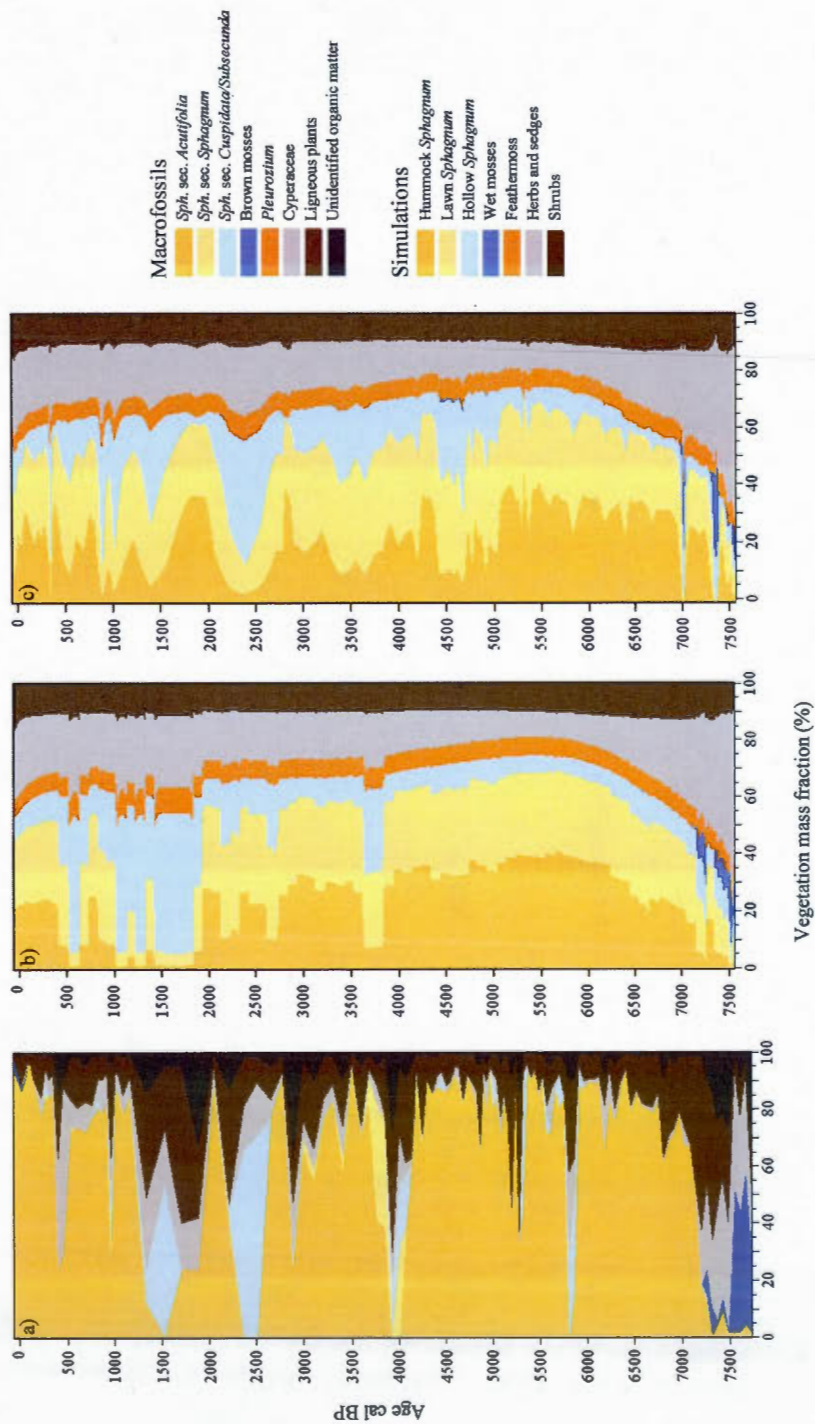


Figure 3.6: a) Macrofossil profile summary, b) distribution of the mass fraction of the different PFTs for P_{LLC} and c) for W_{LLC}. For sake of comparison, HPM's 12 PFTs (see Appendix 3.1) are aggregated into 7 groups of species identifiable in a peat core.

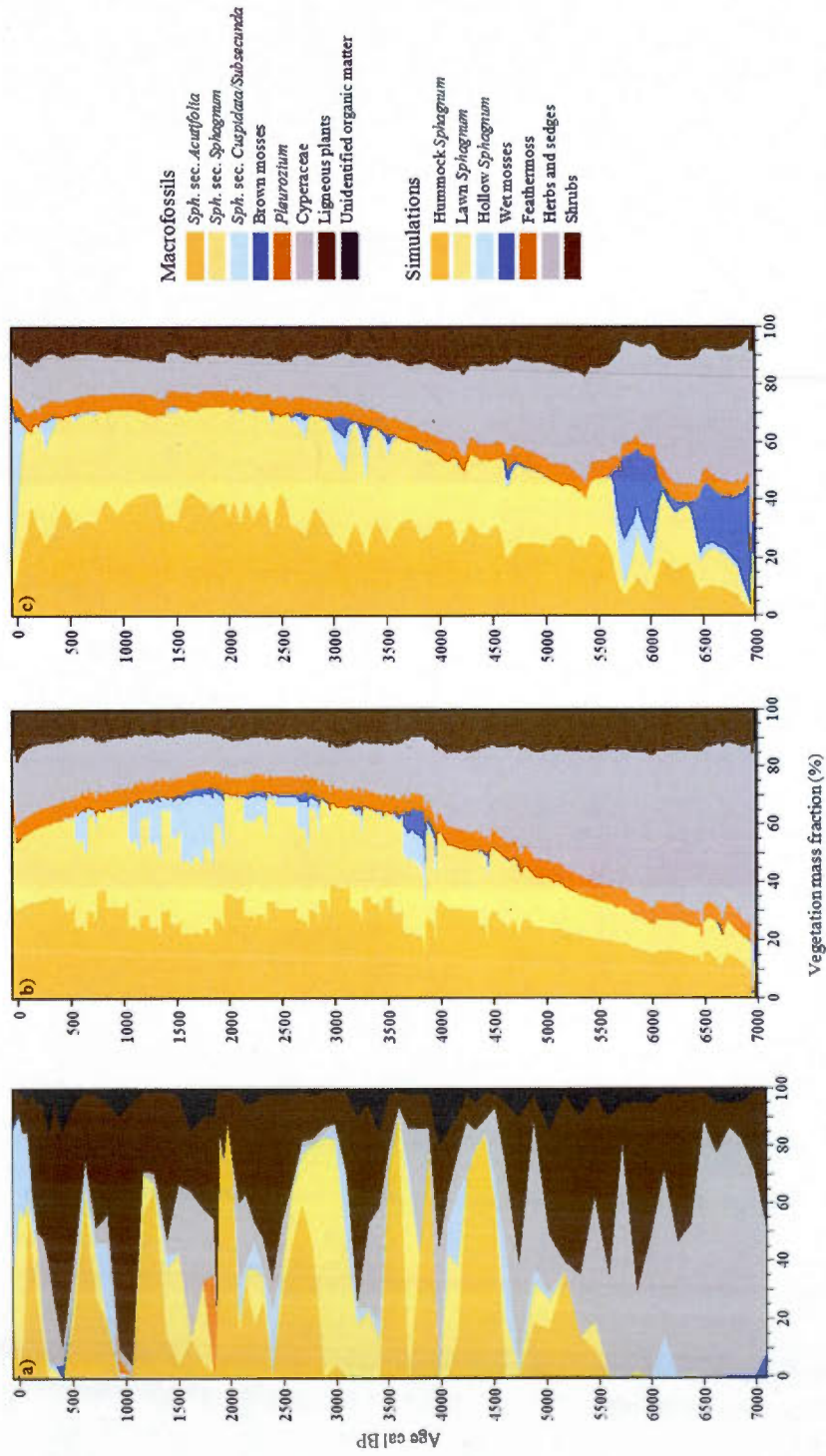


Figure 3.7: a) Macrofossil profile summary, b) distribution of the mass fraction of the different PFTs for PMos and c) for W_Mos. For sake of comparison, HPM's 12 PFTs (see Appendix 3.1) are aggregated into 7 groups of species identifiable in a peat core.

Appendix 3.1: HPM parameters: description and values. Differences between sites are in bold type.

| Parameter description | Units | LLC | MOS |
|--|--|--------------|--------------|
| Simulation length | [yr] | 7562 | 6984 |
| Annual precipitation | [m.yr ⁻¹] | 0.74 | 0.74 |
| Annual potential evotranspiration | [m.yr ⁻¹] | 0.40 | 0.40 |
| WTD threshold for minimal ET | [m] | 0.13 | 0.17 |
| WTD threshold for maximal ET | [m] | 0.24 | 0.24 |
| Potential ET/ Minimal ET | -- | 1.50 | 1.50 |
| Annual runoff adjustment factor | [m.y ⁻¹] | 0.02 | 0.04 |
| Increase in runoff with peat height | [m ⁻¹] | 0.015 | 0.03 |
| Minimum profile relative transmissivity | -- | 0.50 | 0.78 |
| Maximum potential NPP | [kg.m ⁻² .y ⁻¹] | 0.71 | 0.71 |
| Maximum root depth for non-sedge vascular plants | [m] | 0.20 | 0.20 |
| Depth to 80% of the sedge roots | [m] | 0.30 | 0.30 |
| Maximum root depth for sedges | [m] | 2.00 | 2.00 |
| Scale length for the anaerobic effect on decomposition rate | [m] | 0.80 | 0.40 |
| Optimal WFPS for decomposition | -- | 0.45 | 0.45 |
| Decomposition rate multiplier at annual mean water table depth | -- | 0.20 | 0.20 |
| Minimal decomposition rate multiplier | -- | 0.001 | 0.001 |
| Minimum litter/peat degree of saturation | -- | 0.03 | 0.03 |
| Controls litter/peat unsaturated water content function | -- | 0.50 | 0.50 |
| Controls litter/peat unsaturated water content function | [kg.m ⁻³] | 20.00 | 20.00 |
| M/M ₀ at which bulk density reaches half of its amplitude | -- | 0.12 | 0.30 |
| Controls steepness of the bulk density curve | -- | 0.13 | 0.18 |
| Minimum peat bulk density | [kg.m ⁻³] | 40.00 | 50.00 |
| Maximum potential increase in peat bulk density | [kg.m ⁻³] | 53.00 | 55.00 |
| Organic matter particle bulk density | [kg.m ⁻³] | 1300.00 | 1300.00 |

| PFT specific parameter description | Units | Symbol |
|--|--------------------|-------------------|
| Peat depth for optimum productivity | [m] | h_{PDi}^{opt} |
| Productivity range around the optimum | [m] | σ_{PDi} |
| | [m] | σ_{PDi}^+ |
| Water table depth for optimum productivity | [m] | $Z_{W\pi}^{opt}$ |
| Productivity range around the optimum | [m] | $\sigma_{W\pi}$ |
| | [m] | $\sigma_{W\pi}^+$ |
| Relative Net Primary Productivity | [-] | NPP_{rel}^* |
| Above-ground NPP | -- | A_{frac} |
| Decomposition rates | [y ⁻¹] | k_0^{**} |

Lac Le Caron

| PFT | PFT ID | Z^{opt}_{WTi} | $\bar{\sigma}_{WTi}$ | $\hat{\sigma}_{WTi}$ | h^{opt}_{PDi} | $\bar{\sigma}_{PDi}$ | $\hat{\sigma}_{PDi}$ | NPP _{rel} | AG _{fac} | k_0 |
|-------------------------|--------|-----------------|----------------------|----------------------|-----------------|----------------------|----------------------|--------------------|-------------------|--------------------|
| | [-] | [m] | [m] | [m] | [m] | [m] | [m] | [-] | [-] | [y ⁻¹] |
| Grass | 1 | 0.40 | 0.40 | 0.40 | 0.01 | 1.00 | 0.90 | 0.55 | 0.50 | 0.15 |
| Minerotrophic herb | 2 | 0.10 | 0.30 | 0.30 | 0.30 | 1.00 | 0.90 | 0.55 | 0.50 | 0.25 |
| Minerotrophic sedge | 3 | 0.10 | 0.40 | 0.40 | 0.10 | 2.00 | 1.50 | 0.75 | 0.20 | 0.25 |
| Minerotrophic shrub | 4 | 0.20 | 0.20 | 1.00 | 1.00 | 2.00 | 1.50 | 0.50 | 0.50 | 0.20 |
| Brown moss | 5 | 0.01 | 0.20 | 0.05 | 0.10 | 1.50 | 1.50 | 0.50 | 1.00 | 0.10 |
| Hollow <i>Sphagnum</i> | 6 | 0.01 | 0.20 | 0.15 | 2.00 | 1.50 | 19.00 | 0.50 | 1.00 | 0.10 |
| Lawn <i>Sphagnum</i> | 7 | 0.10 | 0.06 | 0.40 | 2.00 | 1.50 | 19.00 | 0.50 | 1.00 | 0.07 |
| Hummock <i>Sphagnum</i> | 8 | 0.20 | 0.10 | 0.50 | 2.00 | 1.50 | 19.00 | 0.50 | 1.00 | 0.05 |
| Feathermoss | 9 | 0.40 | 0.40 | 0.60 | 4.00 | 6.00 | 19.00 | 0.25 | 1.00 | 0.10 |
| Ombrotrophic herb | 10 | 0.20 | 0.20 | 0.20 | 4.00 | 2.00 | 19.00 | 0.25 | 0.50 | 0.25 |
| Ombrotrophic sedge | 11 | 0.20 | 0.30 | 0.30 | 4.00 | 2.00 | 19.00 | 0.50 | 0.20 | 0.15 |
| Ombrotrophic shrub | 12 | 0.30 | 0.30 | 1.00 | 4.00 | 2.00 | 19.00 | 0.50 | 0.50 | 0.15 |

Mosakk

| PFT | PFT ID | Z^{opt}_{WTi} | $\bar{\sigma}_{WTi}$ | $\hat{\sigma}_{WTi}$ | h^{opt}_{PDi} | $\bar{\sigma}_{PDi}$ | $\hat{\sigma}_{PDi}$ | NPP _{rel} | AG _{fac} | k_0 |
|-------------------------|--------|-----------------|----------------------|----------------------|-----------------|----------------------|----------------------|--------------------|-------------------|--------------------|
| | [-] | [m] | [m] | [m] | [m] | [m] | [m] | [-] | [-] | [y ⁻¹] |
| Grass | 1 | 0.40 | 0.40 | 0.40 | 0.01 | 1.00 | 0.90 | 0.55 | 0.50 | 0.15 |
| Minerotrophic herb | 2 | 0.10 | 0.30 | 0.30 | 0.30 | 1.00 | 0.90 | 0.55 | 0.50 | 0.25 |
| Minerotrophic sedge | 3 | 0.10 | 0.40 | 0.40 | 0.10 | 2.00 | 1.50 | 0.75 | 0.20 | 0.25 |
| Minerotrophic shrub | 4 | 0.20 | 0.20 | 1.00 | 1.00 | 2.00 | 1.50 | 0.50 | 0.50 | 0.20 |
| Brown moss | 5 | 0.01 | 0.20 | 0.05 | 0.10 | 1.50 | 1.50 | 0.50 | 1.00 | 0.10 |
| Hollow <i>Sphagnum</i> | 6 | 0.01 | 0.20 | 0.05 | 2.00 | 1.00 | 19.00 | 0.50 | 1.00 | 0.10 |
| Lawn <i>Sphagnum</i> | 7 | 0.10 | 0.09 | 0.40 | 2.00 | 1.50 | 19.00 | 0.50 | 1.00 | 0.07 |
| Hummock <i>Sphagnum</i> | 8 | 0.20 | 0.17 | 0.50 | 2.00 | 1.50 | 19.00 | 0.50 | 1.00 | 0.05 |
| Feathermoss | 9 | 0.40 | 0.40 | 0.60 | 4.00 | 6.00 | 19.00 | 0.25 | 1.00 | 0.10 |
| Ombrotrophic herb | 10 | 0.20 | 0.20 | 0.20 | 4.00 | 2.00 | 19.00 | 0.25 | 0.50 | 0.25 |
| Ombrotrophic sedge | 11 | 0.20 | 0.30 | 0.30 | 4.00 | 2.00 | 19.00 | 0.50 | 0.20 | 0.15 |
| Ombrotrophic shrub | 12 | 0.30 | 0.30 | 1.00 | 4.00 | 2.00 | 19.00 | 0.50 | 0.50 | 0.15 |

CONCLUSION

L'amélioration des connaissances de la dynamique du carbone dans les tourbières est nécessaire à la compréhension et à la modélisation du cycle global du carbone ainsi que du climat global. La modélisation de la dynamique des tourbières représente une étape importante pour leur intégration dans ces modèles globaux. En vue de rendre cette intégration possible, les objectifs de cette thèse consistaient à évaluer la représentation mathématique des processus sous-jacents de la dynamique du carbone dans les tourbières et à en identifier les lacunes. Le « Holocene Peat Model » représente ici un outil de choix pour mener à bien ce projet puisque ce modèle intègre de multiples processus influençant l'accumulation de carbone dans les tourbières mais aussi de nombreuses interactions entre ces processus.

Principales contributions de la thèse

Les travaux présentés dans cette thèse ont contribué à l'avancement des connaissances dans le domaine de la dynamique et de la systématique des tourbières nordiques. Le développement d'une méthodologie originale a permis d'évaluer les processus d'accumulation de carbone dans le modèle en alliant l'évaluation de la dynamique d'échelle fine (échelle du site) et la dynamique de grande échelle (nord du 45^e parallèle) en termes de reproductibilité ainsi que de variabilité. L'évaluation de ces deux aspects a aussi permis de vérifier que ces processus sont adéquatement représentés puisqu'elle tient compte de la grande variabilité des conditions et des caractéristiques des sites simulés et de leur dynamique interne, ce qui est essentiel pour l'intégration des tourbières dans les modèles globaux. De plus la reproductibilité du développement d'une tourbière spécifique après calibration a permis de s'assurer que le modèle est représentatif et répond adéquatement à des conditions régionales et spécifiques au site.

Un autre aspect novateur de la méthodologie consiste en l'utilisation de séries de données paléoécologiques pour compléter l'évaluation des processus du modèle. Cette approche a permis une meilleure comparaison entre les résultats du modèle et des données indépendantes et s'apparente à une analyse paléoécologique intégrée à plusieurs indicateurs (multi-proxy). Cette méthode présente l'avantage d'identifier des lacunes dans le modèle, qu'elles soient d'origine technique ou liées à des manques de connaissance.

L'utilisation de données paléoécologiques dans les simulations a permis d'intégrer des composantes allogènes aux simulations et par conséquent d'assurer la comparaison entre les résultats. Ainsi, il a été possible de comparer les taux d'accumulation de carbone issus des analyses de perte au feu aux taux d'accumulation de carbone simulés et de comparer leurs variations tout en conservant une même chronologie. Ceci a permis de révéler l'occurrence de périodes durant lesquelles la tourbière a pu subir une perte nette de carbone et donc être une source plutôt qu'un puits de carbone. La mise en évidence de ces périodes de perte nette de carbone à l'échelle centenaire n'avait jamais été réalisée à notre connaissance.

Par ailleurs, les trois chapitres de cette étude conduisent à des résultats concernant aussi bien les techniques d'évaluation que la dynamique des systèmes tourbeux. Ainsi, cette étude révèle que les interactions entre les paramètres du modèle revêtent une importance particulière pour les résultats et qu'elles sont de nature complexe. Cette étude a permis également d'identifier les paramètres ayant une influence sur la quantité totale de carbone et étant particulièrement impliqués dans les interactions entre paramètres (tels que la productivité primaire nette, la conductivité hydraulique, le gradient d'anoxie et certains paramètres contrôlant le bilan hydrique et la densité sèche). L'identification de ces interactions est importante puisqu'elle permet de déterminer les causes d'un changement de comportement du modèle. Ces interactions sont fondamentalement indissociables des systèmes adaptatifs complexes que sont les

tourbières, selon la terminologie de Belyea et Baird (2006), et c'est pour cette raison que l'évaluation effectuée ici repose sur une analyse de sensibilité globale.

Au vu des résultats des différents chapitres il appert que le modèle est en mesure de reproduire des dynamiques de développement variées tout en conservant une dynamique réaliste en accord avec les observations faites sur le terrain. Ainsi, plusieurs modes de développement peuvent être simulés et des effets de seuil peuvent être observés dans les simulations à différents stades de leur développement.

Bien que les simulations effectuées dans les deux premiers chapitres n'aient pas intégré de variation des conditions climatiques tout au long des périodes simulées, une grande variabilité des résultats a été obtenue, tant au niveau de la quantité de carbone accumulée durant les simulations qu'au niveau des étapes de développement. Ainsi certaines simulations ont présenté des conditions de forte accumulation de carbone durant les premières centaines d'années de développement qui ont été suivies par une forte baisse de l'accumulation, alors que d'autres ont présenté une accumulation de carbone relativement constante tout au long de la simulation, ou augmentant graduellement durant les derniers millénaires grâce à la prépondérance tardive de sphaignes de platière ou de sphaignes de butte à la décomposition très lente. Ces types de sphaignes ont été identifiés comme des facteurs importants dans l'équilibre du système. Bien que la compétition entre les espèces ne soit représentée que de façon indirecte dans le modèle, ces types de sphaignes ont modifié le régime d'accumulation de carbone dans les simulations.

La dynamique locale de développement des tourbières ayant elle aussi été reproductible, nous pouvons en déduire que les processus représentés dans le modèle sont effectivement représentatifs du système. De plus, bien que le modèle ne soit pas exhaustif, et en tenant compte des limites de sa représentativité, les processus qui le composent suffisent à reproduire ces comportements généraux et sont donc adéquatement représentés.

Limites de l'étude

Plusieurs facteurs limitent l'applicabilité et l'interprétation des résultats de cette thèse. En effet, ces résultats sont applicables à des tourbières ombrotrophes, le cas des autres types de tourbières n'ayant pas été traité. Il serait en conséquence important de procéder au même type d'analyses en comparant les résultats à des données paléoécologiques provenant par exemple de tourbières minérotrophes, puisque le HPM permet également de représenter ces types de milieux.

Intrinsèquement, un modèle ne peut intégrer tous les processus qui sont liés à la systémique du milieu étudié. Le « Holocene Peat Model » ne fait pas exception puisque de nombreuses variables liées à la dynamique des tourbières n'y sont pas représentées (ex : compétition, microtopographie, pergélisol, etc). Certaines de ces lacunes pourraient pourtant engendrer des répercussions sur les résultats présentés et sur leur interprétation. C'est probablement le cas pour les processus impliquant des échanges latéraux d'eau, de carbone ou de nutriments qui font l'objet d'une attention particulière dans le récent développement du DigiBog (Baird, Morris et Belyea, 2012), et qui ne peuvent être représentés actuellement dans le HPM, qui ne possède qu'une dimension.

De plus, l'utilisation d'un régime dynamique de précipitations dans le troisième chapitre a affecté le bilan hydrique des tourbières. Cependant, les précipitations avaient été maintenues à un niveau constant tout au long des simulations utilisées pour l'analyse de sensibilité effectuée dans les deux premiers chapitres, dans le but de comparer les résultats entre eux. Afin de pallier cette déficience, il serait intéressant d'attribuer une valeur aléatoire de variation aux précipitations et d'ajouter ce facteur aux autres paramètres analysés afin d'en mesurer l'incidence sur les résultats.

Par ailleurs, dans le but d'améliorer le modèle, il serait intéressant d'affiner la représentation de la densité sèche qui a été identifiée comme une source d'incertitude

dans le modèle. En effet, la densité sèche est la résultante complexe de plusieurs facteurs (notamment de la décomposition de la tourbe qui elle-même dépend des conditions d'humidité, de température du sol, d'anoxie etc.) et nécessite une meilleure caractérisation afin de limiter les incertitudes qui lui sont associées. Des analyses de décomposition sur des échantillons de tourbe prenant en compte leurs différentes propriétés physiques permettraient d'enrichir les connaissances dans ce domaine. D'autre part, si la masse totale de carbone fait l'objet d'une étude subséquente, le modèle pourrait également être amélioré en supprimant les paramètres identifiés comme non-influents tels que les paramètres associés à la répartition aérienne et souterraine de la biomasse de la végétation, les paramètres liés à la représentation des systèmes racinaires ou certains paramètres associant les niveaux de nappe phréatique aux optimums de productivité de différents TFPs. De plus, le maximum potentiel de la PPN ou le ruissellement net sortant du système pourraient être mieux estimés en intégrant de nouveaux facteurs décrivant ces paramètres (ex. température ou radiation solaire pour la PPN) ou en se basant sur des sorties de modèles globaux.

Pistes de recherche

À partir des résultats obtenus dans cette thèse, plusieurs pistes de recherche peuvent être exploitées. Les nombreuses simulations effectuées pour l'analyse de sensibilité constituent une base de données intéressante pour l'analyse des relations entre différentes composantes du modèle afin de découvrir des comportements récurrents qui peuvent nous renseigner sur la dynamique des tourbières. Par exemple, l'analyse des relations entre l'accumulation de carbone et les niveaux de nappe phréatique permettrait d'identifier différents type de développement des tourbières. Les résultats de cette thèse pourraient également s'avérer utiles pour l'évaluation de la variabilité d'une section de l'espace du modèle correspondant à une région d'étude ou à un

comportement particulier tel que des changements abrupts de densité sèche ou de nappe phréatique.

Dans les deux premiers chapitres de cette étude, les simulations du modèle présentent des réponses d'amplitudes diverses et non anticipées, mais également que la résilience d'un système à l'autre peut être extrêmement variable. Il semble donc essentiel de circonscrire les causes de ce phénomène et de les intégrer dans les modèles afin d'améliorer les résultats. Pour ce faire, il serait tout d'abord nécessaire de caractériser les conditions favorisant ou non la résilience d'un système et de les quantifier. Une analyse de sensibilité axée sur la succession temporelle détaillée des variations d'accumulation de carbone à différents stades de développement permettrait d'étudier les différents processus transitionnels abrupts (sensu Belyea, 2009) qui peuvent s'effectuer à l'échelle centenaire durant le développement d'une tourbière.

Enfin, il serait intéressant d'utiliser de séries de données paléocéologiques ainsi que des chronologies à haute résolution pour effectuer une étude locale détaillée de l'origine des changements de végétation. L'intégration de reconstruction de niveaux de nappe phréatique basés sur des analyses d'abondance de thécamoebiens pourrait également s'avérer utile pour tester les simulations de niveaux de nappe phréatiques dans tous types de modèles basés sur une dynamique à moyen ou à long terme.

En conclusion, les connaissances actuelles permettent une modélisation généralement adéquate de la dynamique du carbone dans les tourbières, qui pourrait être utilisée pour leur intégration dans des modèles globaux. Toutefois, en vue d'assurer l'intégration des tourbières nordiques dans les GCMs, de plus amples évaluations sont nécessaires, celles-ci devant tenir compte des objectifs de l'étude. De plus, le HPM ne calcule pas certaines sorties qui pourraient être nécessaires aux GCM, telles que les échanges de gaz et d'énergie à la surface des tourbières nécessitant le développement d'un arrimage spécifique entre les tourbières et l'atmosphère. Par

ailleurs, en vue de cerner et de reproduire la dynamique locale rapide combinant les facteurs allogènes et autogènes qui gouvernent les changements d'accumulation de carbone et de végétation d'un site particulier, plusieurs efforts de recherche devront être accomplis, notamment en ce qui a trait à l'écohydrologie et à ses implications dans les processus de décomposition.

References

- Anderson, R. L., D. R. Foster et G. Motzkin. 2003. «Integrating lateral expansion into models of peatland development in temperate New England». *Journal of Ecology*, vol. 91, no 1, p. 68-76.
- Baird, A. J., P. J. Morris et L. R. Belyea. 2012. «The DigiBog peatland development model 1: Rationale, conceptual model, and hydrological basis». *Ecohydrology*, vol. 5, no 3, p. 242-255.
- Beaulieu-Audy, V., M. Garneau, P. J. H. Richard et H. Asnong. 2009. «Holocene palaeoecological reconstruction of three boreal peatlands in the la Grande Riviere region, Québec, Canada». *Holocene*, vol. 19, no 3, p. 459-476.
- Belyea, L. R. 2009. «Nonlinear dynamics of peatlands and potential feedbacks on the climate system». In *Carbon cycling in northern peatlands*, sous la dir. de A. J. Baird, L. R. Belyea et X. Comas, p. 5-18. Washington : American Geophysical Union.
- Belyea, L. R., et A. J. Baird. 2006. «Beyond "the limits to peat bog growth": Cross-scale feedback in peatland development». *Ecological Monographs*, vol. 76, no 3, p. 299-322.
- Blaauw, M. 2012. «Out of tune: The dangers of aligning proxy archives». *Quaternary Science Reviews*, vol. 36, p. 38-49.
- Charman, D. J. 2002. *Peatlands and environmental change*. Chichester, 301p.
- Clymo, R. S. 1984. «The limits of peat bogs growth». *Philosophical Transactions of the Royal Society of London, Series B*, vol. 303, p. 605-653.
- 1992. «Models of peat growth». *Suo*, vol. 43, no 4-5, p. 127-136.
- Denman, K. L., G. Brasseur, A. Chidthaisong, P. Ciais, P. M. Cox, R. E. Dickinson, D. Hauglustaine, C. Heinze, E. Holland, D. Jacob, U. Lohmann, S. Ramachandran, P. L. da Silva Dias, S. C. Wofsy et X. Zhang. 2007. «Couplings between changes in the climate system and biogeochemistry». *Climate Change 2007: The Physical Science Basis. Contribution of Working Group I to the Fourth Assessment Report of the Intergovernmental Panel on Climate Change*, p. 500-587.

- Frolking, S., et N. T. Roulet. 2007. «Holocene radiative forcing impact of northern peatland carbon accumulation and methane emissions». *Global Change Biology*, vol. 13, no 5, p. 1079-1088.
- Frolking, S., N. T. Roulet, T. R. Moore, P. J. H. Richard, M. Lavoie et S. D. Muller. 2001. «Modeling northern peatland decomposition and peat accumulation». *Ecosystems*, vol. 4, no spring, p. 479-498.
- Frolking, S., N. T. Roulet, E. Tuittila, J. L. Bubier, A. Quillet, J. Talbot et P. J. H. Richard. 2010. «A new model of Holocene peatland net primary production, decomposition, water balance, and peat accumulation». *Earth System Dynamics*, vol. 1, no 1, p. 1-21.
- Heijmans, M. M. P. D., D. Mauquoy, B. Van Geel et F. Berendse. 2008. «Long-term effects of climate change on vegetation and carbon dynamics in peat bogs». *Journal of Vegetation Science*, vol. 19, no 3, p. 307-320.
- Heinemeyer, A., S. Croft, M. H. Garnett, E. Gloor, J. Holden, M. R. Lomas et P. Ineson. 2010. «The MILLENNIA peat cohort model: Predicting past, present and future soil carbon budgets and fluxes under changing climates in peatlands». *Climate Research*, vol. 45, no 1, p. 207-226.
- Hilbert, D. W., N. T. Roulet et T. R. Moore. 2000. «Modelling and Analysis of Peatlands as Dynamical Systems». *Journal of Ecology*, vol. 88, no 2, p. 230-242.
- Ise, T., A. L. Dunn, S. C. Wofsy et P. R. Moorcroft. 2008. «High sensitivity of peat decomposition to climate change through water-table feedback». *Nature Geoscience*, vol. 1, no 11, p. 763-766.
- Kleinen, T., V. Brovkin et R. J. Getzieh. 2011. «A dynamic model of wetland extent and peat accumulation: Results for the Holocene». *Biogeosciences Discussions*, vol. 8, no 3, p. 4805-4839.
- Lai, D. Y. F. 2009. «Modelling the effects of climate change on methane emission from a northern ombrotrophic bog in Canada». *Environmental Geology*, vol. 58, no 6, p. 1197-1206.
- Lamentowicz, M., M. Obremaska et E. A. D. Mitchell. 2008. «Autogenic succession, land-use change, and climatic influences on the Holocene development of a kettle-hole mire in Northern Poland». *Review of Palaeobotany and Palynology*, vol. 151, no 1-2, p. 21-40.

- Li, T., Y. Huang, W. Zhang et C. Song. 2010. «CH₄MODwetland: A biogeophysical model for simulating methane emissions from natural wetlands». *Ecological Modelling*, vol. 221, no 4, p. 666-680.
- St-Hilaire, F., J. Wu, N. T. Roulet, S. Frohling, P. M. Lafleur, E. R. Humphreys et V. Arora. 2010. «McGill wetland model: Evaluation of a peatland carbon simulator developed for global assessments». *Biogeosciences*, vol. 7, no 11, p. 3517-3530.
- Tang, J., Q. Zhuang, R. D. Shannon et J. R. White. 2010. «Quantifying wetland methane emissions with process-based models of different complexities». *Biogeosciences*, vol. 7, no 11, p. 3817-3837.
- Tuittila, E. S., S. Juutinen, S. Frohling, M. Väiliranta, A. Laine, A. Miettinen, M.-L. Seväkivi, A. Quillet et P. Merilä. 2013. «Wetland chronosequence as a model of peatland development: Vegetation succession, peat and carbon accumulation». *The Holocene*, vol. 23, no 1 January 2013, p. 23-33.
- Tuittila, E. S., M. Väiliranta, J. Laine et A. Korhola. 2007. «Quantifying patterns and controls of mire vegetation succession in a southern boreal bog in Finland using partial ordinations». *Journal of Vegetation Science*, vol. 18, no 6, p. 891-902.
- Turunen, J., E. Tomppo, K. Tolonen et A. Reinikainen. 2002. «Estimating carbon accumulation rates of undrained mires in Finland - Application to boreal and subarctic regions». *Holocene*, vol. 12, no 1, p. 69-80.
- Waddington, J. M., E. Kellner, M. Strack et J. S. Price. 2010. «Differential peat deformation, compressibility, and water storage between peatland microforms: Implications for ecosystem function and development». *Water Resources Research*, vol. 46, no 7, p. W07538.
- Wania, R., L. Ross et I. C. Prentice. 2009. «Integrating peatlands and permafrost into a dynamic global vegetation model: 1. Evaluation and sensitivity of physical land surface processes». *Global Biogeochemical Cycles*, vol. 23, no 3, p. GB3014.
- Yu, Z., D. W. Beilman et M. C. Jones. 2009. «Sensitivity of northern peatland carbon dynamics to Holocene climate change». In *Carbon cycling in northern peatlands*, sous la dir. de A. J. Baird, L. R. Belyea et X. Comas, p. 55-69. Washington: American Geophysical Union.